

29
AUT

~~SECRET~~
~~SECURITY INFORMATION~~

ORNL-1330

CENTRAL RESEARCH LIBRARY
DOCUMENT COLLECTION

546
W.K.

MARTIN MARIETTA ENERGY SYSTEMS LIBRARIES



3 4456 0353143 5

DECLASSIFIED

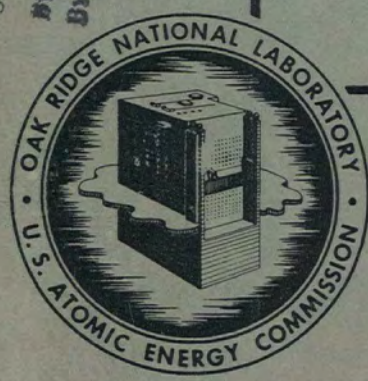
Classified from Original To:
By AUTHORITY OF: AEC
By: [Signature] 10-9-57
11-9-57

HEAT EXCHANGER
DESIGN CHARTS

By

A. P. Fraas
M. E. Laverne

AEC RESEARCH AND DEVELOPMENT REPORT



CENTRAL RESEARCH LIBRARY
DOCUMENT COLLECTION

LIBRARY LOAN COPY

DO NOT TRANSFER TO ANOTHER PERSON

If you wish someone else to see this document, send in name with document and the library will arrange a loan.

OAK RIDGE NATIONAL LABORATORY
OPERATED BY
CARBIDE AND CARBON CHEMICALS COMPANY
A DIVISION OF UNION CARBIDE AND CARBON CORPORATION
OAK RIDGE, TENNESSEE

~~RESTRICTED DATA~~

This document contains restricted data as defined in the Atomic Energy Act of 1946. Its transmittal or the disclosure of its contents in any manner to an unauthorized person is prohibited.

~~SECRET~~
~~SECURITY INFORMATION~~

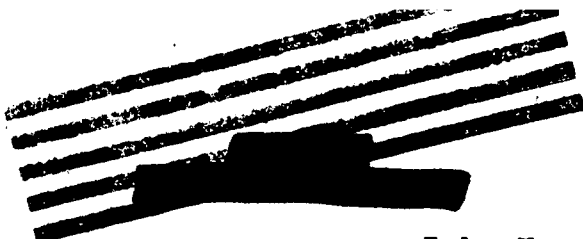
710
AUT

AUT

174
56

Inv. 52

Inv. 59



Index No. ORNL-1330
This document contains 82 pages.
This is copy 54 of 149, Series A.

Subject Category: Reactors-
Research and Power

HEAT EXCHANGER DESIGN CHARTS

A. P. Fraas
M. E. LaVerne

December 7, 1952

OAK RIDGE NATIONAL LABORATORY
Operated by
CARBIDE AND CARBON CHEMICALS COMPANY
A DIVISION OF UNION CARBIDE AND CARBON CORPORATION
Oak Ridge, Tennessee

Contract No. W-7405-eng-26



MARTIN MARIETTA ENERGY SYSTEMS LIBRARIES



3 4456 0353143 5

Distribution, Series A:

- 1-29. Carbide and Carbon Chemicals Company
- 30-40. Argonne National Laboratory
- 41. Armed Forces Special Weapons Project (Sandia)
- 42-46. Atomic Energy Commission, Washington
- 47. Battelle Memorial Institute
- 48-50. Brookhaven National Laboratory
- 51. Bureau of Ships
- 52-53. California Research and Development Company
- 54-65. Carbide and Carbon Chemicals Company (ORNL)
- 66. Chicago Patent Group
- 67. Chief of Naval Research
- 68. Department of the Navy - Op-36
- 69-73. duPont Company
- 74-76. General Electric Company (ANPP)
- 77-80. General Electric Company, Richland
- 81. Hanford Operations Office
- 82-88. Idaho Operations Office
- 89. Iowa State College
- 90-93. Knolls Atomic Power Laboratory
- 94-95. Los Alamos Scientific Laboratory
- 96. Massachusetts Institute of Technology (Kaufmann)
- 97-99. Mound Laboratory
- 100. National Advisory Committee for Aeronautics, Cleveland
- 101. National Advisory Committee for Aeronautics, Washington
- 102-103. New York Operations Office
- 104-105. North American Aviation, Inc.
- 106. Nuclear Development Associates, Inc.
- 107. Patent Branch, Washington
- 108. RAND Corporation
- 109. San Francisco Operations Office
- 110. Savannah River Operations Office, Augusta
- 111. Savannah River Operations Office, Wilmington
- 112-113. University of California Radiation Laboratory
- 114. Vitro Corporation of America
- 115. Walter Kline Nuclear Laboratories, Inc.
- 116-119. Westinghouse Electric Corporation
- 120-134. Wright Air Development Center
- 135-149. Technical Information Service, Oak Ridge

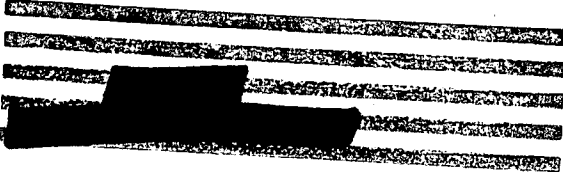
Carbide and Carbon Chemicals Company internal distribution as follows:

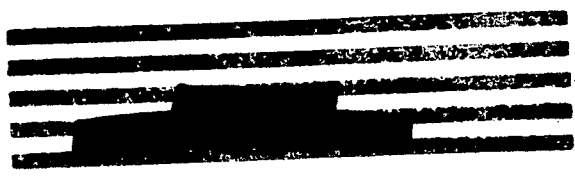
- | | |
|-------------------|----------------------------|
| 1. C. E. Center | 10. M. E. Lerner |
| 2. C. E. Larson | 11. R. N. Lyon |
| 3. L. B. Emet | 12. W. D. Manly |
| 4. W. B. Jones | 13. H. F. Poppendiek |
| 5. J. J. Weisberg | 14. A. J. Miller |
| 6. F. D. Shirley | 15. H. W. Savage |
| 7. E. S. Bettis | 16. R. L. Potter |
| 8. A. C. Briant | 17. F. H. Abernathy |
| 9. J. P. Fraas | 18-25. ANP Reports Office |
| | 26-29. Reports Office, TID |

Issuing Office
Technical Information Department, Y-12 Plant
Date Issued: JAN 13 1953


TABLE OF CONTENTS

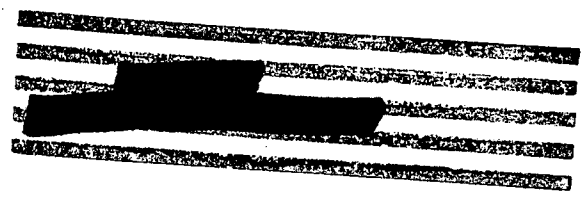
<u>Section</u>	<u>Page No.</u>
INTRODUCTION	9
HEAT EXCHANGER MATRIX GEOMETRY	9
Sample Problem No. 1, Maximum Number of Tubes in Header	20
Sample Problem No. 2, Header Diameter	20
Derivations for Spherical Shell Heat Exchanger	
Tube Inclination Angle	23
Tube Longitude Angle	24
Shell-Thickness to Sphere-Diameter Ratio	25
Tube Length	26
Sample Problem No. 3, Spherical Shell Heat Exchanger	27
Sample Problem No. 4, Tube Bundle Parameters	36
Sample Problem No. 5, Tube Bundle Parameters	37
FLUID FLOW AND PRESSURE LOSSES	51
Sample Problem No. 6, Viscosity and Pressure Drop	51
HEAT TRANSFER COEFFICIENT	57
PERFORMANCE OF A SERIES OF TYPICAL COUNTERFLOW HEAT EXCHANGERS	69
Sample Problem No. 7, Temperature Rise Variation	70
Sample Problem No. 8, Power Density Variation	70
LIST OF TABLES	4
LIST OF ILLUSTRATIONS	5





LIST OF TABLES

<u>Table No.</u>	<u>Title</u>	<u>Page No.</u>
1	Radii and Numbers of Tubes for Circular Headers	15
2	Volumes and Weights of Spheres and Spherical Shells	29
3	Physical Properties	68



LIST OF ILLUSTRATIONS

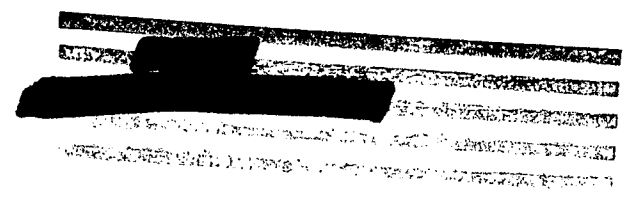
<u>Figure No.</u>	<u>Title</u>	<u>Page No.</u>
1	First ORNL-ANP Heat Exchanger Airflow Model	
	(a) Three-quarter view showing tube shapes and placement of spacers	10
	(b) End view showing details of header plate and tube shapes	11
2	Schematic Longitudinal Cross-Section through Annular Model of Proposed Type of Aircraft Heat Exchanger	12
3	Shower-Head Type Headers	
	(a) Header components	14
	(b) Header assembly	14
4	Circular Header Tube Hole Patterns	
	(a) Coordinate system	19
	(b) Configuration 1	19
	(c) Configuration 2	19
	(d) Configuration 3	19
	(e) Configuration 4	19
5	Cross-Section through a Reactor and Spherical Shell Intermediate Heat Exchanger Arrangement	21
6	Model of Spherical Shell Heat Exchanger	22
7	Spherical Shell Heat Exchanger Geometry	
	(a) Coordinate System	31
	(b) Tube inclination angle as a function of latitude angle	32

List of Illustrations (Continued)

<u>Figure No.</u>	<u>Title</u>	<u>Page No.</u>
	(c) Tube longitude angle as a function of latitude angle	33
	(d) Shell-thickness to sphere-diameter ratio as a function of shell volume to sphere volume ratio and terminal latitude angles	34
	(e) Tube length to sphere diameter ratio as a function of latitude angle	35
8	Various Geometric Parameters for a Square Pitch Tube Bundle as Functions of Ratio of Spacer Thickness to Tube Outside Diameter	
	(a) Ratio of flow area outside tubes to tube matrix frontal area	38
	(b) Ratio of flow area inside tubes to tube matrix frontal area	39
	(c) Ratio of equivalent diameter of flow passage outside tubes to tube outside diameter	40
	(d) Ratio of product of heat transfer surface outside tubes and tube outside diameter to tube matrix volume	41
	(e) Ratio of product of heat transfer surface inside tubes and tube inside diameter to tube matrix volume	42
	(f) Ratio of metal volume in tube walls to tube matrix volume	43
9	Various Geometric Parameters for a Square Pitch 1/8-Inch-Tube Bundle as Functions of Spacer Thickness	
	(a) Ratio of flow area outside tubes to tube matrix frontal area	44
	(b) Ratio of flow area inside tubes to tube matrix frontal area	45

List of Illustrations (Continued)

<u>Figure No.</u>	<u>Title</u>	<u>Page No.</u>
	(c) Equivalent diameter of flow passage outside tubes	46
	(d) Ratio of heat transfer surface outside tubes to tube matrix volume	47
	(e) Ratio of heat transfer surface inside tubes to tube matrix volume	48
	(f) Ratio of metal volume in tube walls to tube matrix volume	49
10	Ratio of Number of Tubes to Tube Matrix Frontal Area as a Function of Spacer Thickness	50
11	Reynolds' Number for Various Fluids in Round Tubes	53
12	Dynamic Pressure for Various Fluids as a Function of Velocity	54
13	Friction Factor for Fluid Flow in Smooth Passages as a Function of Reynolds' Number	55
14	Spacer Friction Factor as a Function of Reynolds' Number in the Tube Bundle	56
15	Heat Transfer Coefficient for Liquid Metals in Round Tubes as a Function of Velocity	
	(a) Li	58
	(b) Na	59
	(c) NaK (56% Na - 44% K)	60
	(d) NaK (22% Na - 78% K)	61
	(e) Bi	62
	(f) Pb	63
16	Heat Transfer Coefficient for Sodium Flowing between Plates as a Function of Velocity. Symmetric Heat Addition	64



List of Illustrations (Continued)

<u>Figure No.</u>	<u>Title</u>	<u>Page No.</u>
17	Heat Transfer Coefficient for Fused Salts in Round Tubes	
	(a) NaOH	65
	(b) Flinak	66
18	Heat Transfer Coefficient for Water in Round Tubes. No Boiling	67
19	Performance of 400,000 KW Heat Exchanger	
	(a) Na-NaK. 1/8" tubes	72
	(b) Flinak-NaK. 1/8" tubes	73
	(c) Flinak-NaK. 3/16" tubes	74
	(d) Flinak-NaK. 1/4" tubes	75
	(e) Flinak-H ₂ O. 1/8" tubes	76
	(f) Funak-Na. 1/8" tubes	77
	(g) Funak-Na. 1/4" tubes	78
	(h) Funak-NaK. 1/8" tubes	79
	(i) Funak-NaK. 3/16" tubes	80
	(j) Funak-NaK. 1/4" tubes	81
	(k) H ₂ O - H ₂ O. 1/8" tubes	82


HEAT EXCHANGER DESIGN CHARTSINTRODUCTION

The ORNL-ANP liquid-to-liquid heat exchanger design and development effort has been based on an exceptionally high performance matrix of closely-spaced small diameter tubes that permits practically pure counter-flow operation. In the course of full-scale aircraft power plant design work a number of charts for this type of heat exchanger has been prepared. These charts were intended in part to show the effects of the various parameters in a readily understandable form, and in part to simplify and to reduce markedly the chore of making detailed design calculations. These charts have proved so helpful it seemed very worthwhile to assemble them into a report along with brief explanations and sample calculations.

HEAT EXCHANGER MATRIX GEOMETRY

Perhaps the best introduction to the type of heat exchanger construction that forms the basis for the charts presented in this report is a series of pictures showing the models that have been built.

The first model was constructed of 1/8-inch diameter copper welding rods bent into the form shown in Figure 1. It was designed for air flow tests to determine the fluid pressure drop across the tube spacers and through the cross-flow region at the end where the tubes are bent into the headers. The tube separation of 0.020 inches in both the horizontal and vertical planes was maintained by using flattened wire spacers. As can be seen in Figure 1(a) the horizontal spacers were placed in one plane at right angles to the axis of the tubes, while the vertical spacers were placed in another plane downstream from the first. This arrangement reduced the resistance to fluid flow across the spacers to a tolerable value. The pressure drop through the cross-flow region, where the tubes enter the header, was reduced to a very low value by shifting the ends of every other column to the left and placing the displaced tubes in between the tubes of the neighboring column. The shifting of the ends of alternate columns of tubes can be clearly seen in Figure 1(b), which was taken with the model partially assembled. It is expected that this type of heat exchanger might well be used in a cylindrical annulus surrounding the reactor core and reflector as indicated in the sketch shown in Figure 2.

Dr. George F. Wislicenus suggested that the fabrication of a heat exchanger of this type would be greatly simplified if it could be assembled using a group of tube bundles with each bundle terminating in a circular disc header instead of a large common header sheet. Thus,



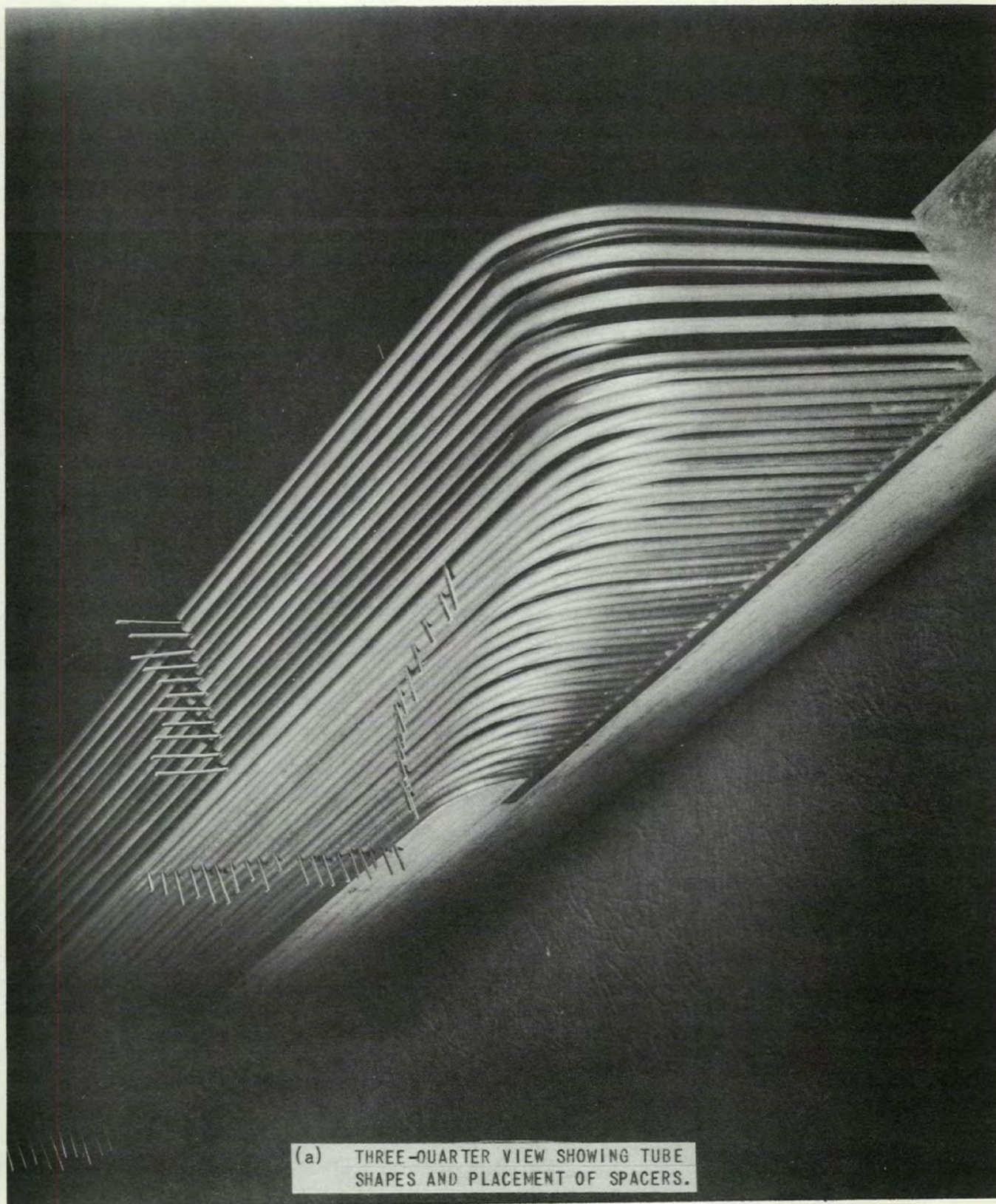
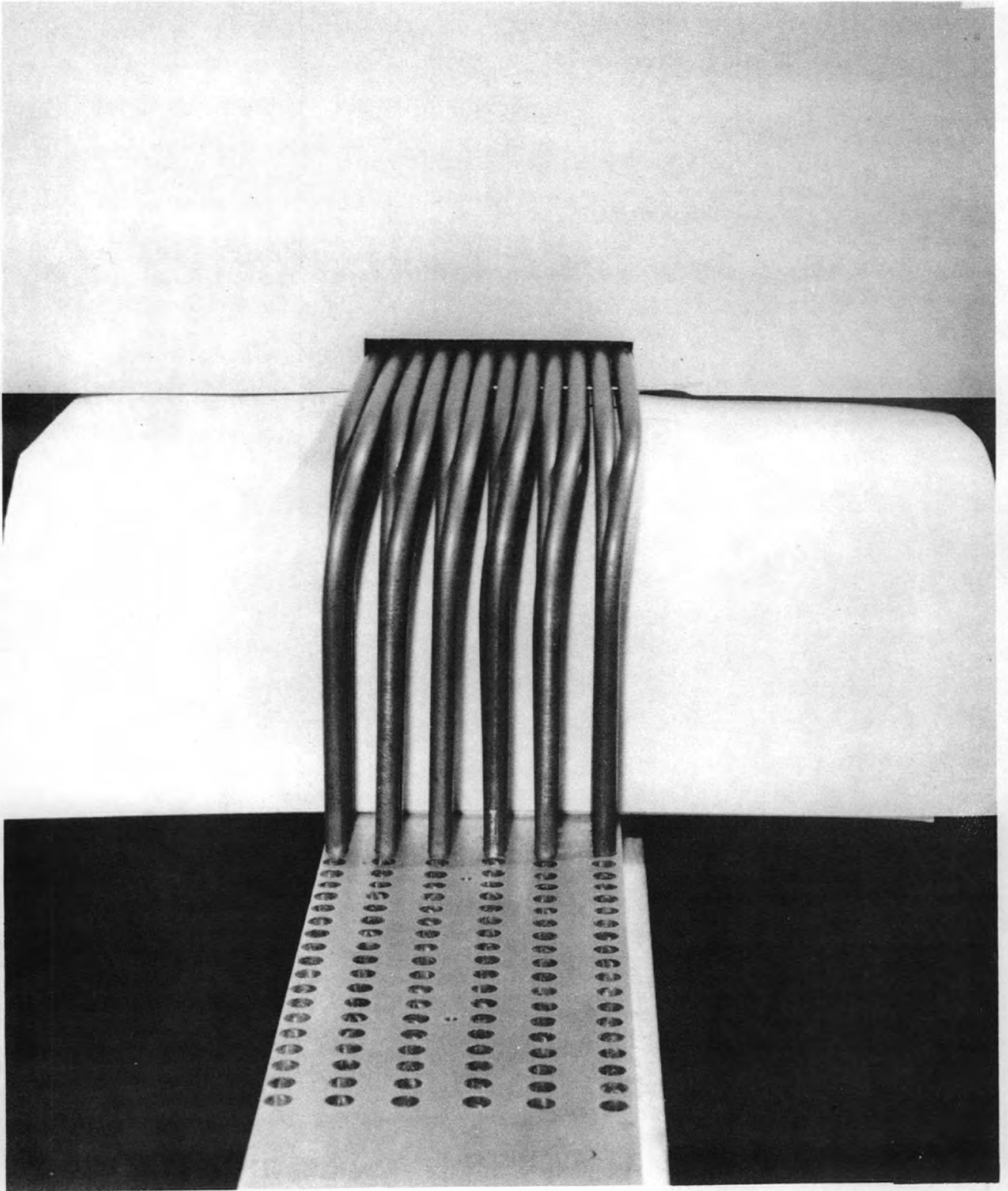


FIGURE 1. FIRST ORNL-ANP HEAT EXCHANGER AIRFLOW MODEL.



(b) END VIEW SHOWING DETAILS OF HEADER PLATE AND TUBE SHAPES.

FIGURE 1, CONCLUDED. FIRST ORNL-ANP HEAT EXCHANGER AIRFLOW MODEL.

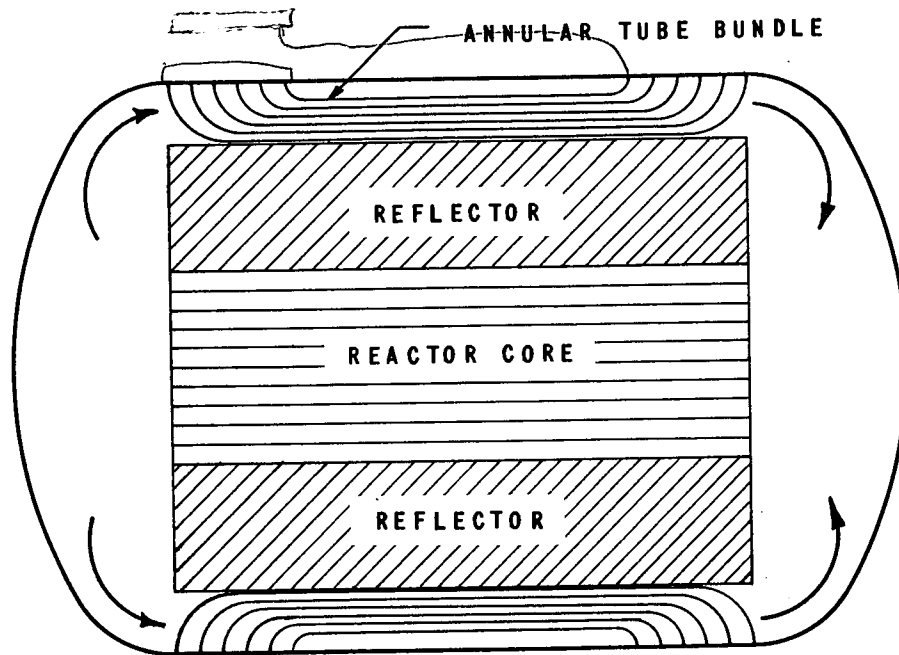


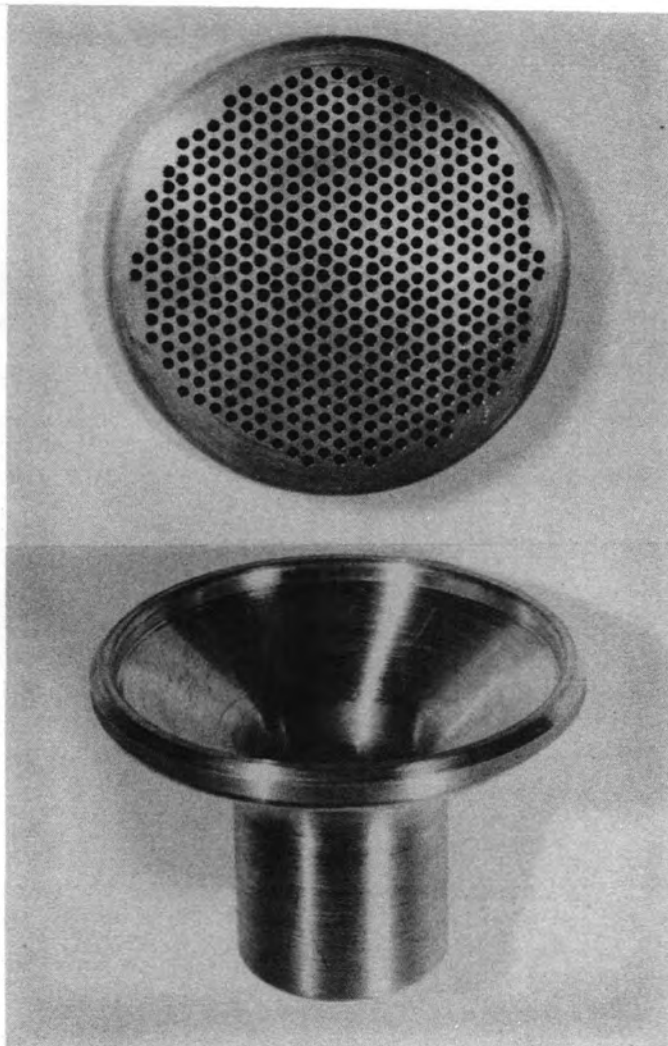
FIGURE NO. 2 - SCHEMATIC LONGITUDINAL CROSS-SECTION THROUGH ANNULAR MODEL OF PROPOSED TYPE OF AIRCRAFT HEAT EXCHANGER.

instead of trying to obtain perhaps 10,000 tube-to-header joints perfect in a single assembly, it would be possible to make use of perhaps 50 sub-assemblies each containing 200 tubes. Each of these could be assembled, welded and/or brazed, inspected, and pressure checked individually. Final assembly could then be made with a single rugged weld between the header disc and the pressure shell. Breaking the header up into a large number of small units has the further advantage that the pipes carrying the secondary circuit fluid through the shield from the intermediate heat exchanger placed close to the reactor are relatively small in diameter, simplifying the problem of allowing for differential thermal expansion. Another salient feature of the multiple-header construction is increased reliability of the external circuit of the reactor. With various components of the power plant connected to separate groups of tube bundles, a leak in any one of the various fluid circuits would have no effect on the others.

Modification of the basic idea is to use a header shaped something like a shower head. Such a header is shown in Figure 3. The "shower head" arrangement has the advantage that it requires a much smaller hole in the pressure shell than a simple circular disc header, hence causing relatively little loss of strength in the header region of the pressure shell. The header, of course, need not be circular but might instead be rectangular in shape in order to utilize the space inside the pressure shell more efficiently.

If circular headers are used, a tabulation of the relation between header size and the greatest number of tubes that can be contained in the header is of value. Such a tabulation is given in Table 1, where the ratio of header diameter to tube spacing for various numbers of tubes on an equilateral triangular pitch is presented. The prime factors of the numbers of tubes are also given for convenience in proportioning the tube bundle where it is rectangular in shape. The column headed "Configuration" identifies the position of the center of the header relative to the hole pattern.

Figure 4 shows the coordinates and tube patterns used in preparing Table 1. The small circles shown represent not the tubes themselves but the loci of points equidistant from the tube surfaces by half the space between tubes. The coordinates of the center of any circle may be expressed as linear functions of the number of tubes per row and the number of rows as shown in Figures 4(b) through 4(e). For any such circle the diameter of the header tangent to the circle may be found easily. If this computation is carried out for a large number of judiciously selected circles and the results are tabulated, the number of circles lying inside a given size of header may be found by inspection. Table 1 was prepared in this fashion for the four locations of header center shown in Figures 4(b) through 4(e).



(a) HEADER COMPONENTS.



(b) HEADER ASSEMBLY.

FIGURE 3. "SHOWER-HEAD" TYPE HEADERS.

Table 1RADII AND NUMBERS OF TUBES FOR CIRCULAR HEADERS

<u>Configuration</u>	<u>Minimum D/S</u>	<u>N</u>	<u>Prime Factors of N</u>
1	1.000	1	1
2	2.000	2	2
3	2.154	3	3
2	2.732	4	2 ²
1	3.000	7	7
2	3.646	8	2 ³
2	4.000	10	2, 5
3	4.056	12	2 ² , 3
1	4.464	13	13
2	4.606	14	2, 7
1	5.000	19	19
2	5.582	22	2, 11
4	5.770	23	23
2	6.000	24	2 ³ , 3
3	6.034	27	3 ³
1	6.292	31	31
1	7.000	37	37
2	7.244	38	2, 19
3	7.430	42	2, 3, 7
4	7.764	44	2 ² , 11
2	8.000	48	2 ⁴ , 3
1	8.212	55	5, 11
2	8.810	56	2 ³ , 7
4	8.858	57	3, 19
2	8.938	60	2 ² , 3, 5
1	9.000	61	61
3	8.082	63	3 ² , 7
2	9.186	64	2 ⁶
3	9.326	69	3, 23
2	9.660	70	2, 5, 7
1	9.718	73	73
2	9.888	74	2, 37
2	10.000	76	2 ² , 19
1	10.166	85	5, 17
2	10.644	88	2 ³ , 11
2	10.848	92	2 ² , 23
4	11.038	96	2 ⁵ , 3
3	11.264	102	2, 3, 17
2	11.536	104	2 ³ , 13
1	11.584	109	109
2	12.000	110	2, 5, 11
3	12.016	114	2 ² , 31
1	12.136	121	11 ²
2	12.532	126	2, 3 ² , 7

Table 1 (Continued)

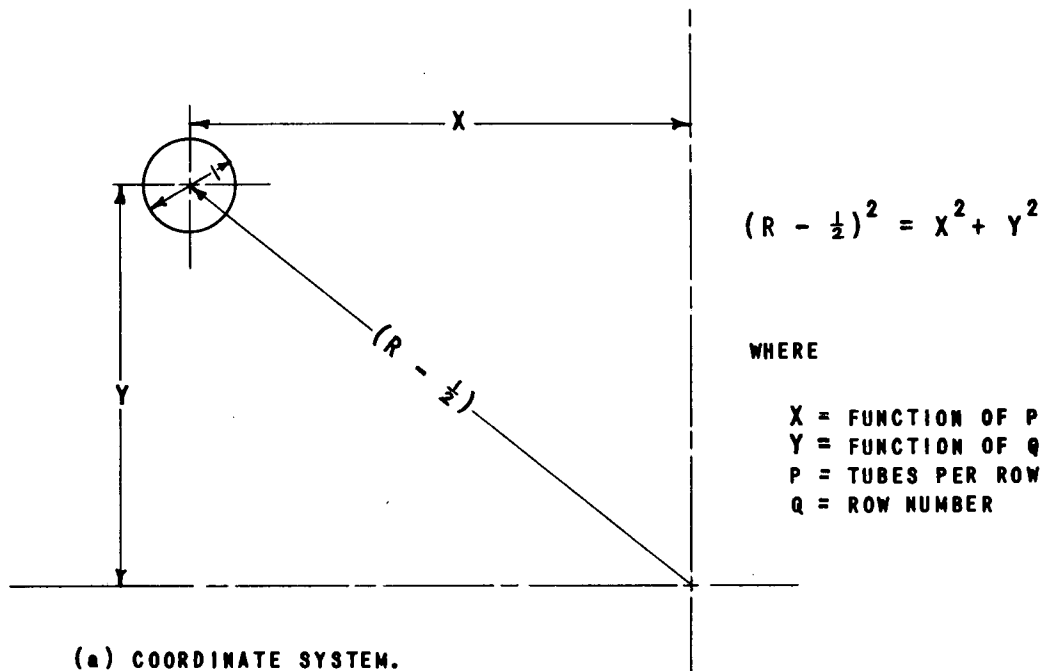
<u>Configuration</u>	<u>Minimum D/S</u>	<u>N</u>	<u>Prime Factors of N</u>
3	12.718	129	3, 43
2	12.790	130	2, 5, 13
4	12.906	131	131
4	12.948	133	7, 19
4	13.032	135	3 ³ , 5
2	13.124	136	2 ³ , 17
1	13.166	139	139
3	13.220	141	3, 47
1	13.490	151	151
2	14.000	154	2, 7, 11
3	14.012	156	2 ² , 3, 13
2	14.076	158	2, 79
1	14.114	163	163
3	14.316	168	2 ³ , 3, 7
2	14.528	170	2, 5, 17
3	14.614	174	2, 3, 29
4	14.812	176	2 ⁴ , 11
2	14.892	178	2, 89
1	15.000	187	11, 17
4	15.344	188	2 ² , 47
4	15.414	190	2, 5, 19
1	15.422	199	199
2	15.798	202	2, 101
2	15.934	206	2, 103
2	16.000	208	2 ⁴ , 13
1	16.100	211	211
2	16.132	212	2 ² , 53
3	16.144	213	3, 71
4	16.256	217	7, 31
3	16.275	219	3, 73
2	16.524	220	2 ² , 5, 11
3	16.534	225	3 ² , 5 ²
2	16.716	230	2, 5, 23
1	16.874	235	5, 47
1	17.000	241	241
3	17.290	246	2, 3, 41
1	17.370	253	11, 23
2	17.644	254	2, 127
2	17.704	258	2, 3, 43
2	17.822	262	2, 131
2	18.000	264	2 ³ , 3, 11
3	18.010	270	2, 3 ³ , 5
4	18.198	274	2, 137
3	18.244	276	2 ² , 3, 23
1	18.436	283	283
2	18.578	284	2 ² , 71
2	18.692	288	2 ⁵ , 3 ²
1	18.776	295	5, 59

Table 1 (Continued)

<u>Configuration</u>	<u>Minimum D/S</u>	<u>N</u>	<u>Prime Factors of N</u>
1	19.000	301	7, 43
3	19.148	306	2, 3 ² , 17
1	19.330	313	313
2	19.520	316	2 ² , 79
3	19.584	321	3, 107
2	19.736	324	2 ² , 3 ⁴
4	19.862	325	5 ² , 13
3	19.904	327	3, 109
4	19.994	329	7, 47
2	20.000	330	2, 3, 5, 11
3	20.008	333	3 ² , 37
1	20.078	337	337
3	20.218	339	3, 113
1	20.288	349	349
4	20.640	351	3 ³ , 13
2	20.672	352	2 ⁵ , 11
1	20.698	361	19 ²
4	20.944	362	2, 181
2	20.974	364	2 ² , 7, 13
1	21.000	367	367
2	21.074	372	2 ² , 3, 31
2	21.224	376	2 ³ , 47
3	21.232	378	2, 3 ³ , 7
1	21.298	379	379
4	21.366	380	2 ² , 5, 19
4	21.390	382	2, 191
3	21.428	384	2 ⁷ , 3
3	21.526	390	2, 3, 5, 13
2	21.664	392	2 ³ , 7 ²
4	21.802	394	2, 197
2	21.808	396	2 ² , 3 ² , 11
1	21.880	397	397
2	21.952	400	2 ⁴ , 5 ²
2	22.00	406	2, 7, 29
1	22.072	409	409
1	22.166	421	421
3	22.572	426	2, 3, 71
1	22.634	433	433
2	22.794	434	2, 7, 31
4	22.858	437	19, 23
2	22.932	442	2, 13, 17
3	23.030	447	3, 149
2	23.114	450	2, 3 ² , 5 ²
3	23.120	453	3, 151
4	23.288	455	5, 7, 13
3	23.300	459	3 ³ , 17

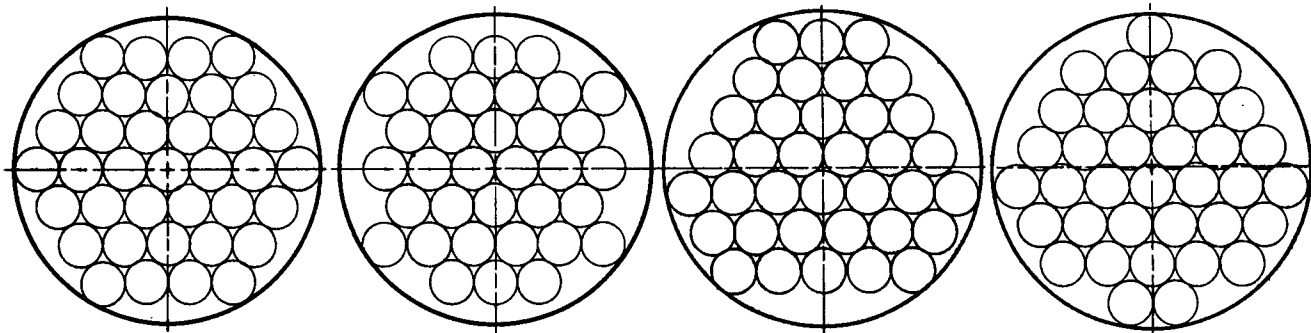
Table 1 (Continued)

<u>Configuration</u>	<u>Minimum D/S</u>	<u>N</u>	<u>Prime Factors of N</u>
4	23.422	461	461
4	23.466	463	463
3	23.480	465	3, 5, 31
2	23.606	468	2 ² , 3 ² , 13
2	23.650	472	23, 59
1	23.716	475	5 ² , 19
2	23.870	476	2 ² , 7, 17
2	23.914	480	2 ⁵ , 3, 5
2	24.000	482	2, 241
4	24.060	483	3, 7, 23
1	24.066	499	499
3	24.438	504	2 ³ , 3 ² , 7
2	24.516	506	2, 11, 23
1	24.580	511	7, 73
2	24.644	514	2, 257
2	24.812	518	2, 7, 37
4	24.848	520	2 ³ , 5, 13
3	24.860	522	2, 3 ² , 29
4	24.974	524	2 ² , 131
4	25.016	526	2, 263
3	25.028	528	2 ⁴ , 3, 11
2	25.062	530	2, 5, 53
3	25.110	534	2 ³ , 17
3	25.194	540	2 ² , 3 ³ , 5
1	25.332	547	547
2	25.556	550	2, 5 ² , 11
1	25.576	559	13, 43
2	25.880	562	2, 281
4	25.934	564	2 ² , 3, 47



$Y_U = Y$ IN UPPER SEMICIRCLE
 $Y_L = Y$ IN LOWER SEMICIRCLE

X	$\frac{1}{2}(P - 1)$	$\frac{1}{2}(P - 1)$	$\frac{1}{2}(P - 1)$	$\frac{1}{2}(P - 1)$
Y_U	$\frac{\sqrt{3}}{2}(Q - 1)$	$\frac{\sqrt{3}}{2}(Q - 1)$	$\frac{\sqrt{3}}{6}(3Q - 2)$	$\frac{\sqrt{3}}{4}(2Q - 1)$
Y_L	"	"	$\frac{\sqrt{3}}{6}(3Q - 1)$	"



(b) CONFIGURATION 1. (c) CONFIGURATION 2. (d) CONFIGURATION 3. (e) CONFIGURATION 4.

FIGURE 4. CIRCULAR HEADER TUBE HOLE PATTERNS.

The following two problems illustrate the use of Table 1:

Sample problem No. 1

For a header diameter D of 4" and a tube center-to-center spacing S of .30" find the maximum number of tubes insertable on an equilateral triangular pitch.

- 1) $D/S = 4/.3 = 13.33$
- 2) The nearest tabulated entries are 13.220 and 13.538. Select the smaller value. The number of tubes is found to be 141 and the configuration is that shown in Figure 4(d).

Sample problem No. 2

What is the header diameter for 200 tubes on a .250" spacing?

- 1) The nearest tabulated entries are for 199 and 202 tubes. Select the larger value and omit two tubes from the pattern. The configuration is shown in Figure 4(c).
- 2) The tabulated $D/S = 15.798$

$$D = (.250)(15.798) = 3.95"$$

While the application of this type of heat exchanger to an annular arrangement in a right circular cylinder as suggested in Figure 2 is relatively straightforward, its application to a heat exchanger in the form of a spherical shell may be rather difficult to grasp at first. Figures 5 through 7 have been prepared with the intention of alleviating this difficulty.

Figure 5 shows a cross-section through a reactor and intermediate heat exchanger combination that appears to offer many interesting possibilities. The primary fluid can be circulated down through the reactor and then upward through the space between the reflector and the pressure shell. This return passage can be filled with tube bundles terminating in "shower head" type headers of the sort shown in Figure 3. A model of a heat exchanger of this type is shown in Figure 6. While the tube bundle shape is quite unusual, fabrication of the heat exchanger ought not be too difficult. After jigs had been prepared for building up a tube bundle, one bundle after another could be assembled, brazed and/or welded into its headers, pressure tested, inspected, and assembled into the spherical steel shell. A simple fillet weld between the header and the pressure shell would suffice to complete the installation.

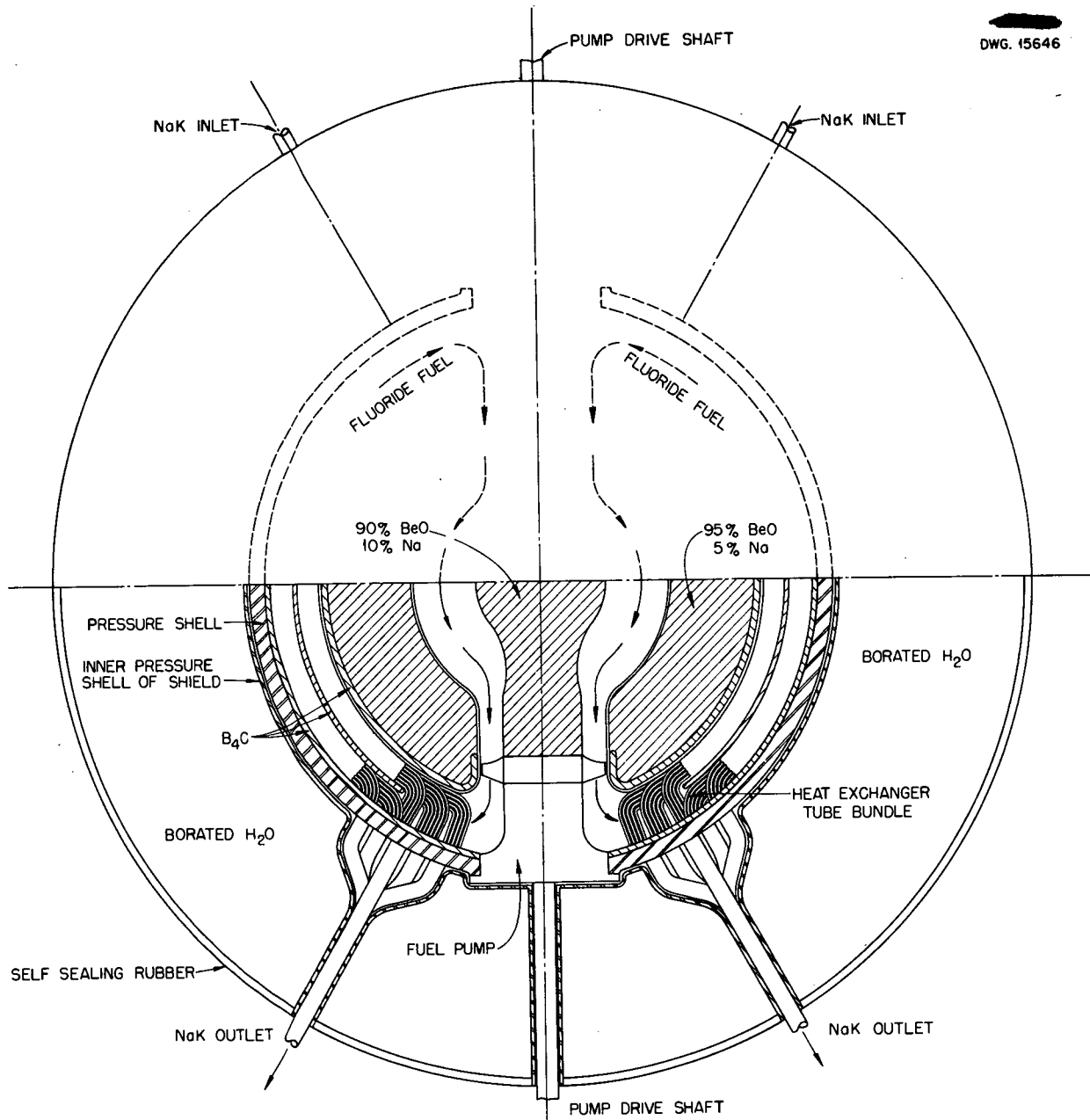


FIGURE 5 CROSS-SECTION THROUGH A REACTOR AND SPHERICAL SHELL INTERMEDIATE HEAT EXCHANGER ARRANGEMENT.

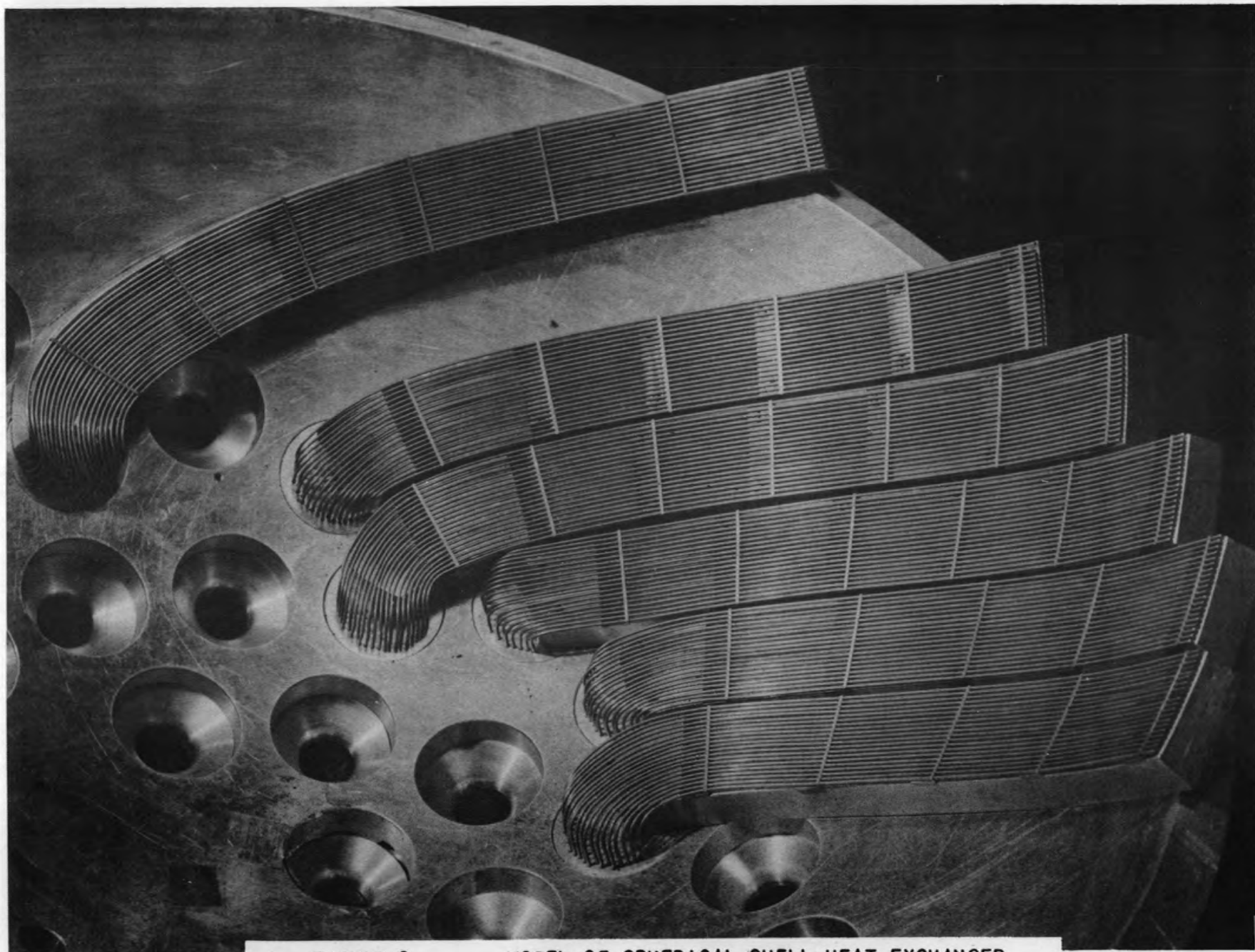


FIGURE 6. MODEL OF SPHERICAL SHELL HEAT EXCHANGER.

Although the spherical shell type of heat exchanger appears to be geometrically complicated, it has many advantages. The problem of differential thermal expansion between the tubes and the pressure shell in a conventional tube-and-shell heat exchanger is a very serious one in units designed for high temperature operation; however, in the spherical arrangement expansion of the tubes relative to the pressure shell simply results in a slight warping of the tubes from their original paths but no particular trouble should be experienced. A second and perhaps the most important feature is the major shield weight reduction possible with this design, largely because of its extreme compactness.

By analogy with the coordinate system used on the earth's surface, the pump shafts in Figure 5 may be considered to lie along the polar axis of the sphere. The points at which the shafts penetrate the sphere then represent the north and south poles and the equator lies midway between them on the sphere's surface. The latitude of any point on the surface is then the angular distance from the equatorial plane measured along a great circle passing through the poles. The longitude of that point is the angular distance from some reference great circle measured at constant latitude. Figure 7(a), which shows the coordinate system used, illustrates these points.

In order to obtain efficient use of the space inside the spherical shell the tube bundles must follow some path other than, say, the lines of longitude. The desirable path is one in which the tube center-to-center spacing is independent of latitude. This spacing can be obtained if the tubes follow a certain variable pitch helix from one header to the other.

Detailed design work on this geometry, while of a relatively complex nature, is greatly simplified through the use of Table 2 and the charts presented in Figure 7. Table 2 gives volumes and weights of spheres and spherical shells having a specific gravity equal to one. Figure 7(a) illustrates the coordinate system used for the spherical shell heat exchanger and defines the various terms such as the longitude angle α , the latitude angle θ , the tube inclination angle ϕ , tube spacing S , and sphere radius R . Tube inclination angle and longitude angle are given as functions of latitude angle in Figures 7(b) and 7(c), respectively. The ratio of the exchanger shell thickness to the diameter of the sphere on which it is wrapped is given in Figure 7(d) as a function of the required heat exchanger volume and the two terminal latitude angles. Finally, Figure 7(e) presents the ratio of tube length to sphere diameter as a function of latitude angle.

These charts were constructed from the following geometrical considerations:

Tube Inclination Angle

At any latitude θ , N heat exchanger tubes cross the latitude circle

at an angle ϕ . Tube spacing S is measured perpendicular to the tubes so that

$$\sin \phi = \frac{SN}{2\pi R \cos \theta}$$

At $\theta = 0$,

$$\begin{aligned} \sin \phi &= \frac{SN}{2\pi R} \\ &= \sin \phi_0 \end{aligned}$$

giving

$$\sin \phi = \frac{\sin \phi_0}{\cos \theta} \quad (1)$$

or

$$\phi = \sin^{-1} \frac{\sin \phi_0}{\cos \theta} \quad (2)$$

Figure 7(b) is plotted from equation (2).

Tube Longitude Angle

From Figure 7(a),

$$\frac{Rd\theta}{rd\alpha} = \tan \phi$$

and

$$r = R \cos \theta$$

giving

$$\frac{d\alpha}{d\theta} = \frac{\cos \phi}{\sin \phi \cos \theta} \quad (3)$$

From equation (1),

$$\sin \phi = \frac{\sin \phi_0}{\cos \theta} \quad (4)$$

Also,

$$\cos \phi = \sqrt{1 - \sin^2 \phi} \quad (5)$$

Substituting in equation (3) from equations (4) and (5) then gives

$$\begin{aligned} \frac{d\alpha}{d\theta} &= \frac{1}{\cos \theta} \sqrt{\frac{\cos^2 \theta}{\sin^2 \phi_0} - 1} \\ &= \sqrt{\csc^2 \phi_0 - \sec^2 \theta} \end{aligned}$$

The longitude angle is then given by

$$\alpha = \int_0^{\theta} \sqrt{\csc^2 \phi_0 - \sec^2 x} \, dx \quad (6)$$

Equation (6) is presented in graphical form in Figure 7(c).

Shell-Thickness to Sphere-Diameter Ratio

The volume of a hemisphere = $\frac{2}{3} \pi r^3$, where r is the radius of the hemisphere; the volume of a spherical sector = $\frac{2}{3} \pi r^3 (1 - \sin \theta)$, where θ is the latitude angle. Hence, the volume of a spherical shell from equator to latitude θ_1 is given by

$$V_1 = \frac{2\pi \sin \theta_1}{3} (r_0^3 - r_1^3)$$

where r_0 and r_1 are the outer and inner radii, respectively, of the shell.

$$r_0 = r_1 + t$$

where t is the thickness of the shell, so that

$$V_1 = \frac{2\pi \sin \theta_1}{3} (3 r_1^2 t + 3 r_1 t^2 + t^3)$$

or

$$\frac{V_1}{\frac{2\pi r_1^3}{3}} = \left[3\left(\frac{t}{r_1}\right) + 3\left(\frac{t}{r_1}\right)^2 + \frac{t}{r_1} \right]^3 \sin \theta_1$$

$$= 2 \frac{V_1}{V_1}$$

where

$$V_1 = \frac{4\pi}{3} r_1^3$$

= volume of inner sphere.

Similarly,

$$2 \frac{V_2}{V_1} = \left[3 \frac{t}{r_1} + 3\left(\frac{t}{r_1}\right)^2 + \left(\frac{t}{r_1}\right)^3 \right] \sin \theta_2$$

where θ_2 = latitude on the opposite side of the equator from θ_1 .

The total shell volume $V = V_1 + V_2$

so that

$$2 \frac{V}{V_1} = \left[3 \frac{t}{r_1} + 3\left(\frac{t}{r_1}\right)^2 + \left(\frac{t}{r_1}\right)^3 \right] (\sin \theta_1 + \sin \theta_2)$$

or

$$\frac{V}{V_1} = \left[3 \frac{t}{d_1} + 6\left(\frac{t}{d_1}\right)^2 + 4\left(\frac{t}{d_1}\right)^3 \right] (\sin \theta_1 + \sin \theta_2) \quad (7)$$

Equation (7) is plotted in Figure 7(d).

Tube Length

From Figure 7(a),

$$\frac{Rd\theta}{dL} = \sin \phi$$

From equation (1),

$$\sin \phi = \frac{\sin \phi_0}{\cos \theta}$$

so that

$$\frac{1}{R} \frac{dL}{d\theta} = \frac{\cos \theta}{\sin \phi_0}$$

and

$$\begin{aligned} \frac{L}{R} &= \frac{1}{\sin \phi_0} \int_0^\theta \cos x \, dx \\ &= \frac{\sin \theta}{\sin \phi_0} \end{aligned}$$

or

$$\frac{L}{D} = \frac{\sin \theta}{2 \sin \phi_0} \quad (8)$$

where

$$D = 2R$$

Equation (8) is presented graphically in Figure 7(e).

A sample problem to illustrate the use of Figure 7 is given below:

Sample problem No. 3

A spherical heat exchanger geometry is specified as follows:

- a) The tubes run from forty degrees south latitude to fifty degrees north latitude;
- b) the equatorial crossing angle for all tubes is forty degrees.
- c) The shell has an inside diameter of 48 inches;
- d) The required heat exchanger volume is 13.4 cubic feet.

Find:

- 1) Tube inclination angles at ends of a tube bundle;
- 2) longitude angles at ends of a tube bundle;
- 3) heat exchanger thickness;
- 4) length of tubes closest to and farthest from the pressure shell.

Sample problem No. 3 (Continued)

Solution:

- 1) Use Figure 8(b) with $\phi_0 = 40^\circ$. For $\theta = 40^\circ$, $\phi = 57^\circ$.
For $\theta = 50^\circ$, $\phi = 90^\circ$.
- 2) Use Figure 7(c) with $\phi_0 = 40^\circ$. For $\theta = 40^\circ$, $\alpha = 44^\circ$.
For $\theta = 50^\circ$, $\alpha = 50^\circ$. These two values of α are, of course, oppositely directed, i.e., whichever one is east of the point at which the tube crosses the sphere's equator, the other is west.
- 3) From Table 2 for a diameter of 48 inches, $V_1 = 33.51 \text{ ft}^3$. Then $V/V_1 = 13.4/33.51 = .40$. Figure 7(d) gives, for $\theta_1 = 40^\circ$, $\theta_2 = 50^\circ$, and $V/V_1 = .40$, $T/D_1 = .083$. Then, thickness of shell = $(.083)(48) = 4$ inches.
- 4) Use Figure 7(e) with $\phi_0 = 40^\circ$. For $\theta = 40^\circ$, $L/D = .50$.
For $\theta = 50^\circ$, $L/D = .59$. Then over-all $L/D = .50 + .59 = 1.09$. Minimum $D = 48$ inches. Maximum $D = 48 + (2)(4) = 56$ inches. Then the length of the tube farthest from the pressure shell = $(1.09)(48) = 52.3$ inches; while the length of the tube closest to the pressure shell = $(1.09)(56) = 61.0$ inches.

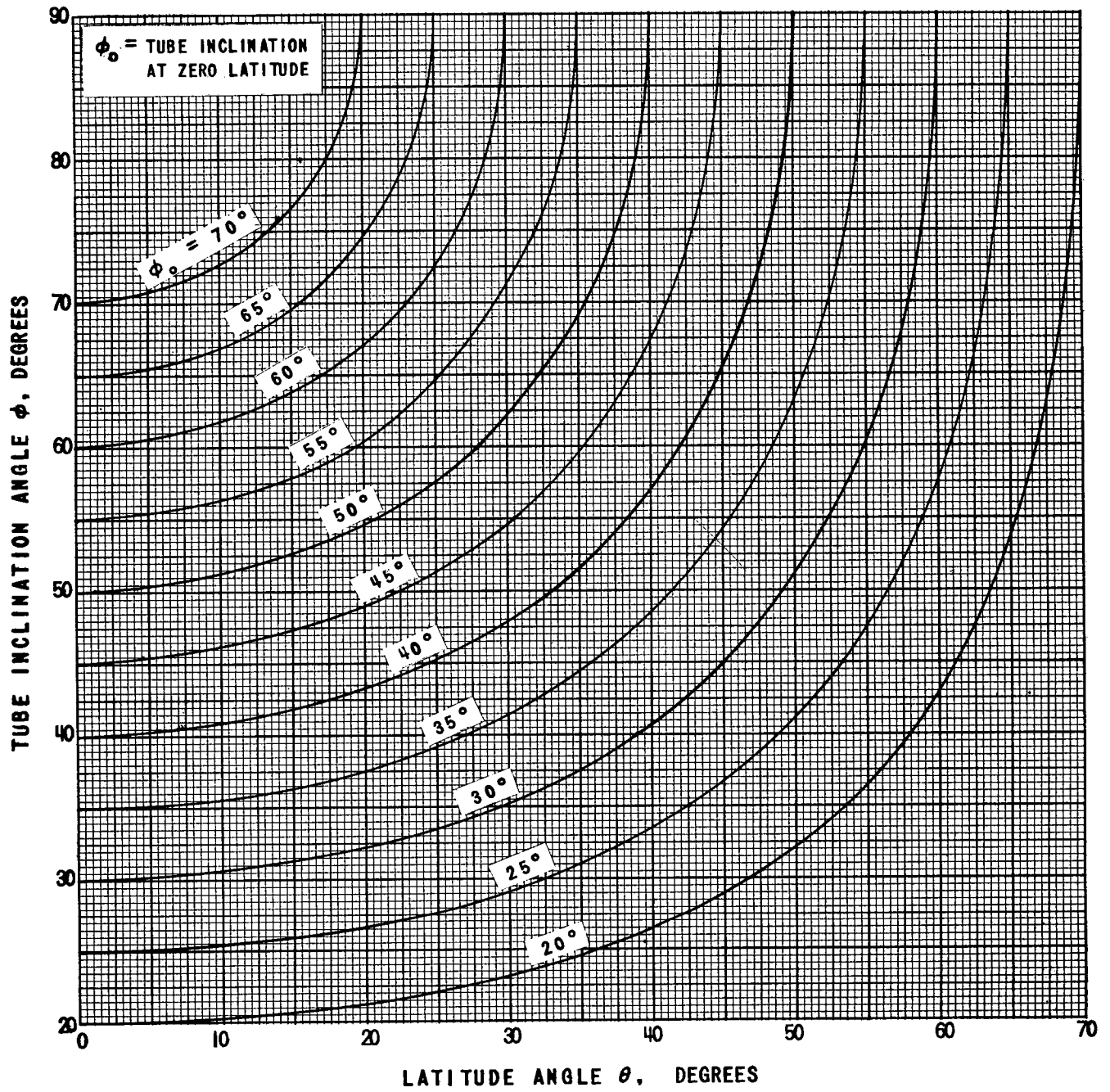
These lengths do not include the curved portions forming the cross-flow regions at the ends where the tubes are bent to enter the headers. In this case if the bend radius were 1" for tubes closest to the pressure shell it would be 5" for the tubes farthest away. For a 90° bend, the length of tube along the arc is roughly 1.5 times the radius. Thus, the total length of the tube closest to the pressure shell becomes $61.0 + (2)(1)(1.5) = 64$ inches, while the total length of the tube farthest from the pressure shell becomes $52.3 + (2)(5)(1.5) = 67.3$ inches.

TABLE 2

VOLUMES AND WEIGHTS OF SPHERES AND SPHERICAL SHELLS

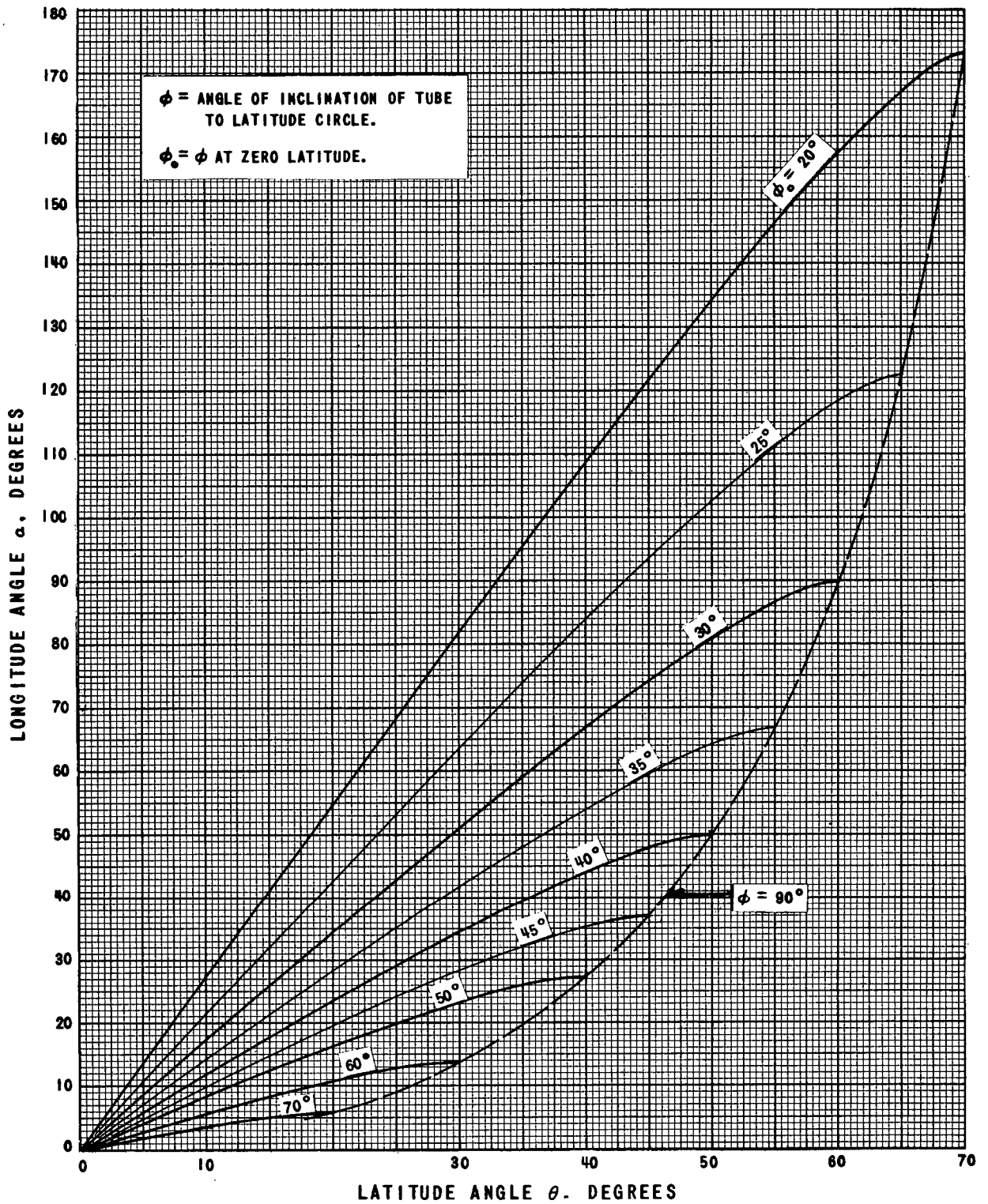
Size			Sphere		Spherical Shell 1" Thick	
Outer Dia. In.	Outer Radius In. Cm.		Volume Ft ³	H ₂ O Wt. Lb.	Volume Ft ³	H ₂ O Wt. Lb.
10	5	12.70	.303	18.9	.147	9.22
12	6	15.24	.523	32.6	.220	13.76
14	7	17.78	.831	51.8	.307	19.20
16	8	20.32	1.241	77.4	.409	25.56
18	9	22.86	1.767	110.2	.526	32.82
20	10	25.40	2.424	151.2	.657	40.99
22	11	27.94	3.226	201.3	.802	50.06
24	12	30.48	4.188	261.3	.962	60.05
26	13	33.02	5.325	332.3	1.136	70.94
28	14	35.56	6.651	415.0	1.325	82.72
30	15	38.10	8.181	510.5	1.529	95.44
32	16	40.64	9.929	619.5	1.747	109.0
34	17	43.18	11.90	743.1	1.980	123.5
36	18	45.72	14.13	882.1	2.227	139.0
38	19	48.26	16.62	1037	2.489	155.3
40	20	50.80	19.39	1210	2.765	172.5
42	21	53.34	22.44	1400	3.056	190.7
44	22	55.88	25.81	1610	3.362	209.8
46	23	58.42	29.49	1840	3.682	229.7
48	24	60.96	33.51	2091	4.016	250.6
50	25	63.50	37.87	2363	4.365	272.4
52	26	66.04	42.60	2658	4.729	295.1
54	27	68.58	47.71	2977	5.107	318.7
56	28	71.12	53.21	3320	5.500	343.2
58	29	73.66	59.12	3689	5.907	368.6
60	30	76.20	65.44	4084	6.329	394.9
62	31	78.74	72.21	4506	6.765	422.1
64	32	81.28	79.43	4956	7.216	450.3
66	33	83.82	87.11	5435	7.681	479.3
68	34	86.36	95.27	5945	8.161	509.2
70	35	88.90	103.9	6485	8.656	540.1
72	36	91.44	113.0	7057	9.165	571.8
74	37	93.98	122.7	7661	9.689	604.5
76	38	96.52	133.0	8300	10.22	638.1
78	39	99.06	143.7	8972	10.78	672.6
80	40	101.6	155.1	9680	11.34	708.0
82	41	104.1	167.0	10425	11.92	744.3
84	42	106.6	179.5	11206	12.52	781.5
86	43	109.2	192.7	12026	13.13	819.6
88	44	111.7	206.4	12885	13.76	858.7
90	45	114.3	220.8	13783	14.40	898.6

Size			Sphere		Spherical Shell 1" Thick	
Outer Dia. In.	Outer Radius In.	Cm.	Volume Ft ³	H ₂ O Wt. Lb.	Volume Ft ³	H ₂ O Wt. Lb.
92	46	116.8	235.9	14723	15.05	939.4
94	47	119.3	251.6	15704	15.72	981.2
96	48	121.9	268.0	16728	16.40	1023
98	49	124.4	285.1	17795	17.10	1067
100	50	127.0	303.0	18907	17.81	1111
102	51	129.5	321.5	20065	18.54	1157
104	52	132.0	340.8	21268	19.28	1203
106	53	134.6	360.8	22519	20.04	1250
108	54	137.1	381.7	23818	20.81	1298
110	55	139.7	403.3	25166	21.60	1347
112	56	142.2	425.7	26564	22.40	1397
114	57	144.7	448.9	28012	23.21	1448
116	58	147.3	472.9	29513	24.04	1500
118	59	149.8	497.8	31066	24.88	1553
120	60	152.4	523.5	32672	25.74	1606
122	61	154.9	550.2	34333	26.61	1661
124	62	157.4	577.7	36049	27.50	1716
126	63	160.0	606.1	37822	28.40	1772
128	64	162.5	635.4	39652	29.32	1829
130	65	165.1	665.7	41540	30.25	1887
132	66	167.6	696.9	43487	31.20	1946
134	67	170.1	729.0	45493	32.16	2006
136	68	172.7	762.2	47561	33.13	2067
138	69	175.2	796.3	49690	34.12	2129
140	70	177.8	831.4	51882	35.12	2191
142	71	180.3	867.6	54138	36.14	2255
144	72	182.8	904.7	56458	37.17	2319
146	73	185.4	943.0	58843	38.22	2385
148	74	187.9	982.2	61294	39.28	2451
150	75	190.5	1022	63813	40.36	2518



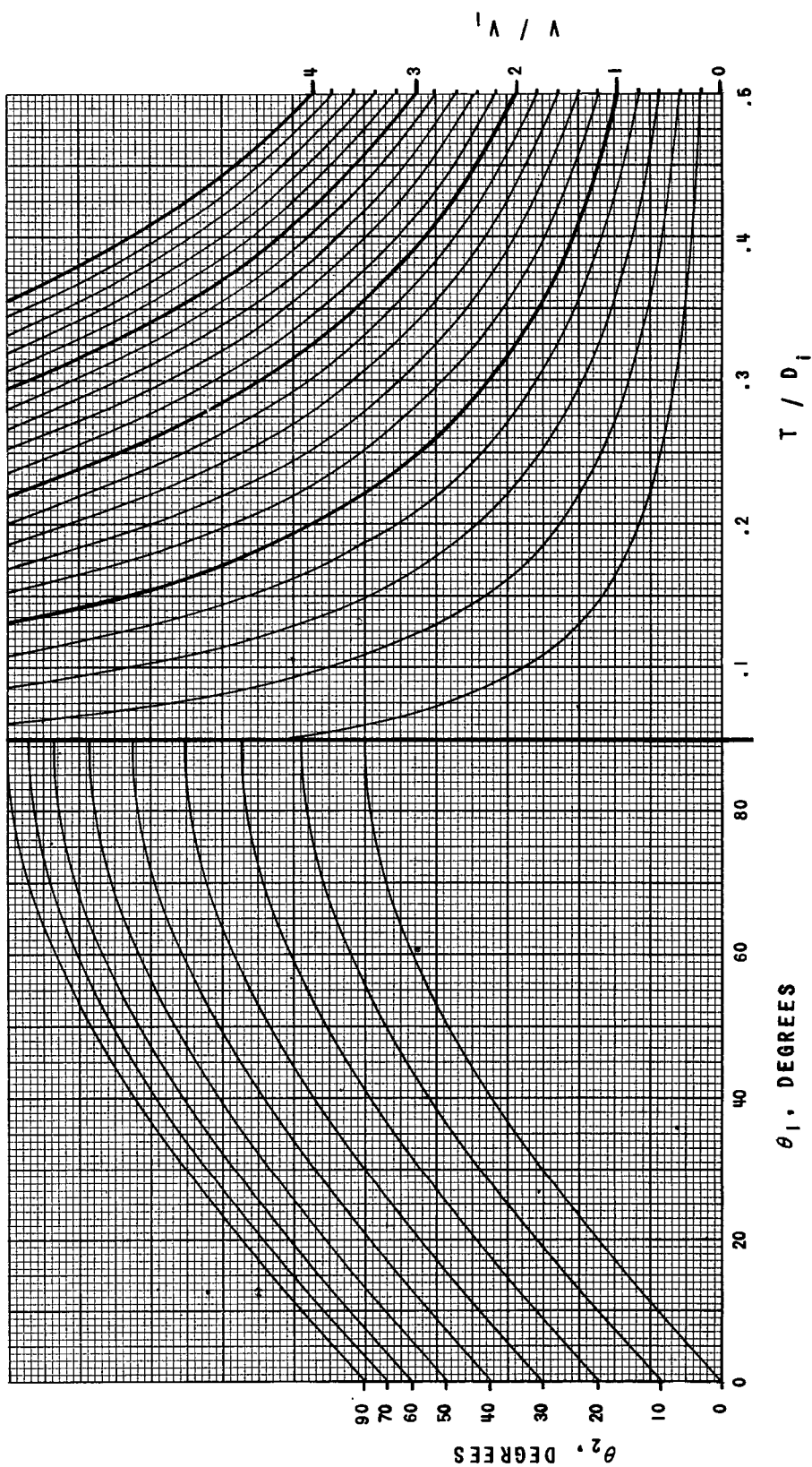
(b) TUBE INCLINATION ANGLE AS A FUNCTION OF LATITUDE ANGLE.

FIGURE 7. SPHERICAL SHELL HEAT EXCHANGER GEOMETRY.



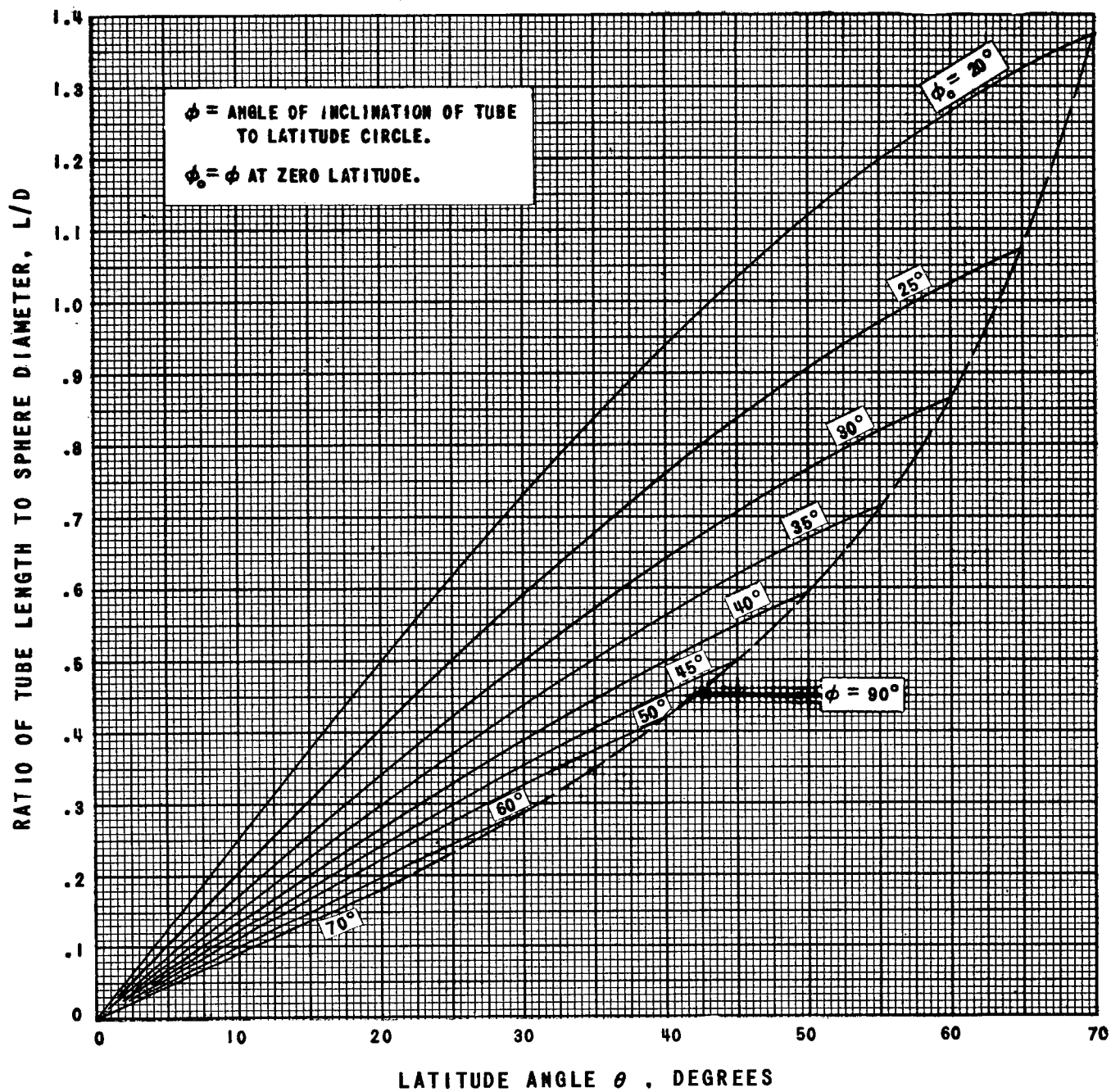
(c) TUBE LONGITUDE ANGLE AS A FUNCTION OF LATITUDE ANGLE.

FIGURE 7. SPHERICAL SHELL HEAT EXCHANGER GEOMETRY.



(d) SHELL THICKNESS TO SPHERE DIAMETER RATIO AS A FUNCTION OF SHELL VOLUME TO SPHERE VOLUME RATIO AND TERMINAL LATITUDE ANGLES.

FIGURE 7. SPHERICAL SHELL HEAT EXCHANGER GEOMETRY.



(e) TUBE LENGTH TO SPHERE DIAMETER RATIO AS A FUNCTION OF LATITUDE ANGLE.

FIGURE 7. SPHERICAL SHELL HEAT EXCHANGER GEOMETRY.

In the preparation of detailed designs for tube bundles for either spherical or cylindrical annulus types of heat exchangers, the calculation of flow passage areas, heat transfer surface areas, number of tubes, etc., as functions of spacer thickness and tube diameters proves to be rather time consuming. The charts in Figures 8, 9, and 10 should considerably simplify such calculations. Figure 8 presents various geometric parameters in dimensionless form; any consistent set of units is therefore directly applicable. Figure 9 presents these parameters for a specific size of tube; here most of the parameters are dimensional so that conversion is necessary if different units are desired. Figure 10 gives the number of tubes per square foot as a function of spacer thickness for various tube diameters.

Sample problems utilizing Figures 8, 9, and 10 are presented below.

Sample problem No. 4 (Figure 8)

Suppose the heat exchanger of the previous example to be made up from rectangular tube bundles, each bundle containing 200 tubes on a square pitch in a 20 x 10 array. If tube outside diameter $D_o = 3/16"$, wall thickness $T_w = .020"$, spacer thickness $T_s = .032"$, find for a tube bundle:

- 1) Flow area outside tubes A_o ;
- 2) Flow area inside tubes A_i ;
- 3) Equivalent diameter of flow passage outside tubes D_e ;
- 4) Heat transfer surface outside tubes S_o ;
- 5) Heat transfer surface inside tubes S_i ;
- 6) Volume of metal in tube walls V_w .

Solution:

$$1) \quad T_s/D_o = .171 \quad A_f = [(20)(.188 + .032)][(10)(.188 + .032)] \\ = 9.68 \text{ in}^2.$$

Figure 8(a) gives $A_o/A_f = .429$.

$$A_o = (9.68) (.429) = 4.15 \text{ in}^2.$$

- 2) $T_w/D_o = .107$. An interpolation in Figure 8(b) gives

$$A_i/A_f = .355.$$

$$A_i = (9.68) (.355) = 3.44 \text{ in}^2.$$

- 3) From Figure 8(c), $D_e/D_o = .74$. $D_e = (.74)(.188) = .139"$.

(Note; n on Figure is number of tubes in bundle.)

Sample problem No. 4 (Figure 8) (Continued)Solution:

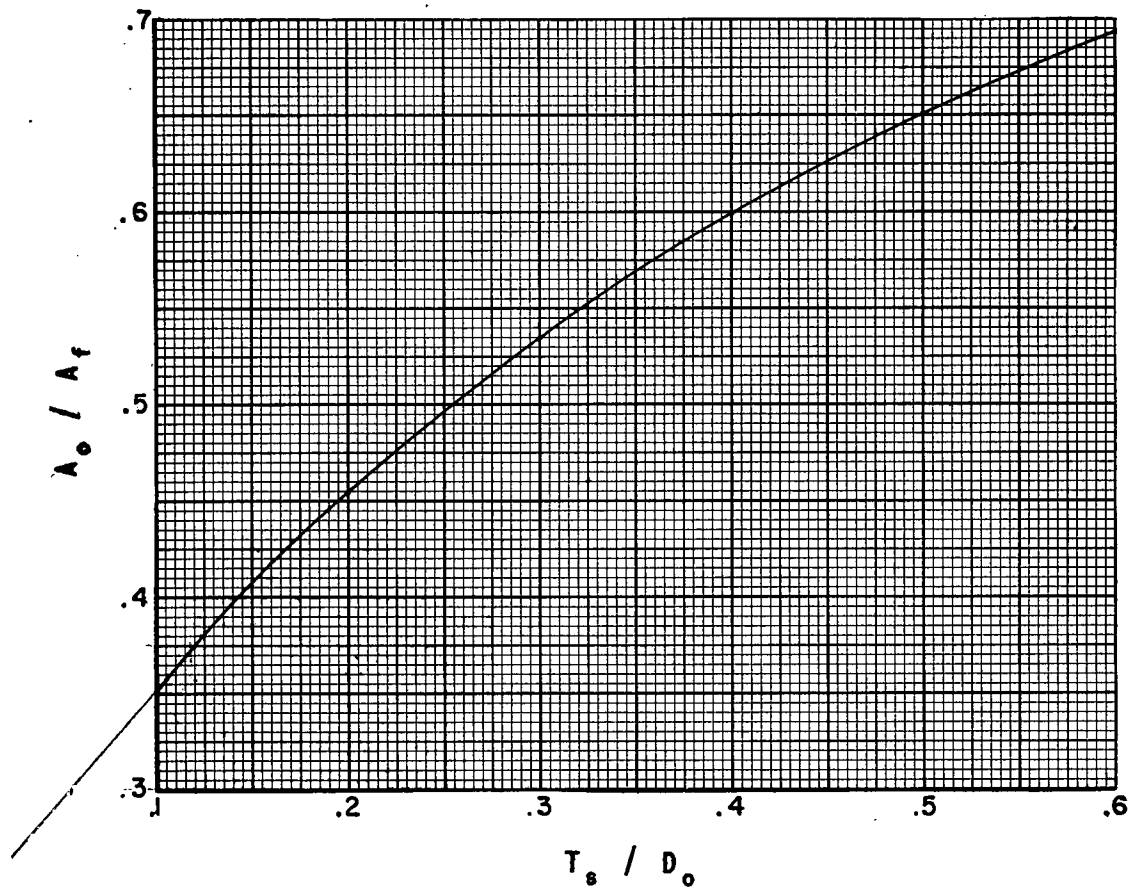
- 4) From the previous example, mean length of tube = $1/2 (52.3 + 61.0) = 56.65$ ". Then matrix volume $V_m = (56.65) (9.68) = 548 \text{ in}^3$. Figure 8(d) gives $S_o D_o / V_m = 2.30$. $S_o = (2.30) (548) / .188 = 6720 \text{ in}^2$.
- 5) From Figure 8(e), $S_i D_i / V_m = 1.41$, $S_i = (1.41) (548) / .188 = 4120 \text{ in}^2$.
- 6) From Figure 8(f), $V_w / V_m = .238$, $V_w = (.238) (548) = 130.5 \text{ in}^3$.

Sample problem No. 5 (Figures 9 and 10)

If the tube bundle in Problem 3 is changed to $1/8$ " tubes with wall thickness = $.020$ " and spacer thickness = $.020$ ", find A_o , A_i , D_e , S_o , S_i , and V_w . Find, also, the number of tubes per square foot of matrix frontal area.

Solution:

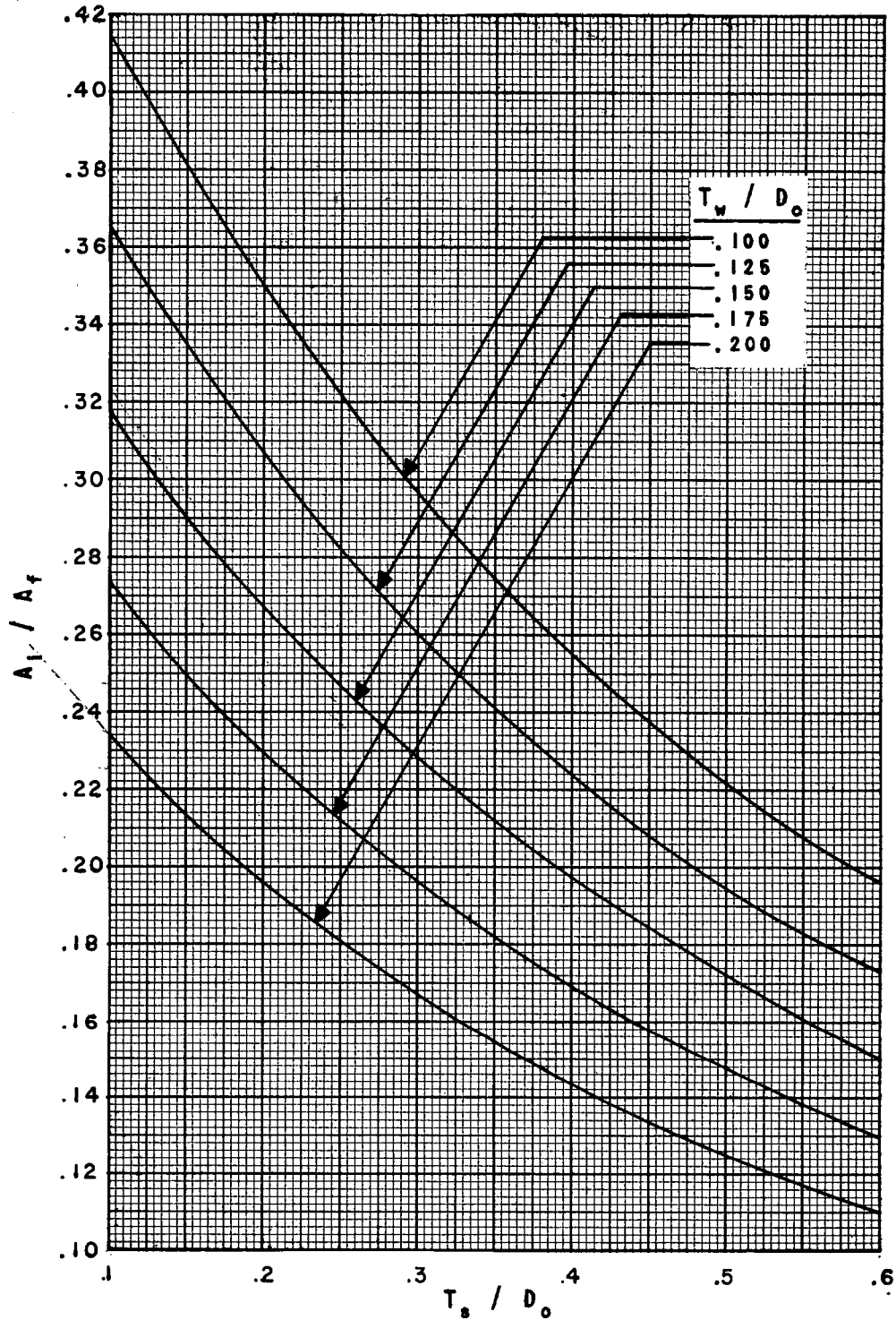
- 1) $A_f = [(20)(.125 + .020)] [(10)(.125 + .020)] = 4.2 \text{ in}^2$
 From Figure 9(a), $A_o / A_f = .417$, $A_o = (4.2)(.417) = 1.75 \text{ in}^2$
- 2) Figure 9(b) gives $A_i / A_f = .271$, $A_i = (4.2)(.271) = 1.14 \text{ in}^2$
- 3) Figure 9(c) gives $D_e = .0074 \text{ ft} = .089 \text{ in}$.
- 4) $V_m = (4.2)(56.65) = 238 \text{ in}^3$. From Figure 9(d),
 $S_o / V = 224 \text{ ft}^{-1} = 18.67 \text{ in}^{-1}$, $S_o = (238)(18.67) = 4440 \text{ in}^2$
- 5) Figure 9(e) gives $S_i / V_m = 152 \text{ ft}^{-1} = 12.67 \text{ in}^{-1}$, $S_i = (238) (12.67) = 3015 \text{ in}^2$
- 6) From Figure 9(f), $V_w / V_m = .3125$ $V_w = 74.4 \text{ in}^3$
- 7) The number of tubes per square foot may be computed from the above information or it may be determined directly from Figure 10. For a spacer thickness of $.020$ " and a tube diameter of $1/8$ ", Figure 10 gives $N / A_f = 6860 \text{ tubes/ft}^2$.



(a) RATIO OF FLOW AREA OUTSIDE TUBES TO TUBE MATRIX
FRONTAL AREA.

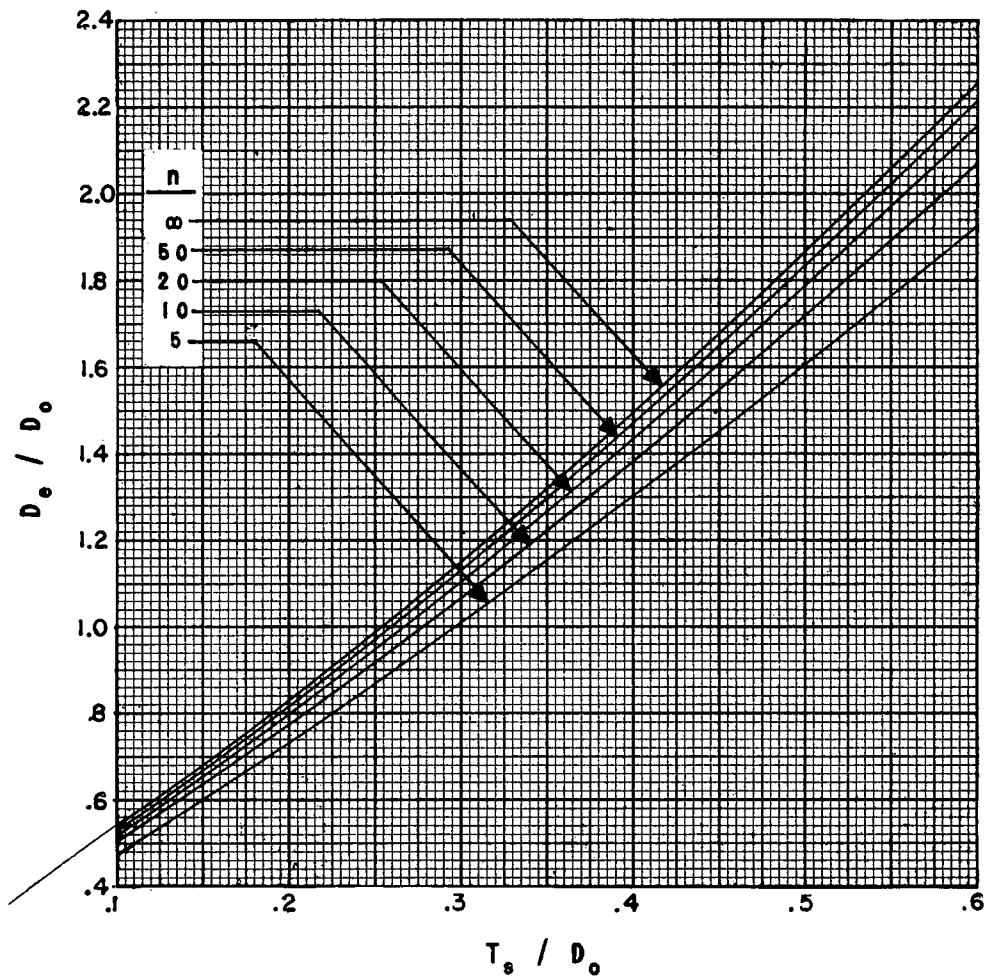
FIGURE 8.

VARIOUS GEOMETRIC PARAMETERS FOR A SQUARE PITCH TUBE
BUNDLE AS FUNCTIONS OF RATIO OF SPACER THICKNESS TO
TUBE OUTSIDE DIAMETER.



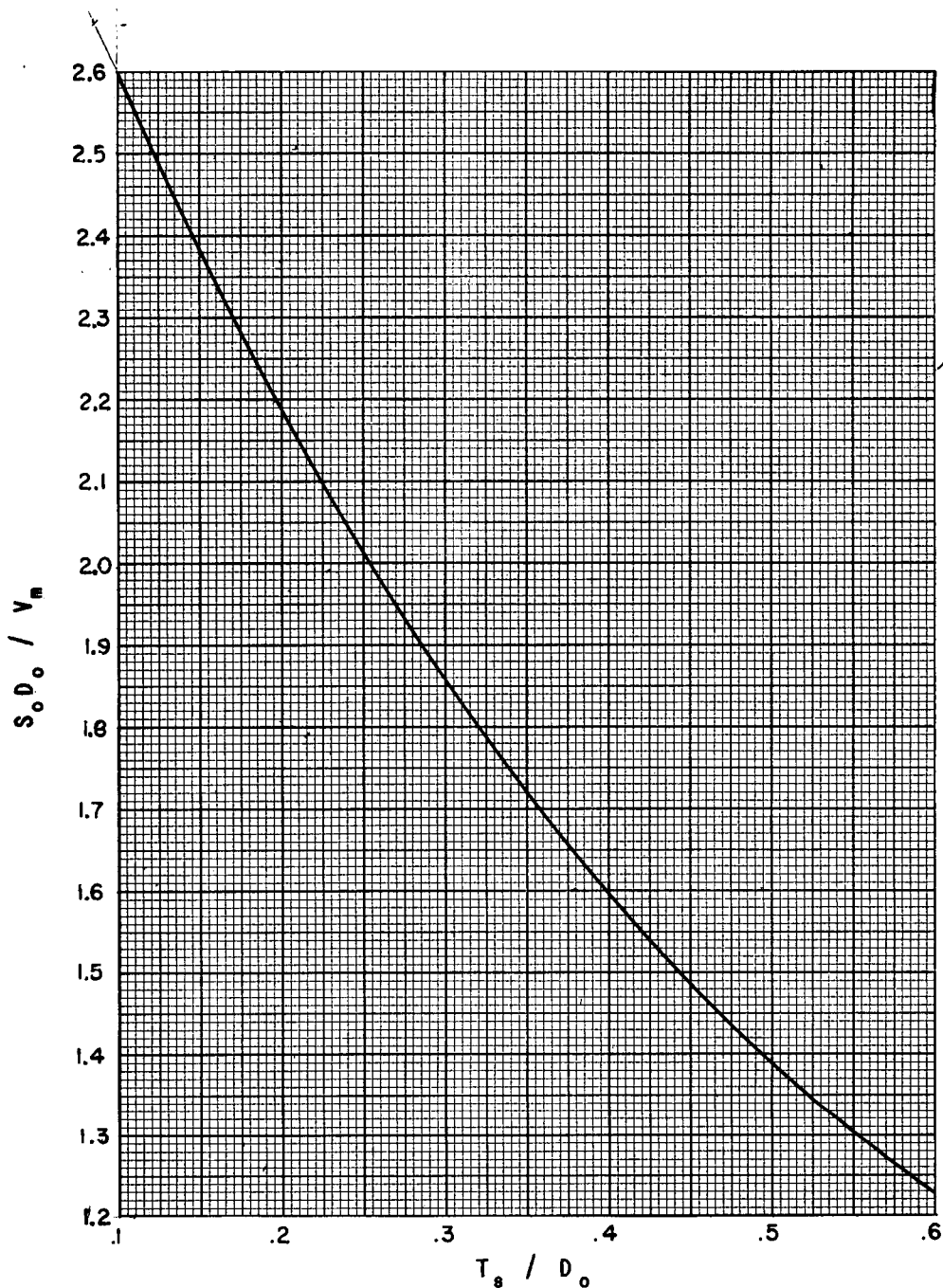
(b) RATIO OF FLOW AREA INSIDE TUBES TO TUBE MATRIX FRONTAL AREA.

FIGURE 8. CONTINUED. VARIOUS GEOMETRIC PARAMETERS FOR A SQUARE PITCH TUBE BUNDLE AS FUNCTIONS OF RATIO OF SPACER THICKNESS TO TUBE OUTSIDE DIAMETER.



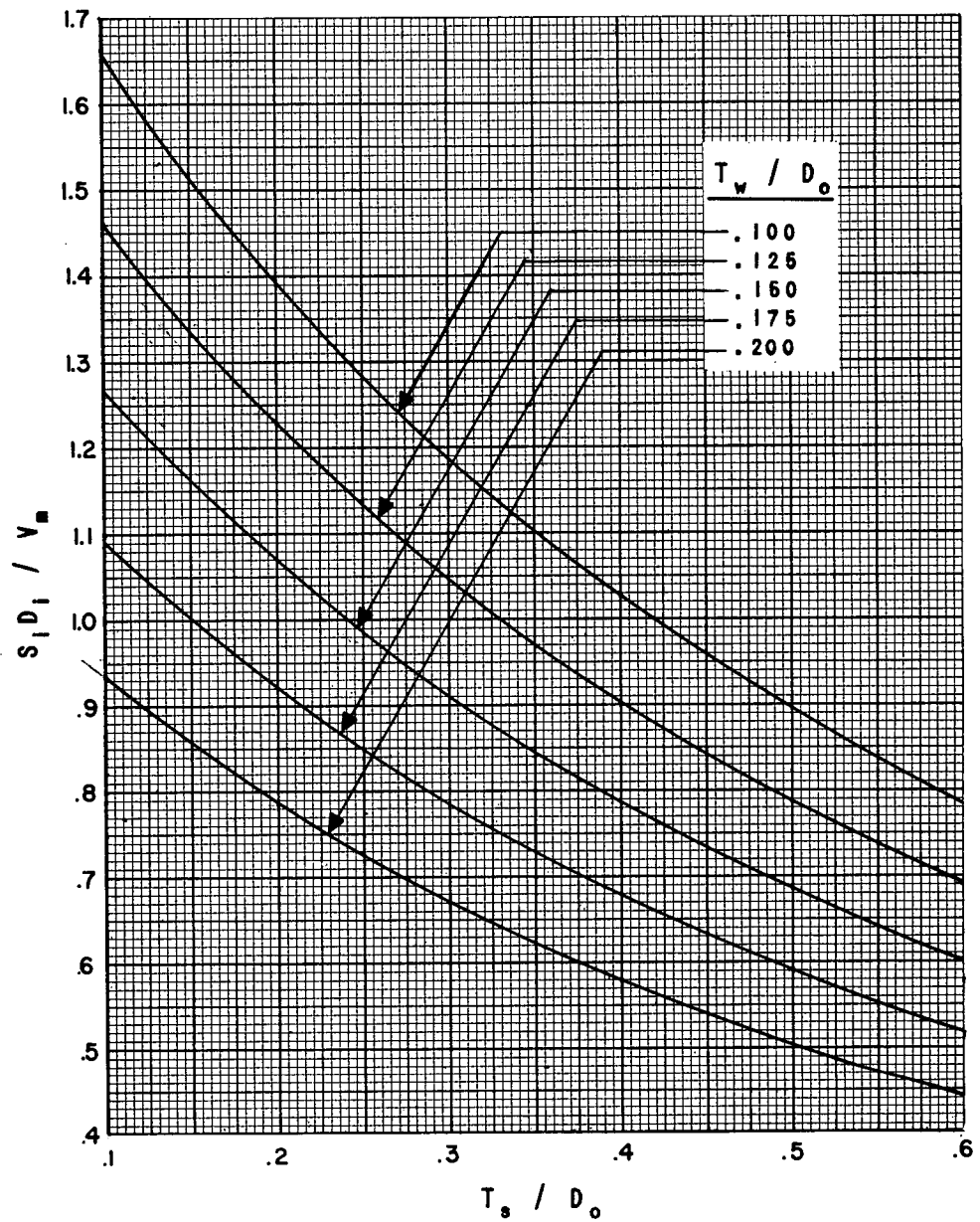
(c) RATIO OF EQUIVALENT DIAMETER OF FLOW PASSAGE OUTSIDE TUBES TO TUBE OUTSIDE DIAMETER.

FIGURE 8. CONTINUED. VARIOUS GEOMETRIC PARAMETERS FOR A SQUARE PITCH TUBE BUNDLE AS FUNCTIONS OF RATIO OF SPACER THICKNESS TO TUBE OUTSIDE DIAMETER.



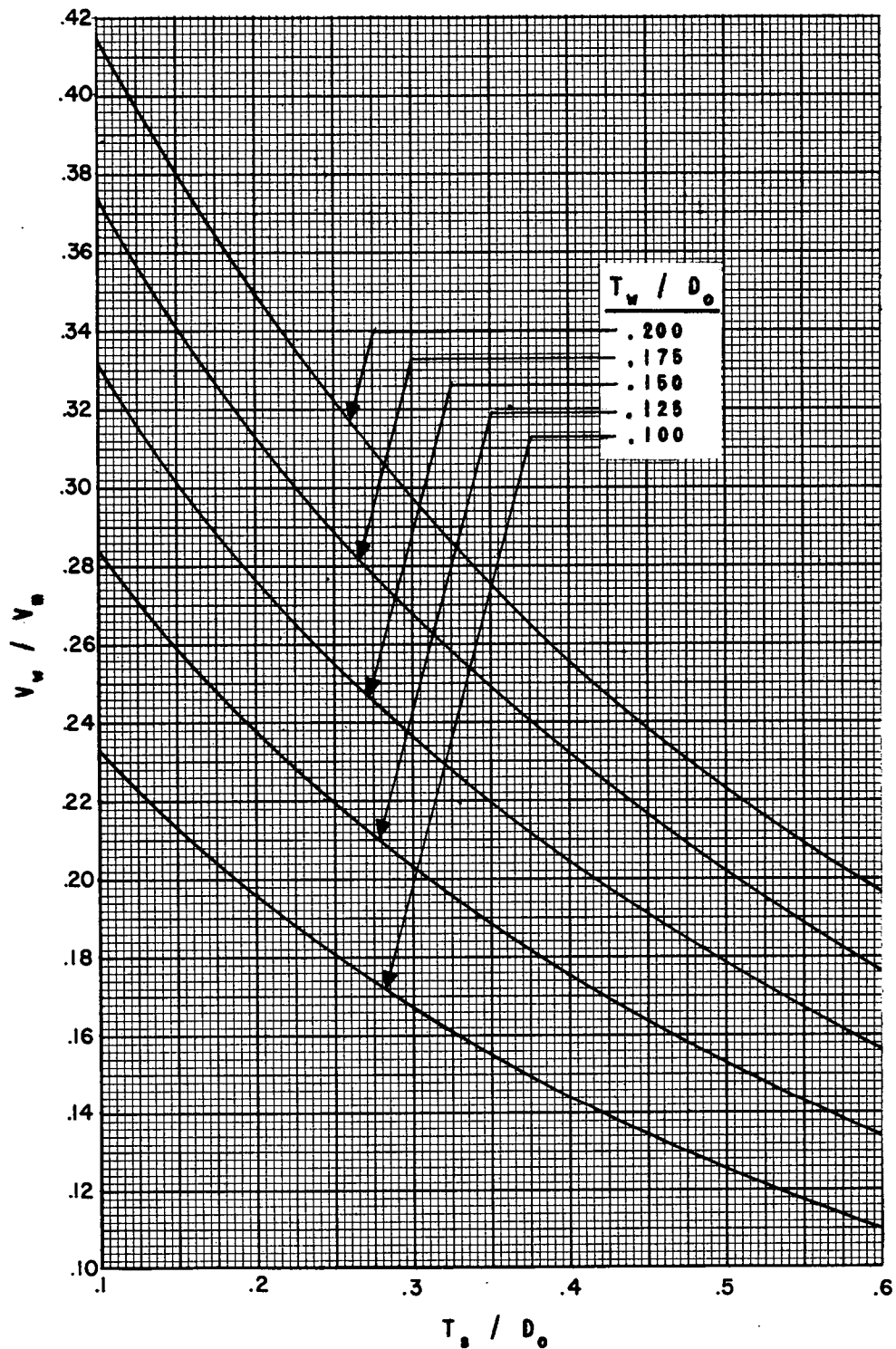
(d) RATIO OF PRODUCT OF HEAT TRANSFER SURFACE OUTSIDE TUBES AND TUBE OUTSIDE DIAMETER TO TUBE MATRIX VOLUME.

FIGURE 8. CONTINUED. VARIOUS GEOMETRIC PARAMETERS FOR A SQUARE PITCH TUBE BUNDLE AS FUNCTIONS OF RATIO OF SPACER THICKNESS TO TUBE OUTSIDE DIAMETER.



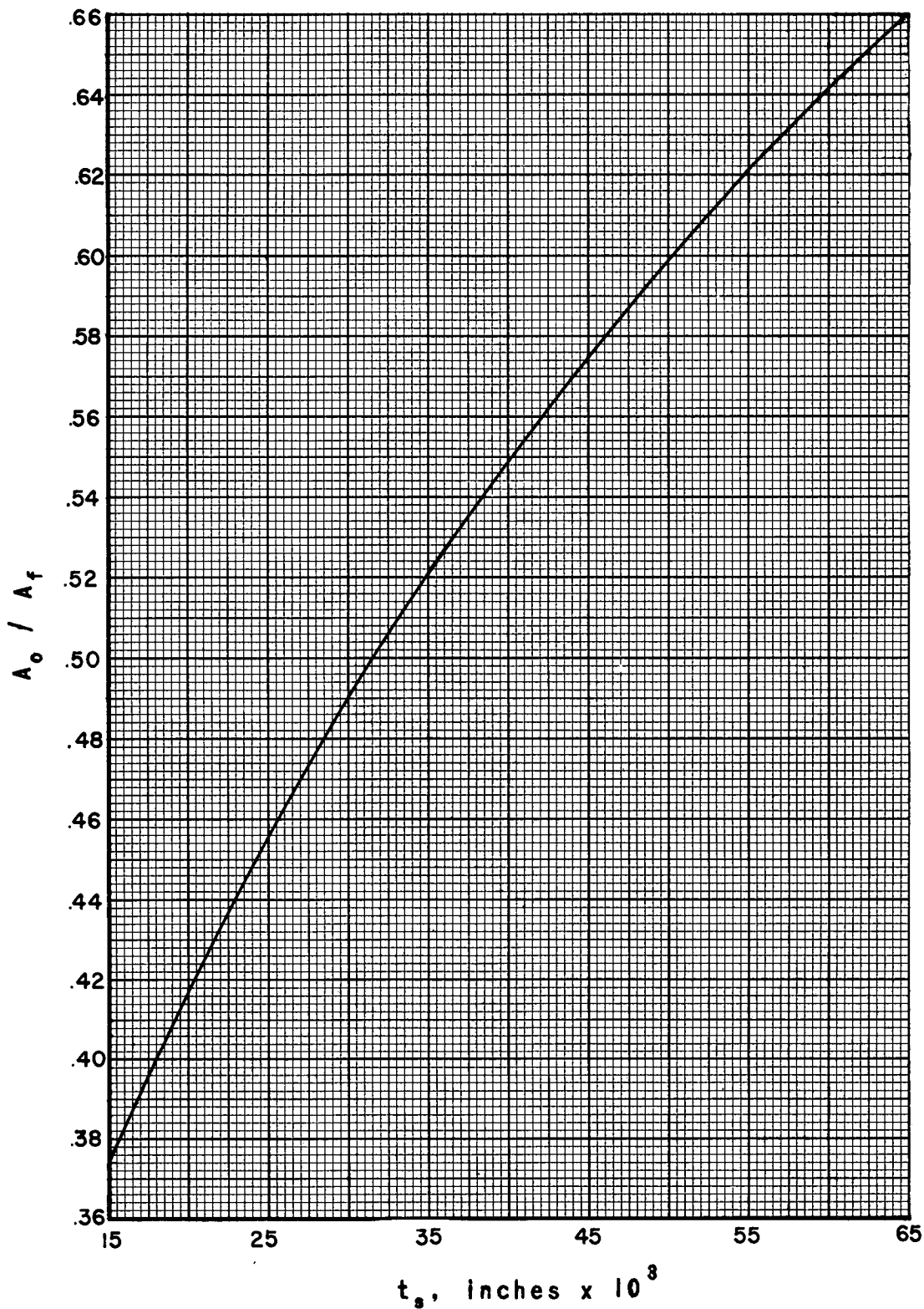
(e) RATIO OF PRODUCT OF HEAT TRANSFER SURFACE INSIDE TUBES AND TUBE INSIDE DIAMETER TO TUBE MATRIX VOLUME.

FIGURE 8. CONTINUED. VARIOUS GEOMETRIC PARAMETERS FOR A SQUARE PITCH TUBE BUNDLE AS FUNCTIONS OF RATIO OF SPACER THICKNESS TO TUBE OUTSIDE DIAMETER



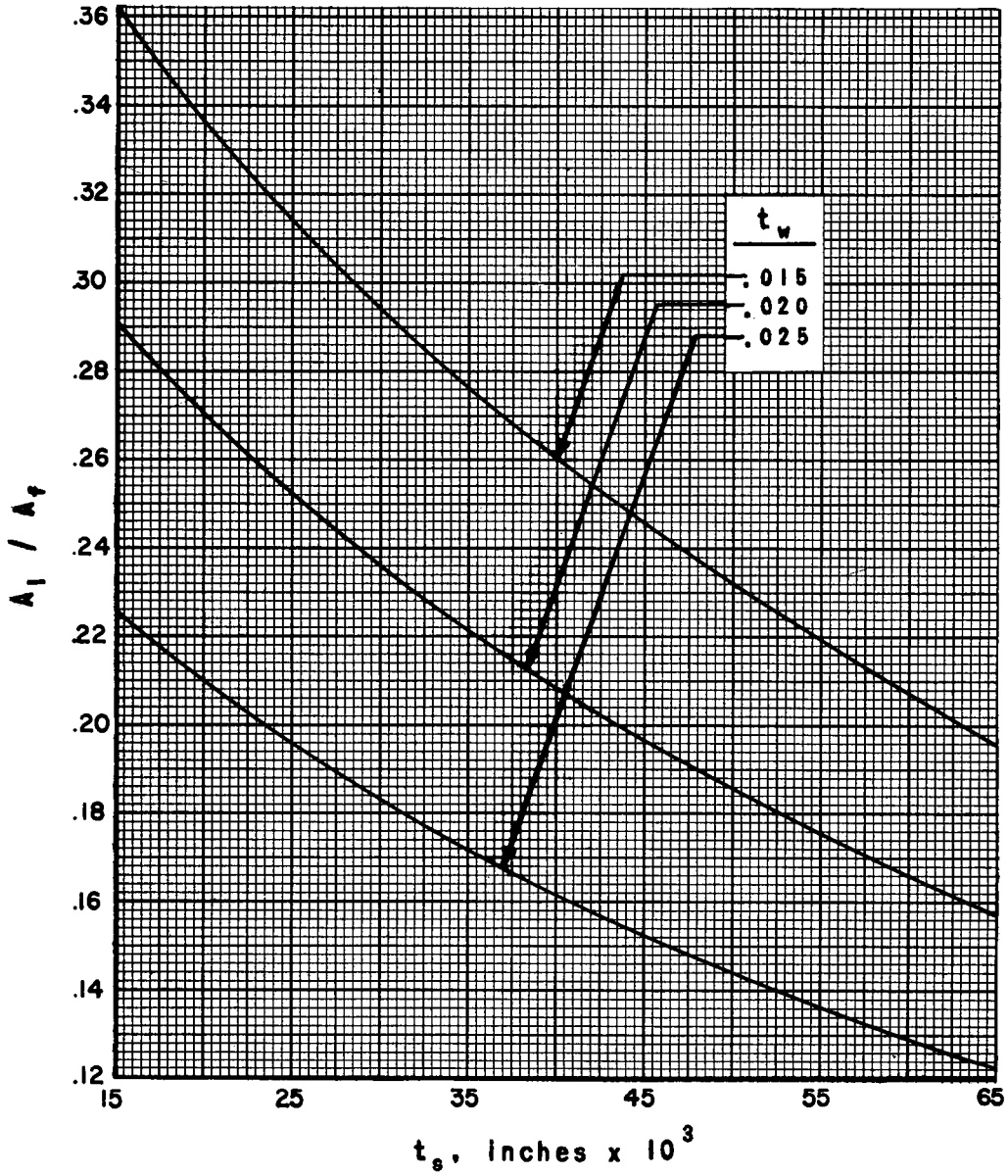
(f) RATIO OF METAL VOLUME IN TUBE WALLS TO TUBE MATRIX VOLUME.

FIGURE 8. CONCLUDED. VARIOUS GEOMETRIC PARAMETERS FOR A SQUARE PITCH TUBE BUNDLE AS FUNCTIONS OF RATIO OF SPACER THICKNESS TO TUBE OUTSIDE DIAMETER.



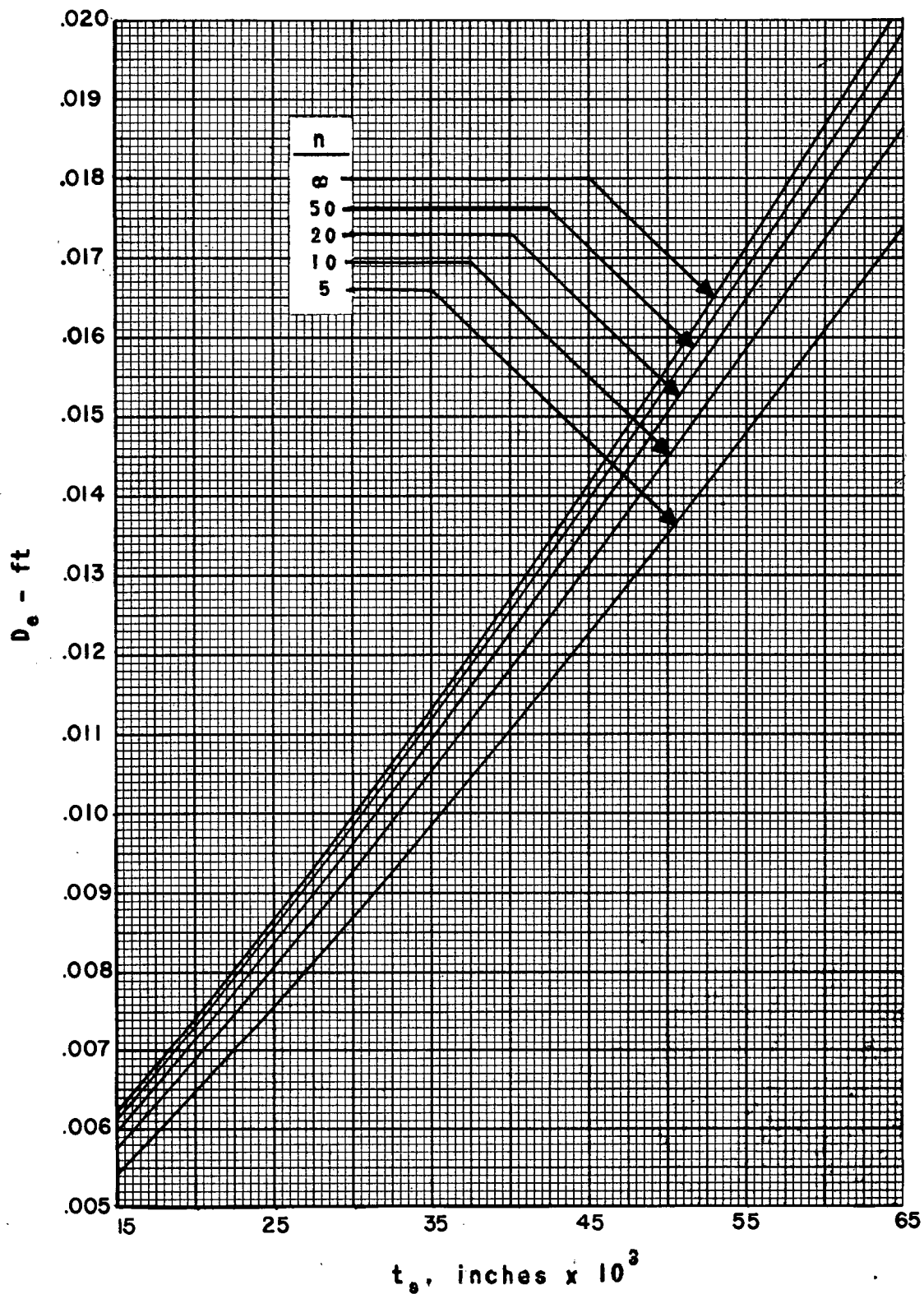
(a) RATIO OF FLOW AREA OUTSIDE TUBES TO TUBE MATRIX FRONTAL AREA.

FIGURE 9. VARIOUS GEOMETRIC PARAMETERS FOR A SQUARE PITCH 1/8-INCH-TUBE BUNDLE AS FUNCTIONS OF SPACER THICKNESS.



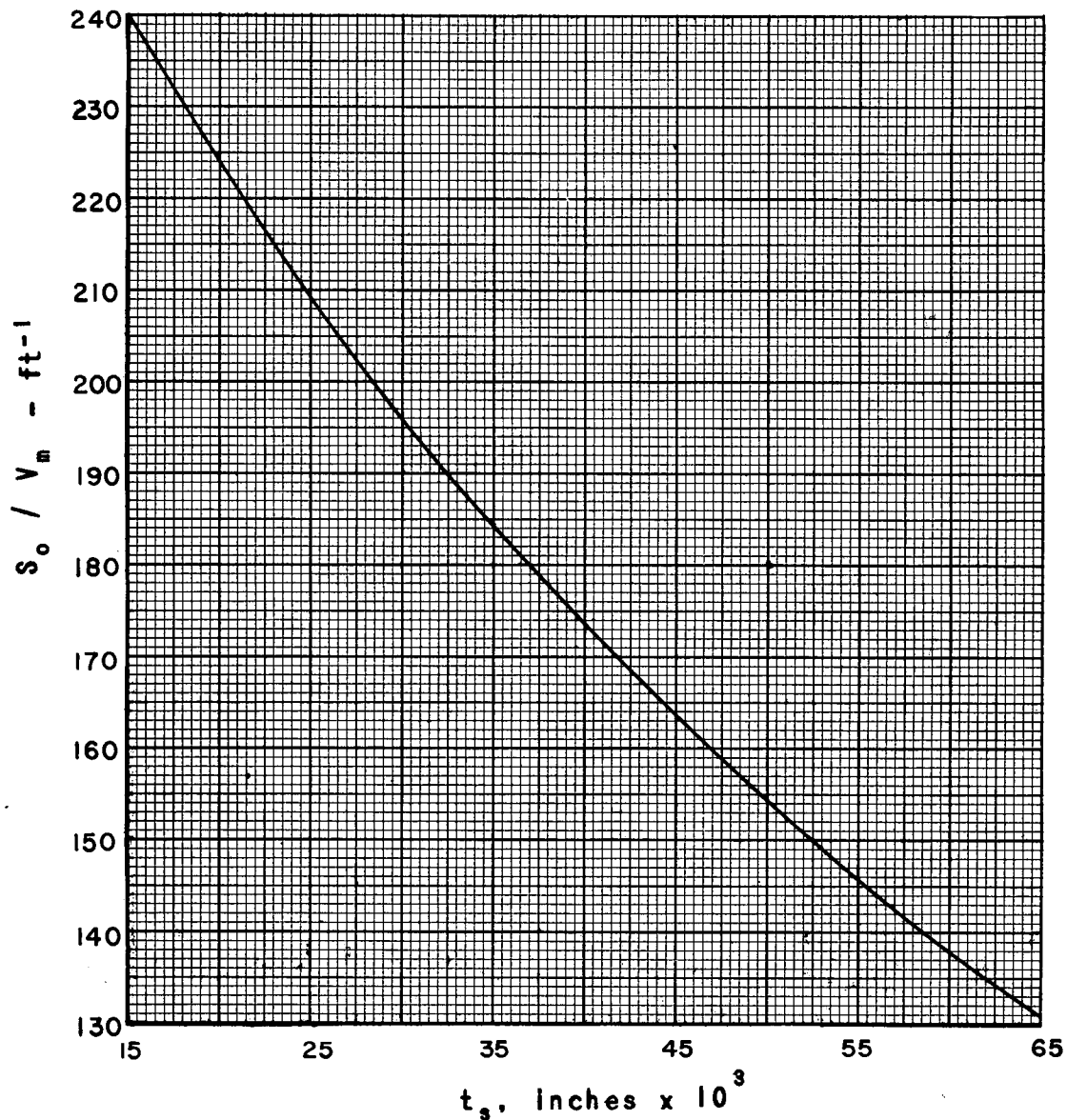
(b) RATIO OF FLOW AREA INSIDE TUBES TO TUBE MATRIX FRONTAL AREA.

FIGURE 9. CONTINUED. VARIOUS GEOMETRIC PARAMETERS FOR A SQUARE PITCH 1/8-INCH-TUBE BUNDLE AS FUNCTIONS OF SPACER THICKNESS.



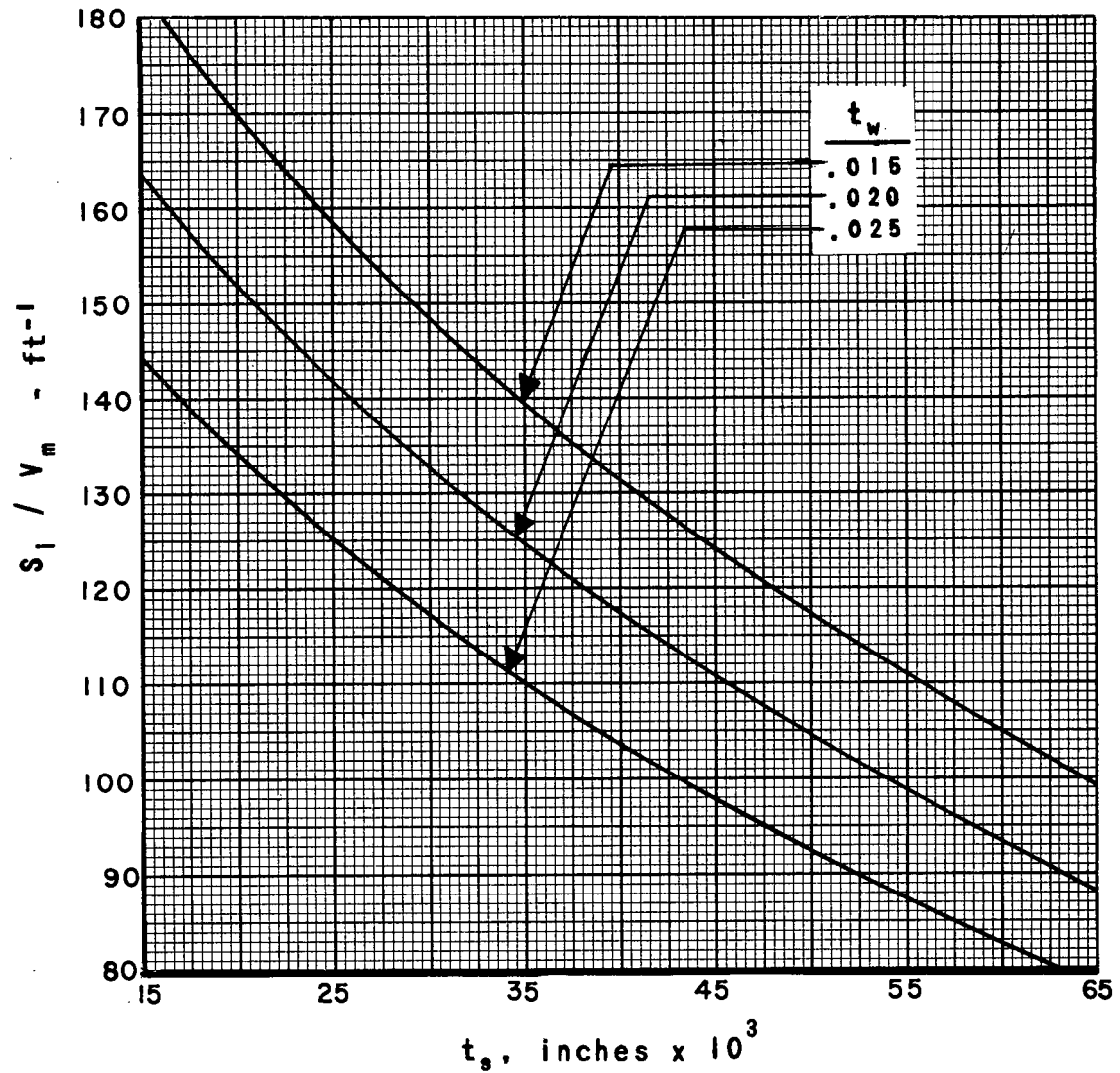
(c) EQUIVALENT DIAMETER OF FLOW PASSAGE OUTSIDE TUBES.

FIGURE 9. CONTINUED. VARIOUS GEOMETRIC PARAMETERS FOR A SQUARE PITCH 1/8-INCH-TUBE BUNDLE AS FUNCTIONS OF SPACER THICKNESS.



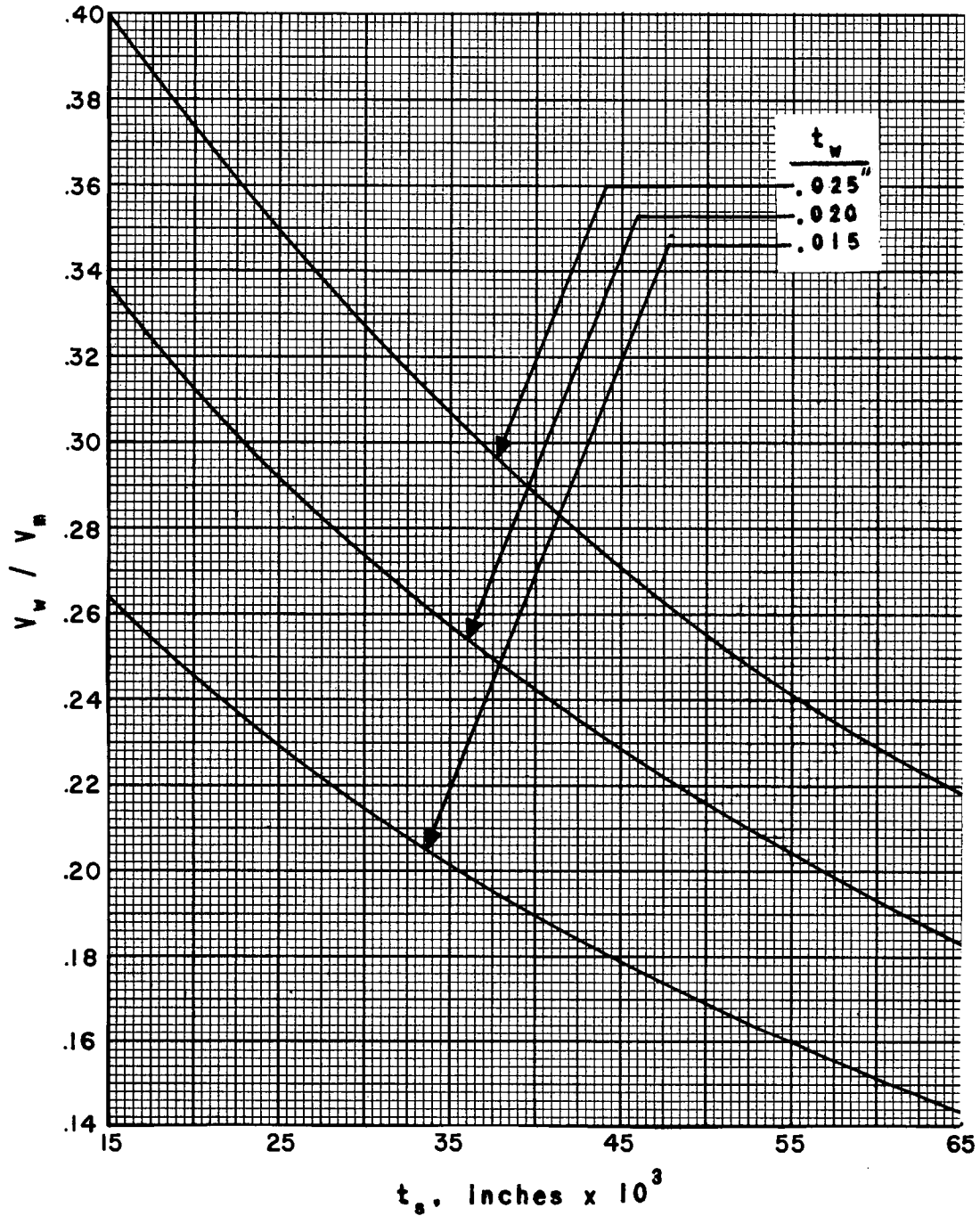
(d) RATIO OF HEAT TRANSFER SURFACE OUTSIDE TUBES TO TUBE MATRIX VOLUME.

FIGURE 9. CONTINUED. VARIOUS GEOMETRIC PARAMETERS FOR A SQUARE PITCH 1/8-INCH-TUBE BUNDLE AS FUNCTIONS OF SPACER THICKNESS.



(e) RATIO OF HEAT TRANSFER SURFACE INSIDE TUBES TO TUBE MATRIX VOLUME.

FIGURE 9. CONTINUED. VARIOUS GEOMETRIC PARAMETERS FOR A SQUARE PITCH 1/8-INCH-TUBE BUNDLE AS FUNCTIONS OF SPACER THICKNESS.



(f) RATIO OF METAL VOLUME IN TUBE WALLS TO TUBE MATRIX VOLUME.

FIGURE 9. CONCLUDED. VARIOUS GEOMETRIC PARAMETERS FOR A SQUARE PITCH 1/8-INCH-TUBE BUNDLE AS FUNCTIONS OF SPACER THICKNESS.

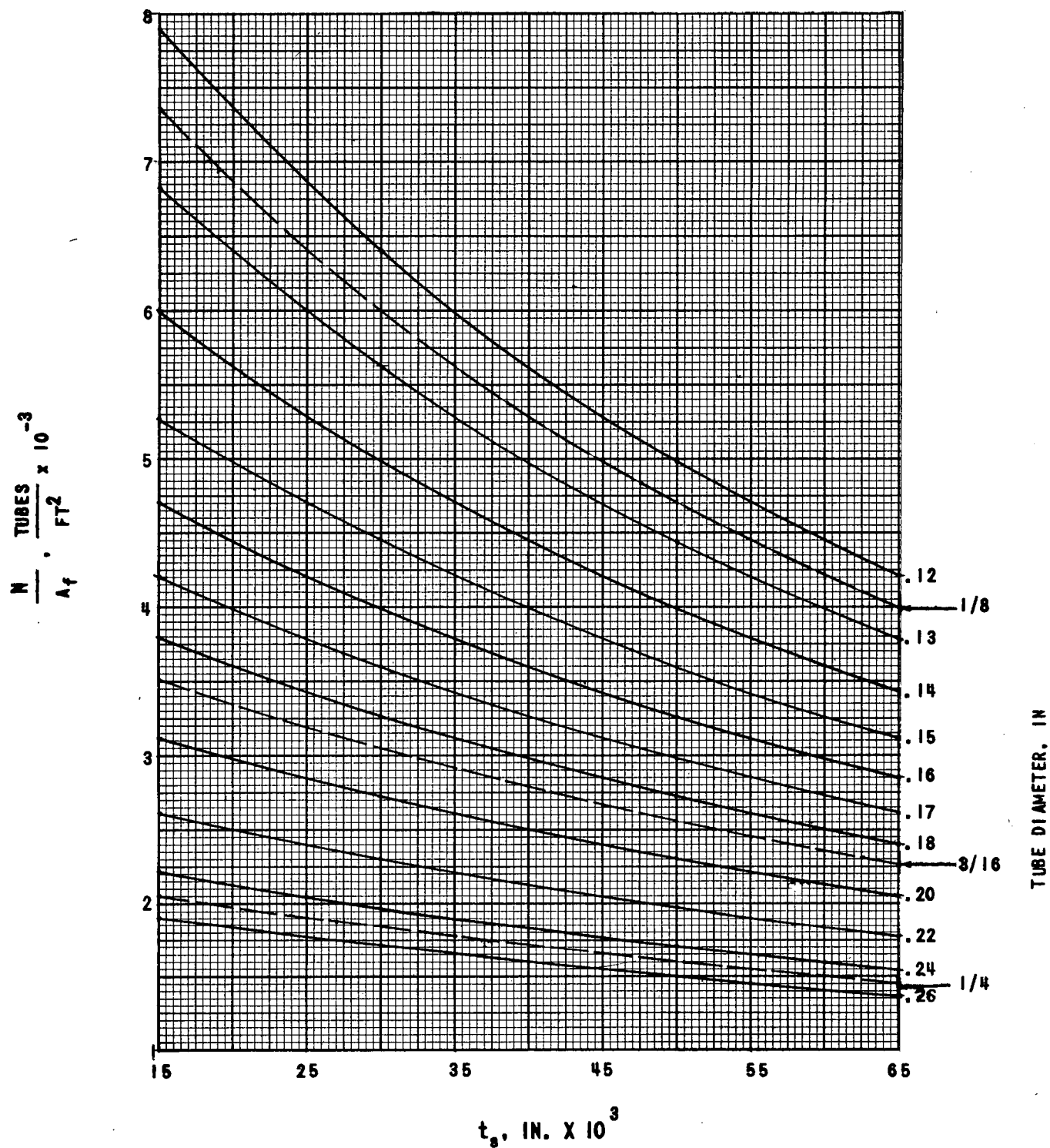


FIGURE 10. RATIO OF NUMBER OF TUBES TO TUBE MATRIX FRONTAL AREA AS A FUNCTION OF SPACER THICKNESS.

FLUID FLOW AND PRESSURE LOSSES

The state of the art at the time of writing is such that data for the physical properties of liquid metals and molten salts in the temperature range of interest is rather difficult to get and in some instances contradictory. Thus the calculation of Reynolds' number, for example, can often be a most annoying job. Figure 11 gives the best data available at the time of writing for the kinematic viscosity of some representative fluids as a function of temperature, as well as a chart from which Reynolds' number can be determined quickly for flow involving any of these fluids.

Pressure losses in heat exchangers or other system components are a function of Reynolds' number and dynamic head (or pressure). Figure 12 gives the dynamic pressure as a function of fluid velocity for a variety of molten metals, fused salts, and water.

The friction factor for flow through smooth tubes is shown as a function of Reynolds' number in Figure 13. Experimental data (see ORNL-1215) has shown that this same friction factor can be applied to the passages between circular tubes on an equivalent diameter basis if turbulent flow conditions prevail. The friction factor for flow past flattened wire tube spacers of the type used in Figure 1 is given in Figure 14 as a function of Reynolds' number and spacer-thickness to tube-diameter ratio. The effect of spacer width can be evaluated from the curve in the upper right-hand corner of Figure 14. This curve is given in the form of a correction factor plotted as a function of spacer thickness-to-width ratio.

The following problem is given to demonstrate the use of the charts in this section.

Sample problem No. 6

In the tube bundle of Problem 4, sodium at 1200°F flows around the tubes at 12 ft/sec. Spacers are .032" thick and .064" wide with 2 vertical and 2 horizontal sets per foot.

Find:

- 1) Kinematic viscosity of the sodium;
- 2) Over-all pressure drop per foot in the tube bundle.

Solution:

- 1) From Figure 11, $\nu = .0093 \text{ ft}^2/\text{hr}$.
- 2) From Problem 4, equivalent diameter = .139". Then from Figure 11 for $\nu = .0093$, $N_R/V = 4250$. $N_R = (12)(4250) = 51,000$.

Sample problem No. 6 (Continued)Solution:

From Figure 12, dynamic pressure = .77 psi at 12 ft/sec.

From Figure 13, $f = .021$ at $N_R = 51,000$. From Problem 4,

$T_s/D_o = .171$. Figure 14 then gives $f_s = .66$ at $N_R =$

51,000. The spacer thickness to width ratio = $.032/.064 =$

.50. Then $K = .98$ and corrected $f_s = (.98)(.66) = .65$.

For a one-foot long tube bundle, $L/D = \frac{12}{.139} = 86.3$. Then

ΔP outside tubes = $(.021)(86.3)(.77) = 1.4$ psi. Spacer

$\Delta P = (.65)(4)(.77) = 2.0$ psi. Therefore, over-all ΔP

= $1.4 + 2.0 = 3.4$ psi per foot.

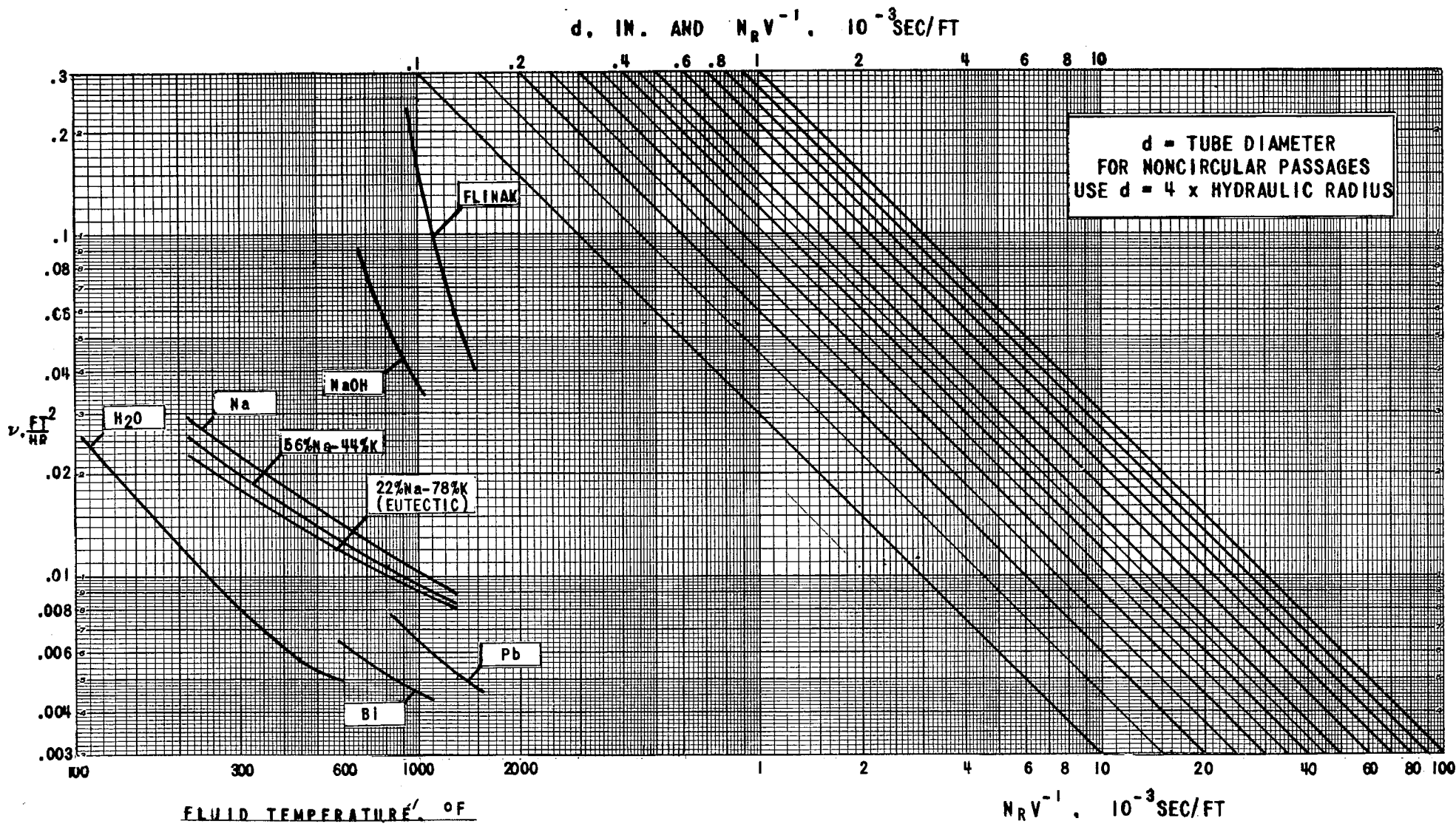


FIGURE 11. REYNOLDS' NUMBER FOR VARIOUS FLUIDS IN ROUND TUBES.

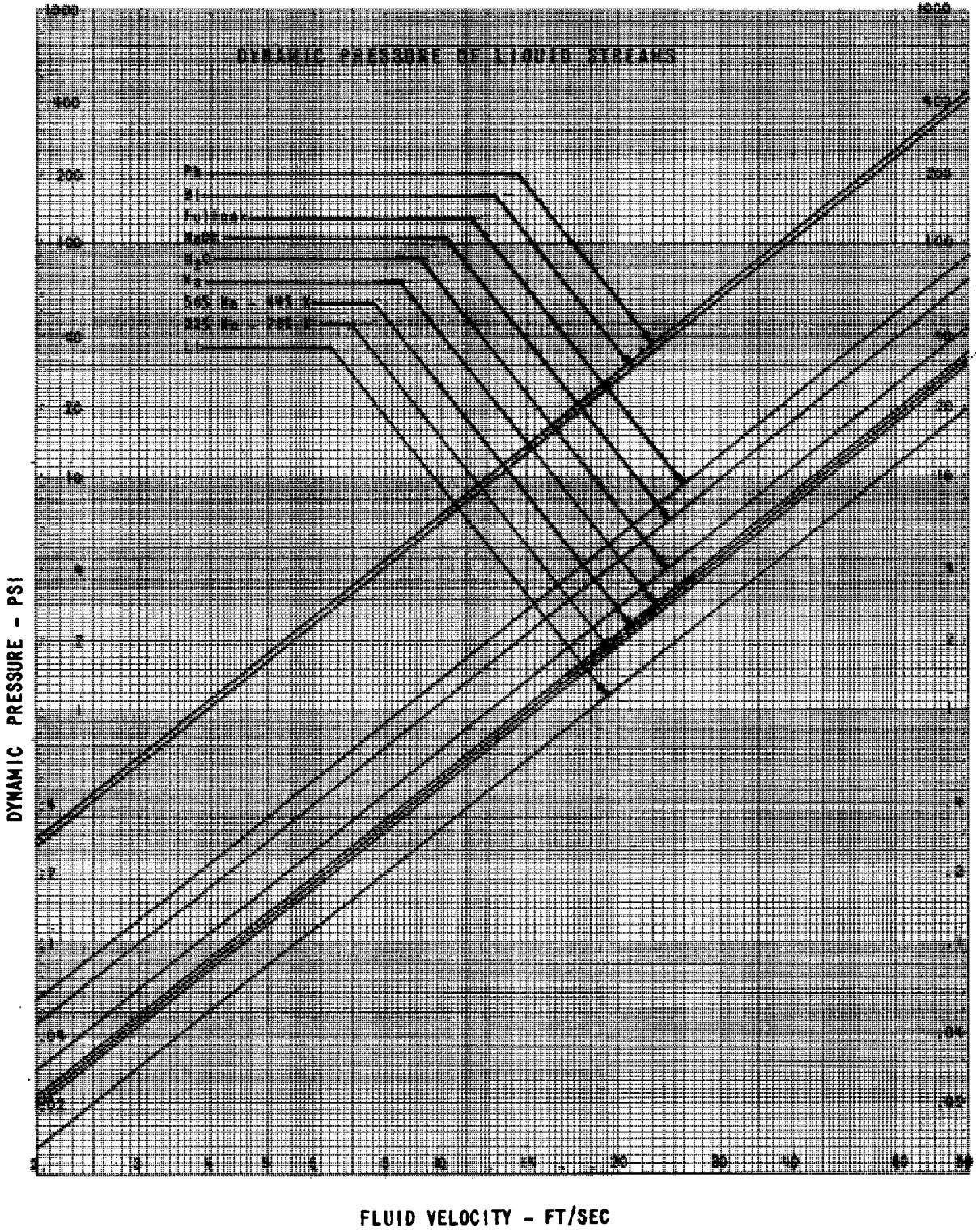
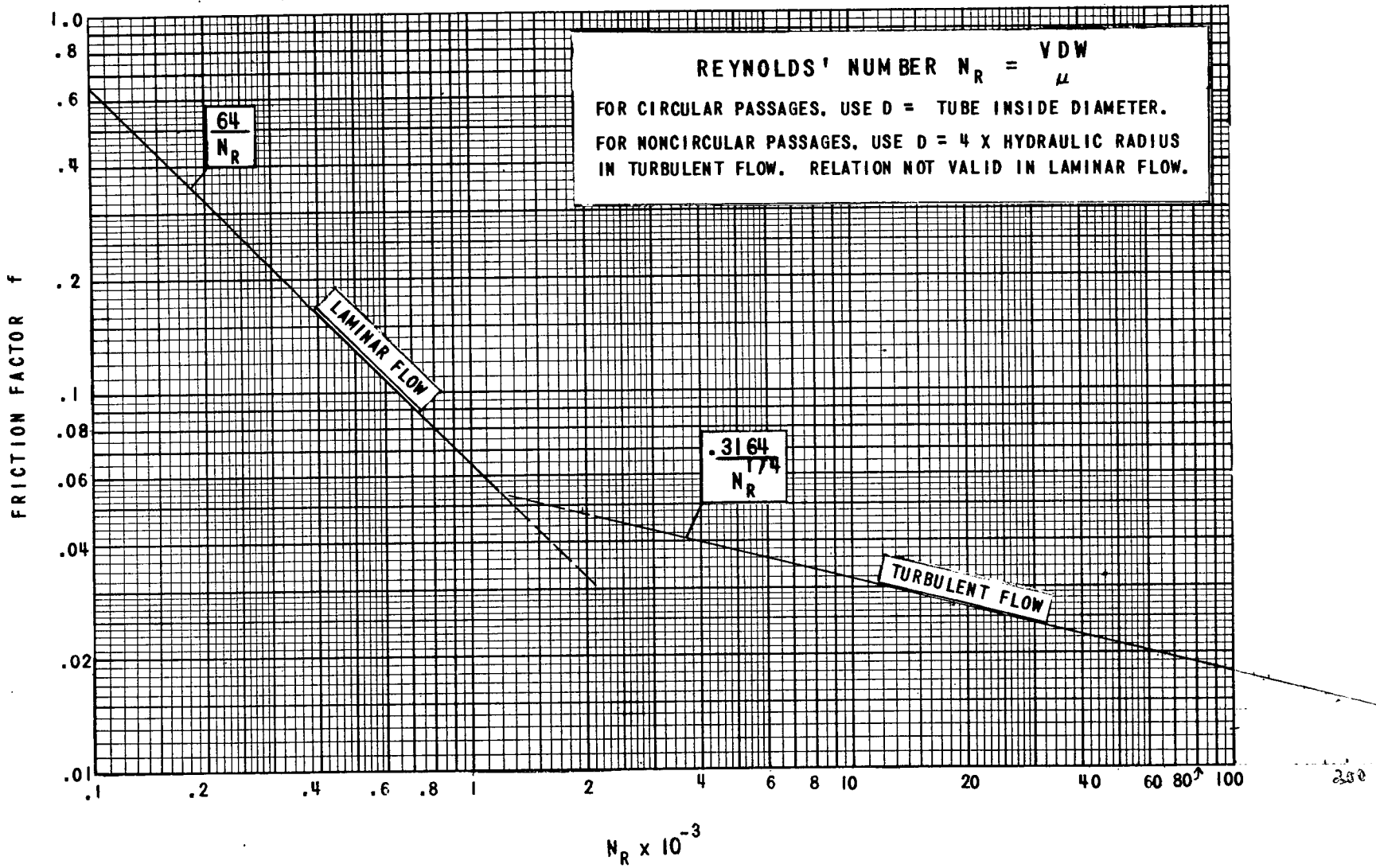


FIGURE 12. DYNAMIC PRESSURE FOR VARIOUS FLUIDS AS A FUNCTION OF VELOCITY.

FIGURE 13. FRICTION FACTOR FOR FLUID FLOW IN SMOOTH PASSAGES AS A FUNCTION OF REYNOLDS' NUMBER.



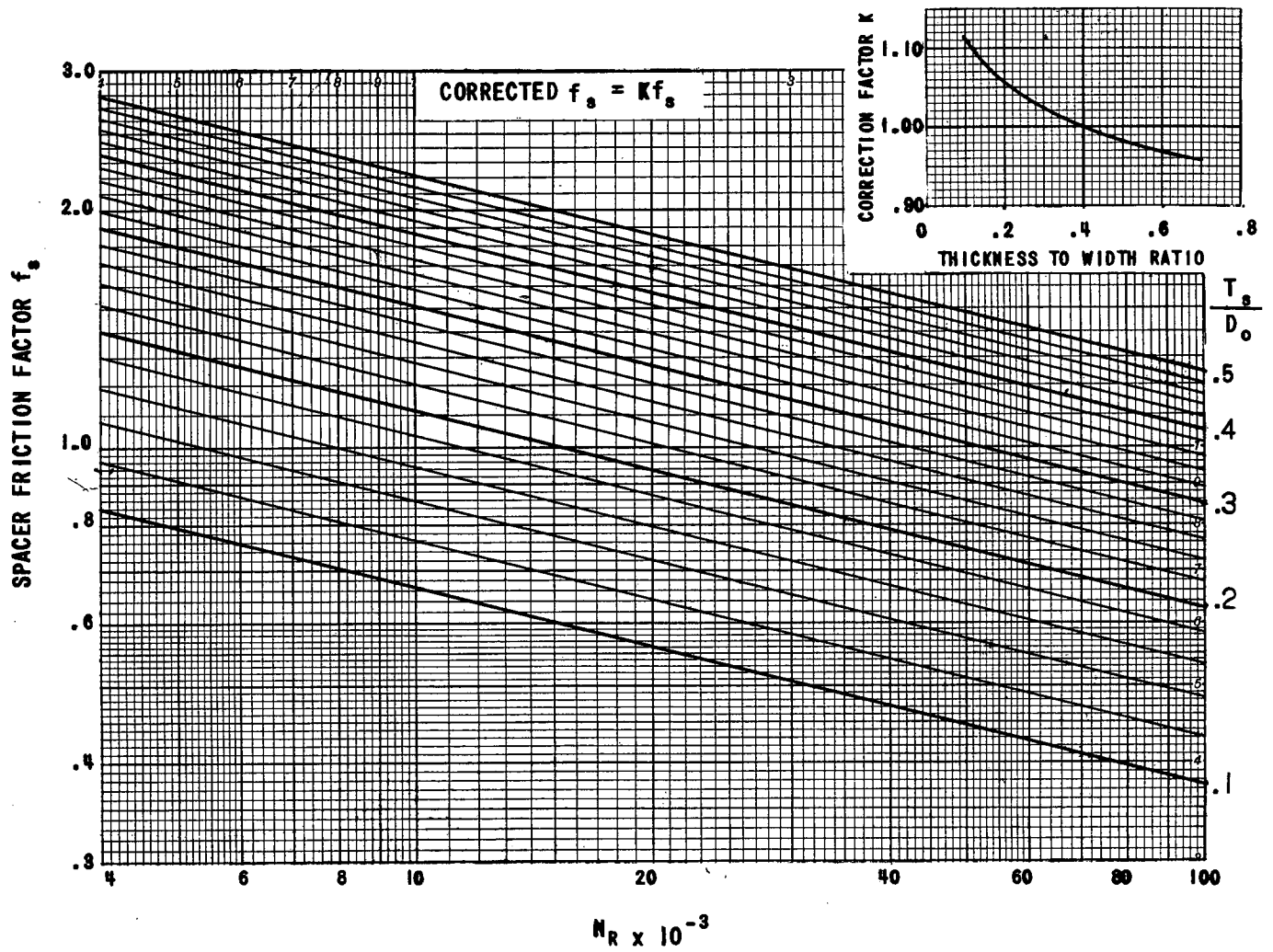


FIGURE 14. SPACER FRICTION FACTOR AS A FUNCTION OF REYNOLDS' NUMBER IN THE TUBE BUNDLE.

HEAT TRANSFER COEFFICIENT

The calculation of heat transfer coefficients from physical property data for the fluids of interest for reactor design work is usually a troublesome task. A set of consistent physical properties was selected after a careful survey of the literature and heat transfer coefficients were calculated from them. These charts are presented in Figures 15 through 18.

Lyons' formula

$$\frac{hD}{k} = 7 + 0.025 \left[\frac{C \mu}{k} \right]^{0.8} \left[\frac{VDW}{\mu} \right]^{0.8}$$

was used for the molten metal heat transfer coefficients in Figures 15(a) through 15(f).

Available data for sodium flowing between flat plates with symmetric heat addition were correlated by

$$\frac{2 hs}{k} = 10.5 + 0.026 \left[\frac{C \mu}{k} \right]^{0.8} \left[\frac{2 VsW}{\mu} \right]^{0.8}$$

where twice the plate spacing s replaces tube diameter. The coefficients in Figure 16 are computed from this equation.

For the non-metals, McAdams' equation

$$\frac{h D}{k} = 0.023 \left[\frac{C \mu}{k} \right]^{0.4} \left[\frac{VDW}{\mu} \right]^{0.8}$$

was used to calculate the heat transfer coefficients in Figures 17 and 18. Figure 17 presents the results for two fused salts. The salts chosen, NaOH and Flinak, were considered representative of those likely to be used. Figure 18 is a chart for water.

Physical properties used in computing Figures 15 through 18 are given in Table 3.

FIGURE 15. HEAT TRANSFER COEFFICIENT FOR LIQUID METALS IN ROUND TUBES AS A FUNCTION OF VELOCITY.

(a) LI

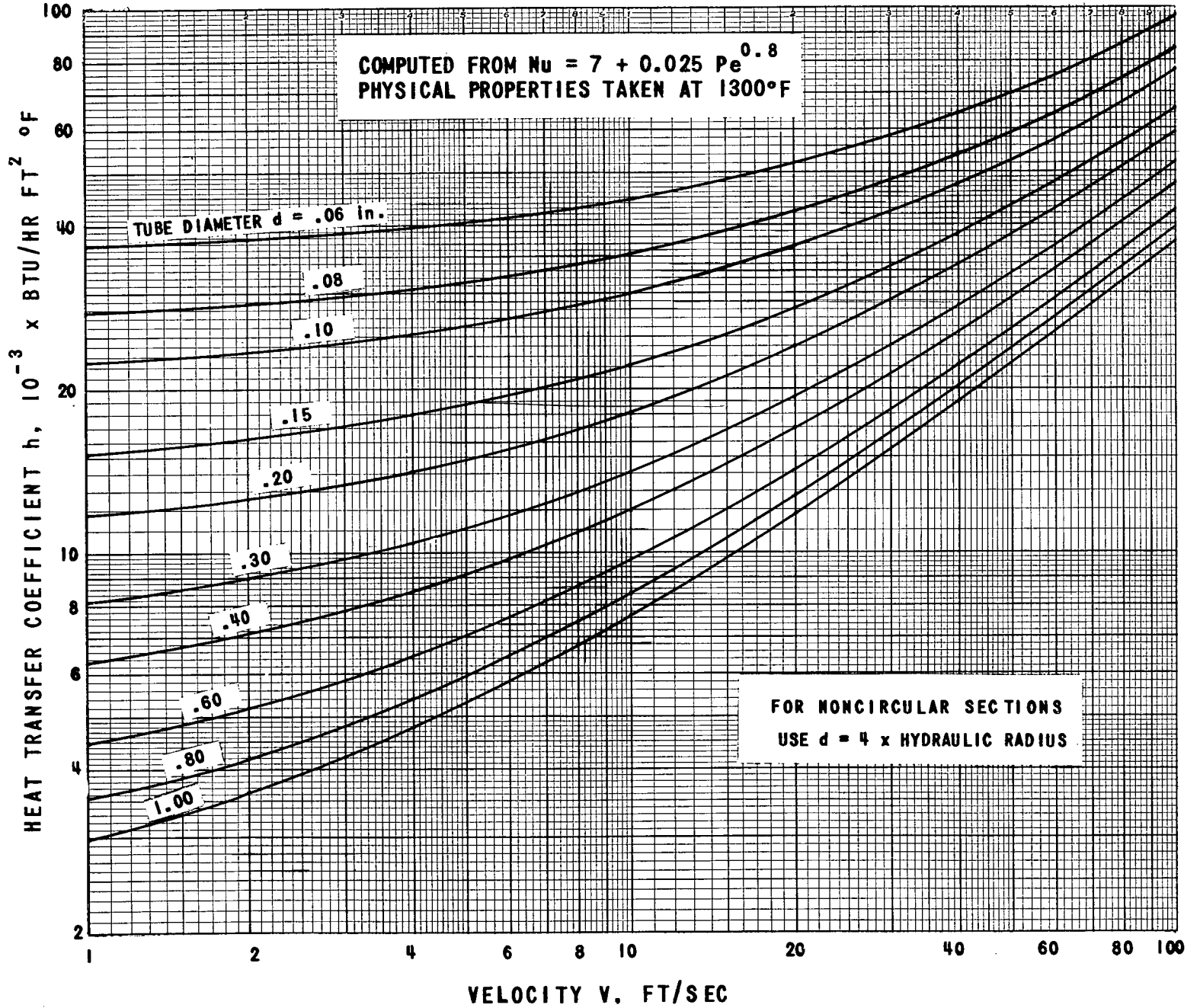


FIGURE 15 CONTINUED. HEAT TRANSFER COEFFICIENT FOR LIQUID METALS IN ROUND TUBES AS A FUNCTION OF VELOCITY.

(b) Na

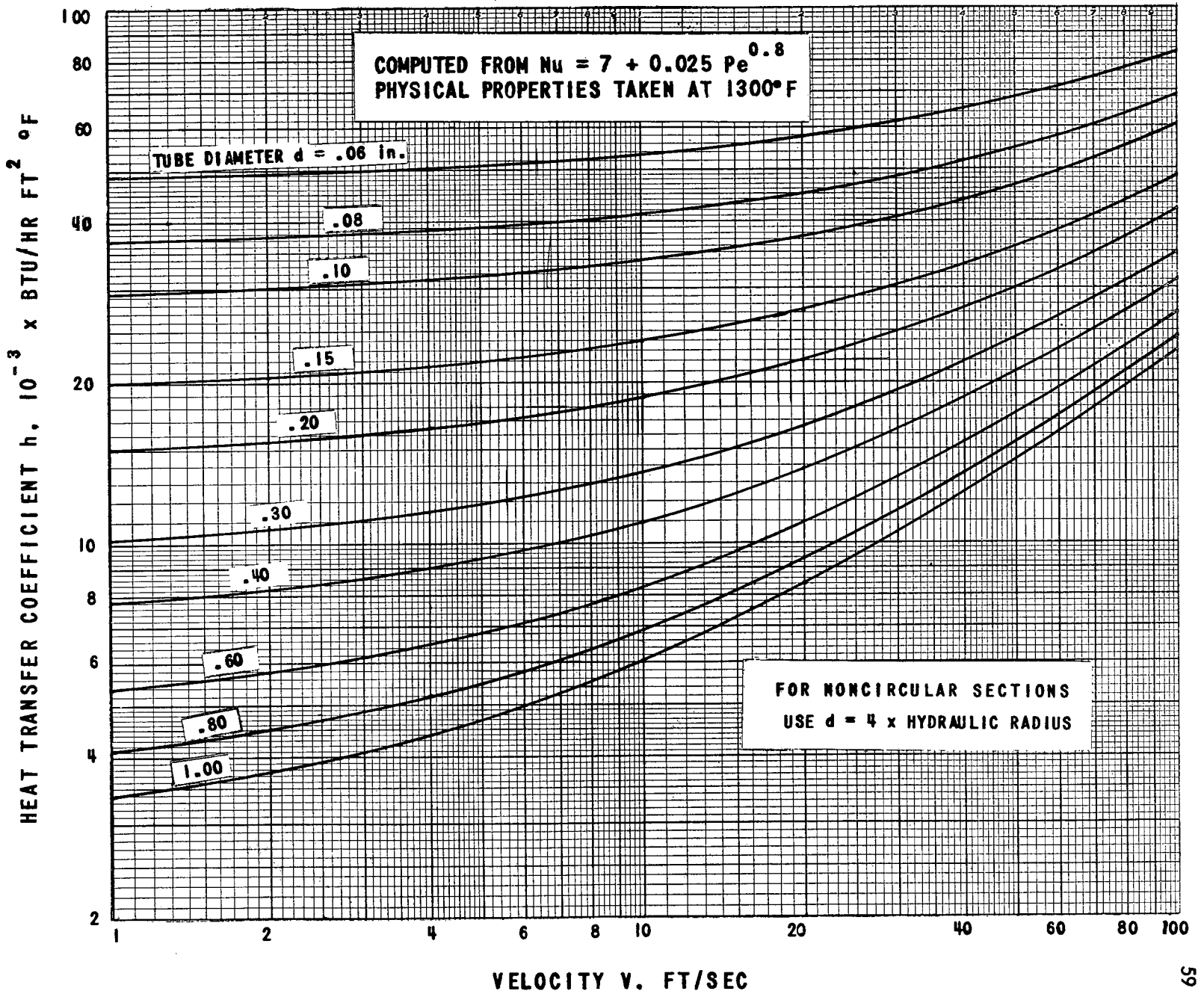


FIGURE 15 . CONTINUED. HEAT TRANSFER COEFFICIENT FOR LIQUID METALS IN ROUND TUBES AS A FUNCTION OF VELOCITY.

(c) Na_K (56% Na - 44% K)

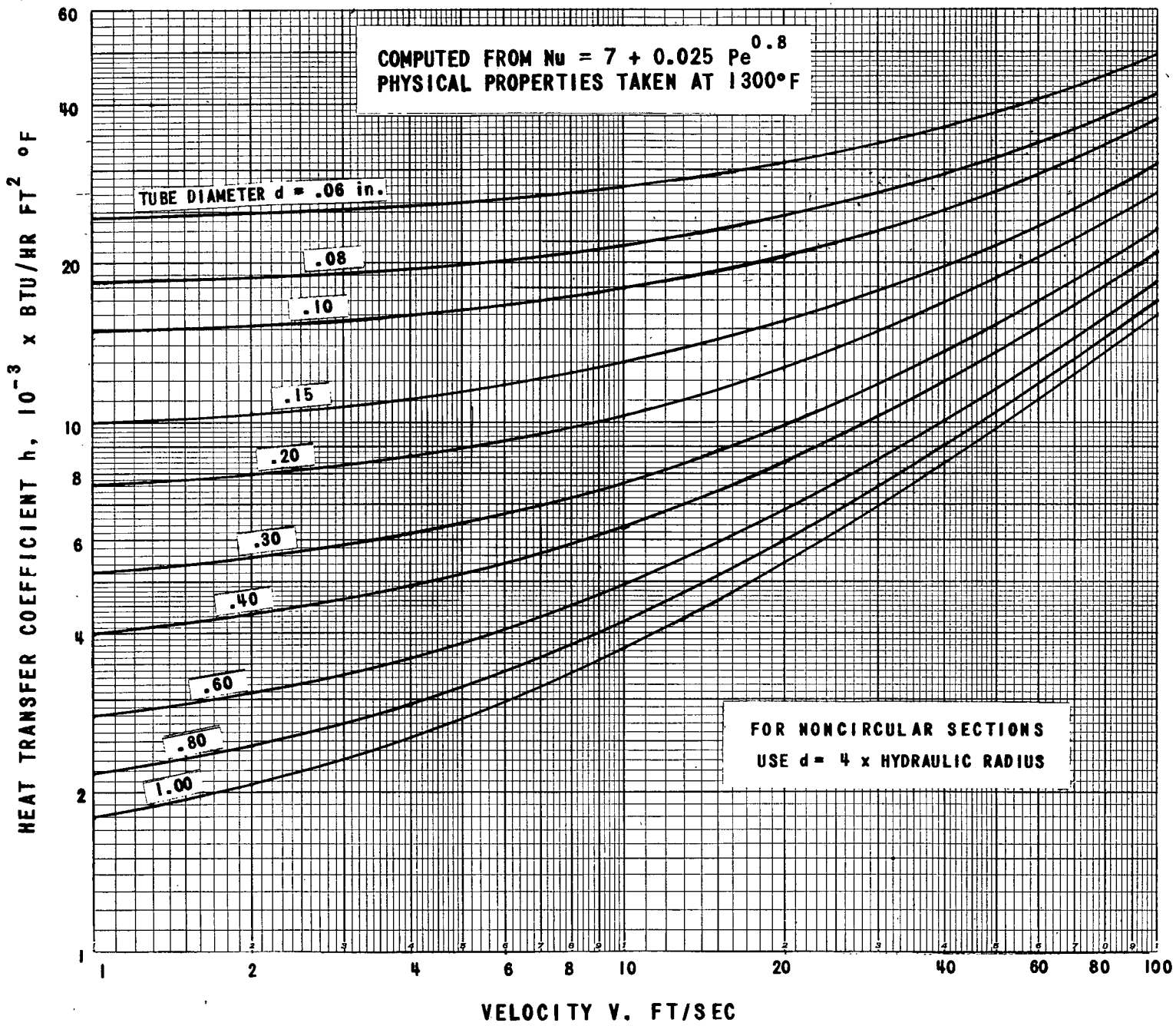


FIGURE 15 . CONTINUED. HEAT TRANSFER COEFFICIENT FOR LIQUID METALS IN ROUND TUBES AS A FUNCTION OF VELOCITY.

(D) NaK (22% Na - 78% K)

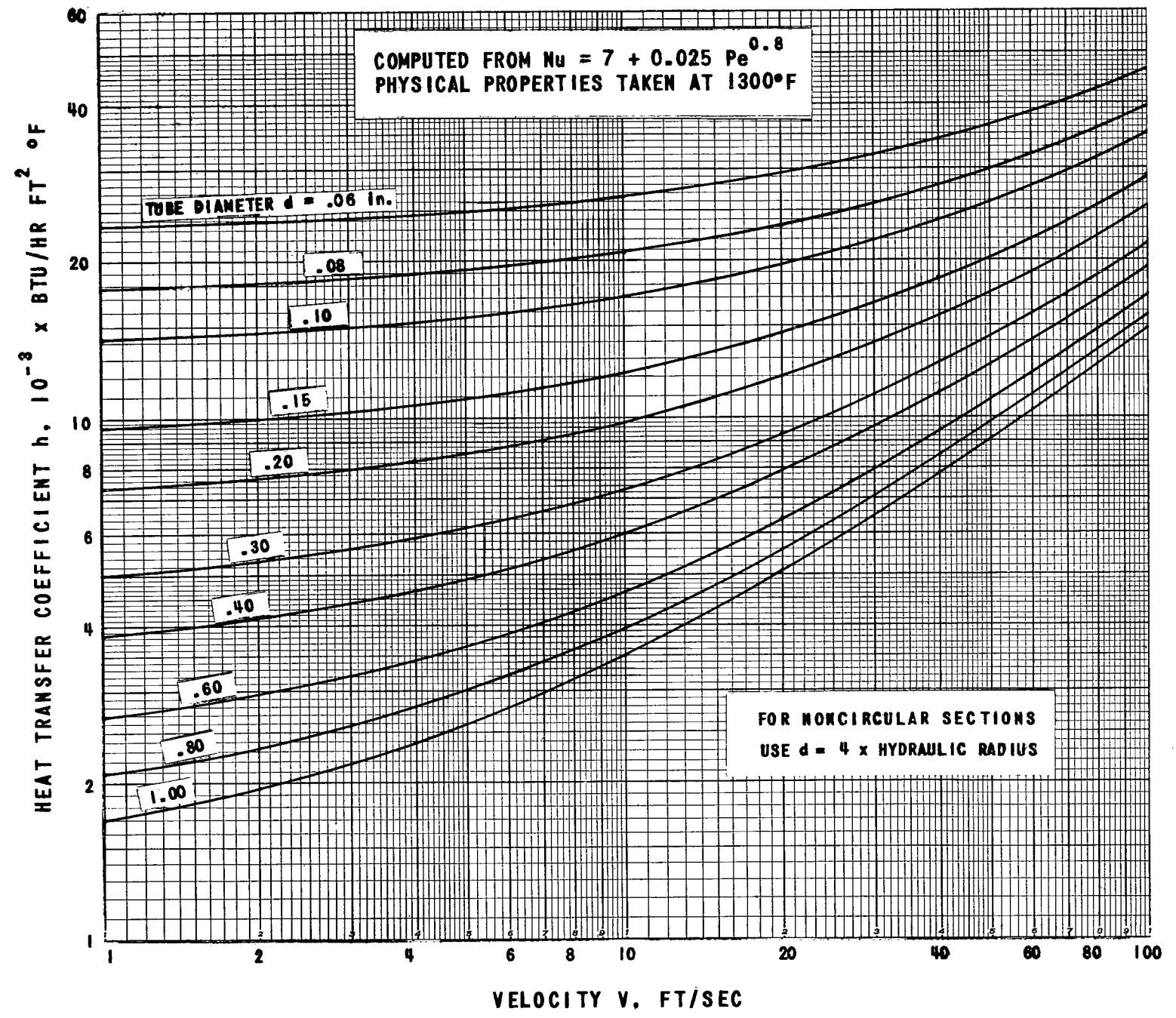


FIGURE 15 CONTINUED. HEAT TRANSFER COEFFICIENT FOR LIQUID METALS IN ROUND TUBES AS A FUNCTION OF VELOCITY

(a) B1

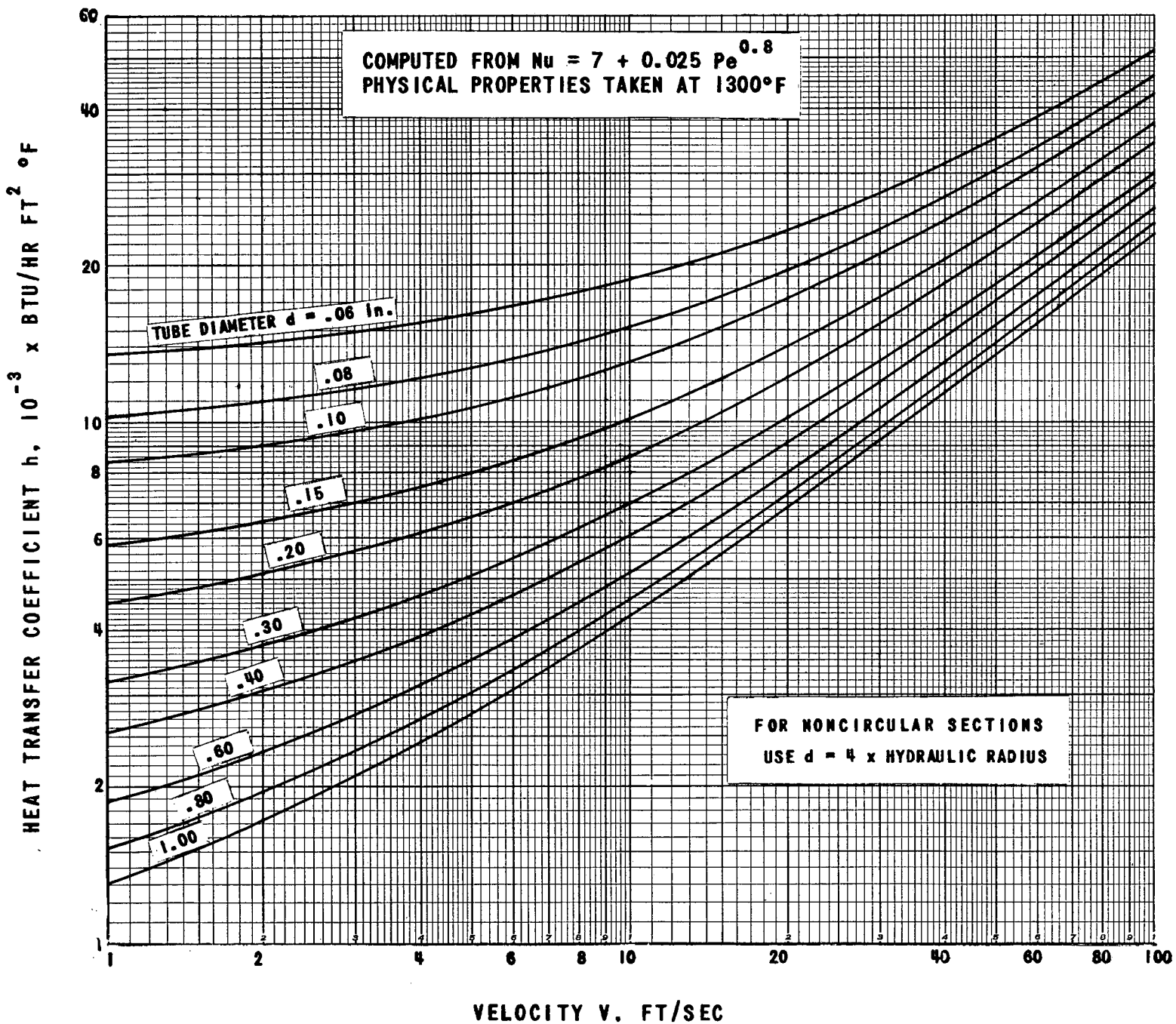


FIGURE 15 . CONCLUDED. HEAT TRANSFER COEFFICIENT FOR LIQUID METALS IN ROUND TUBES AS A FUNCTION OF VELOCITY

(f) Pb

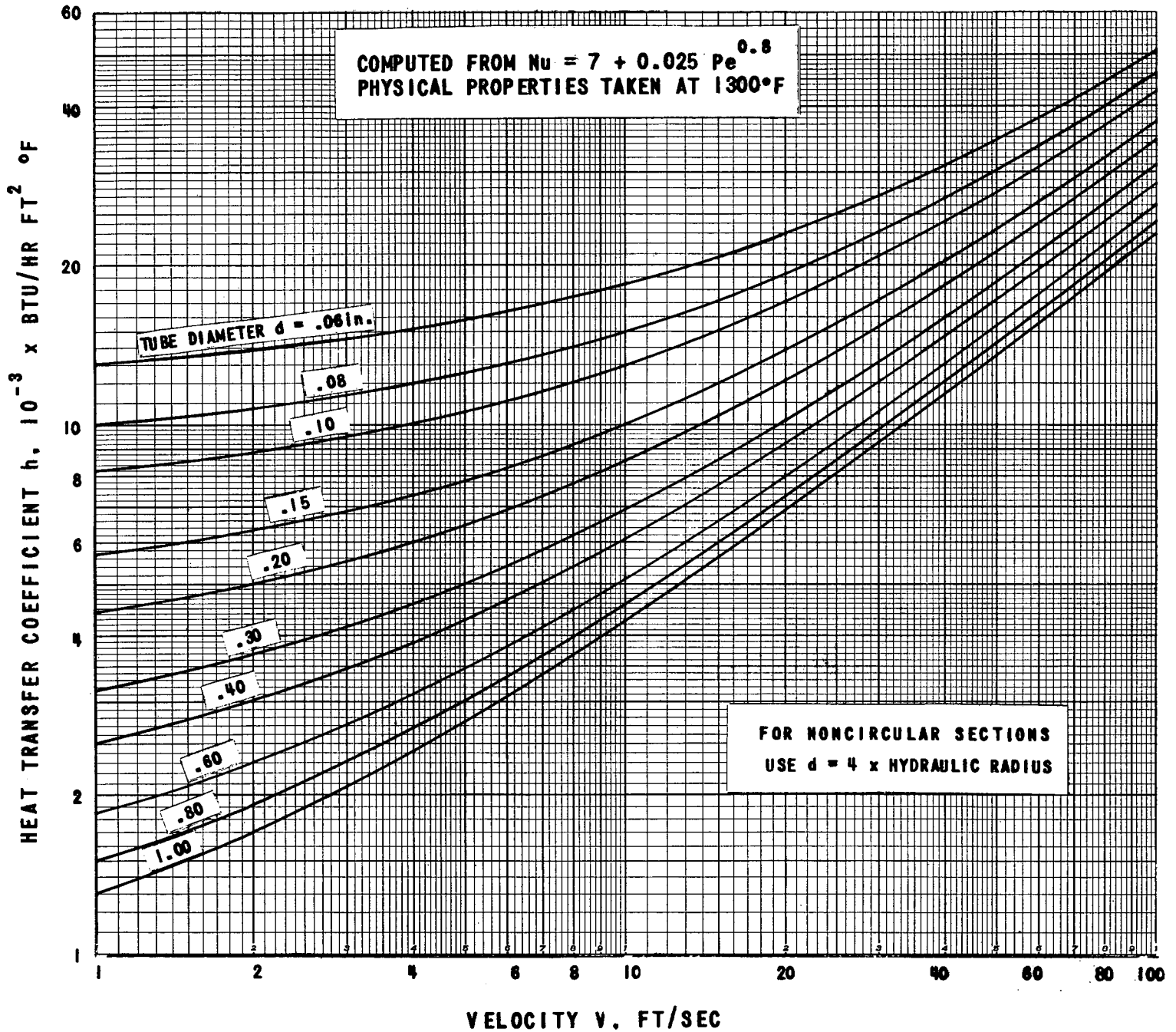
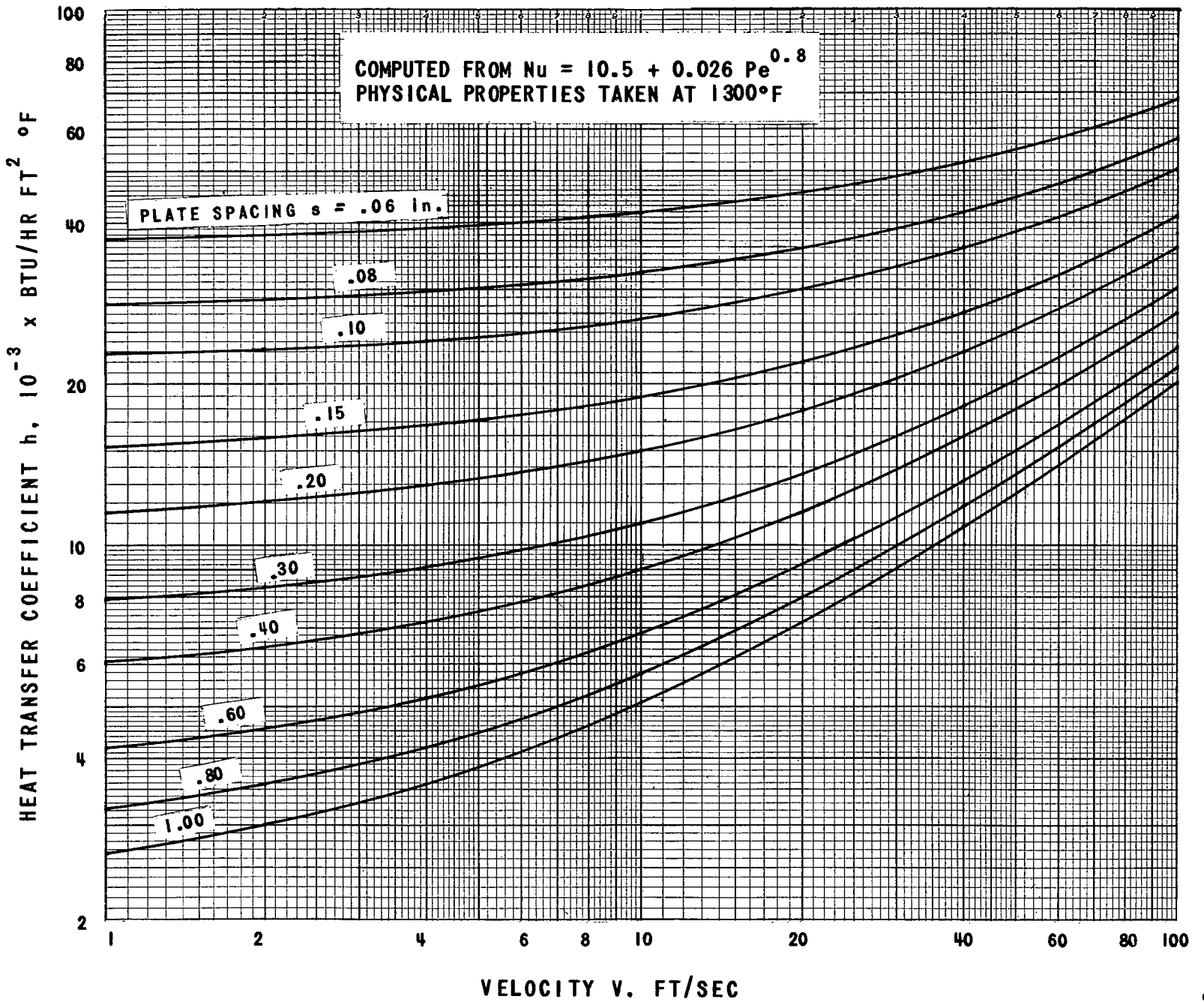
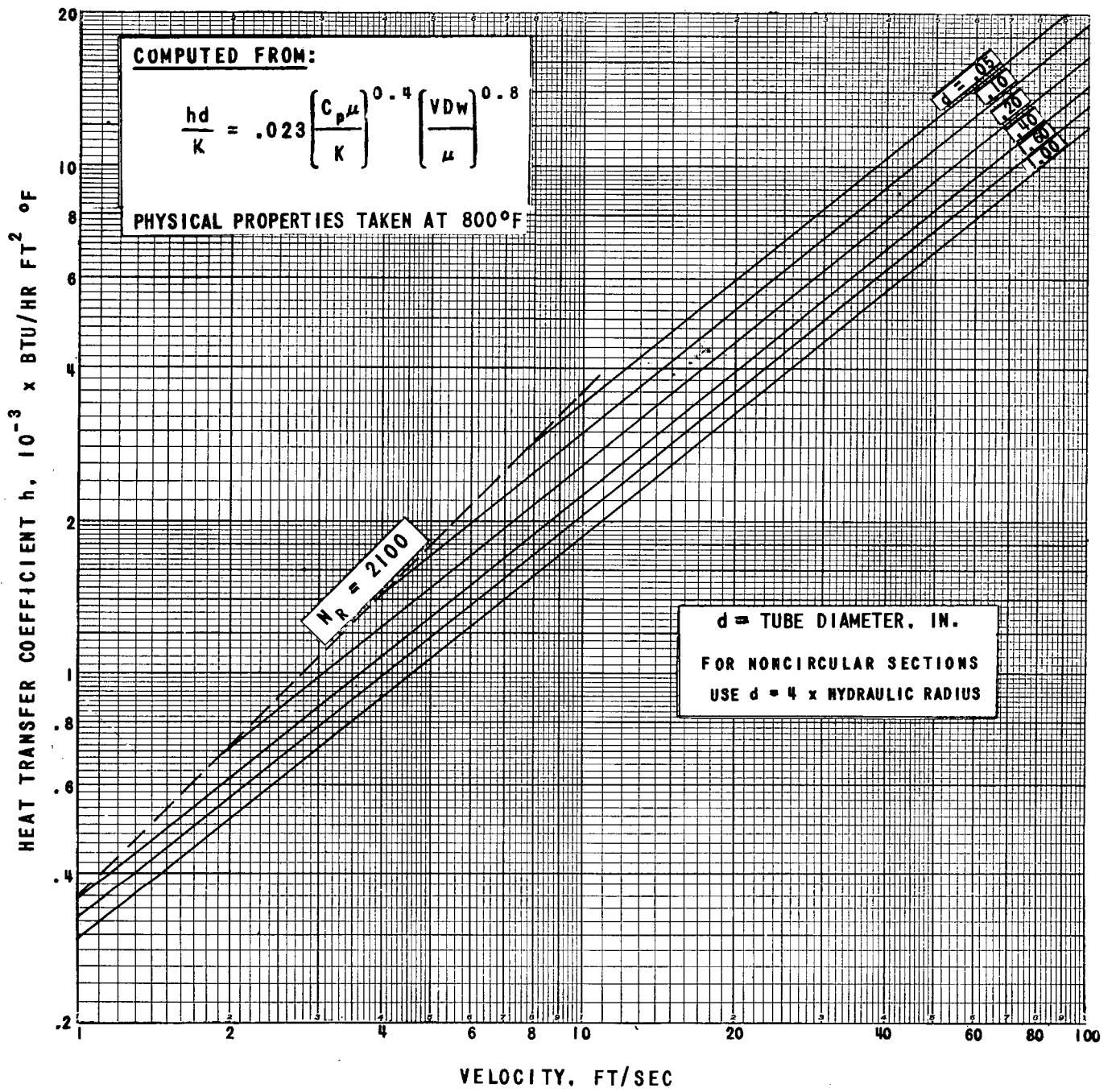


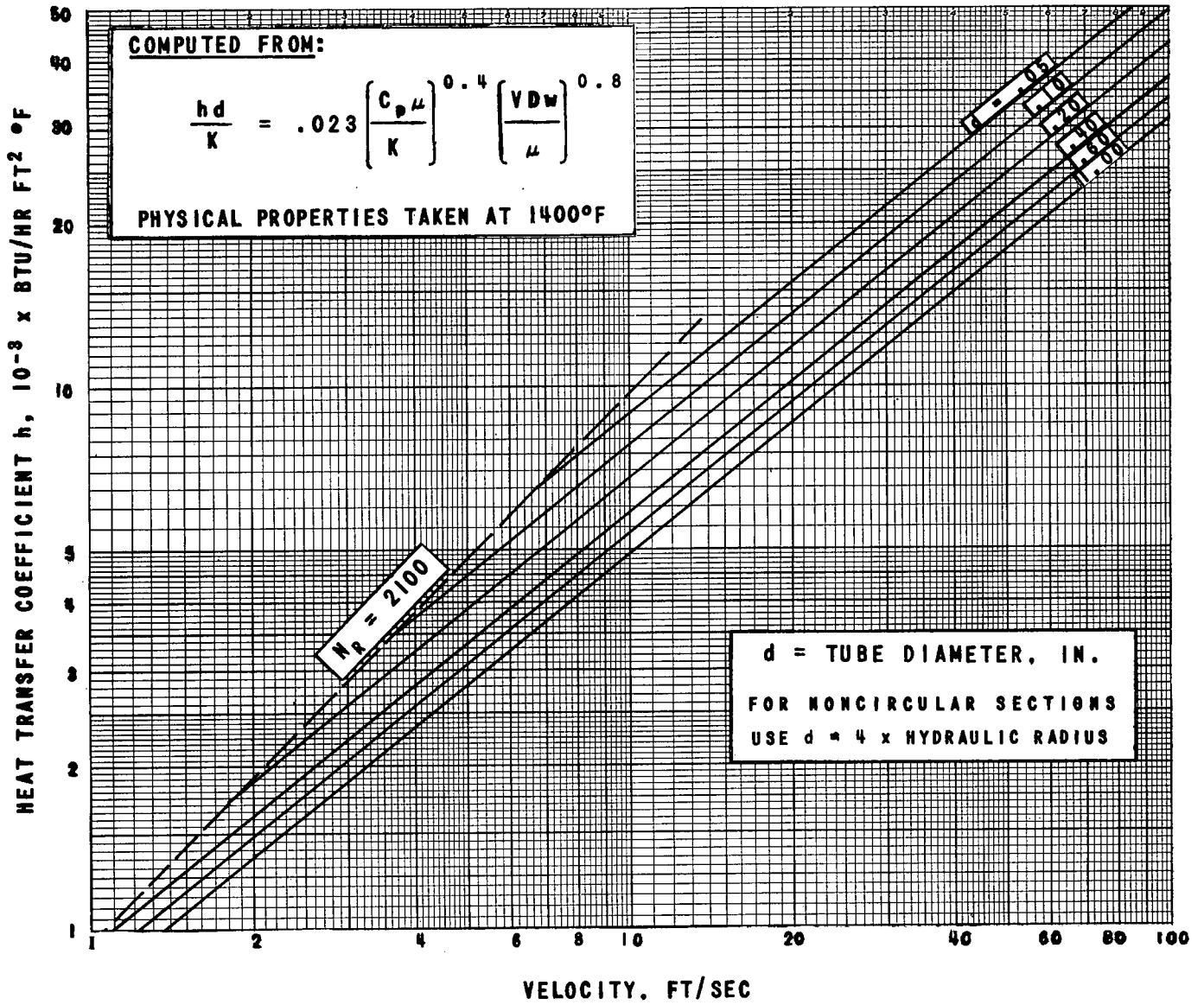
FIGURE 16. HEAT TRANSFER COEFFICIENT FOR SODIUM FLOWING BETWEEN FLAT PLATES AS A FUNCTION OF VELOCITY. SYMMETRIC HEAT ADDITION.





(a) NaOH

FIGURE 17. HEAT TRANSFER COEFFICIENT FOR FUSED SALTS IN ROUND TUBES.



(b) FLINAK (11.5% NaF - 42% KF - 46.5% LiF)

FIGURE 17. HEAT TRANSFER COEFFICIENT FOR FUSED SALTS IN ROUND TUBES.

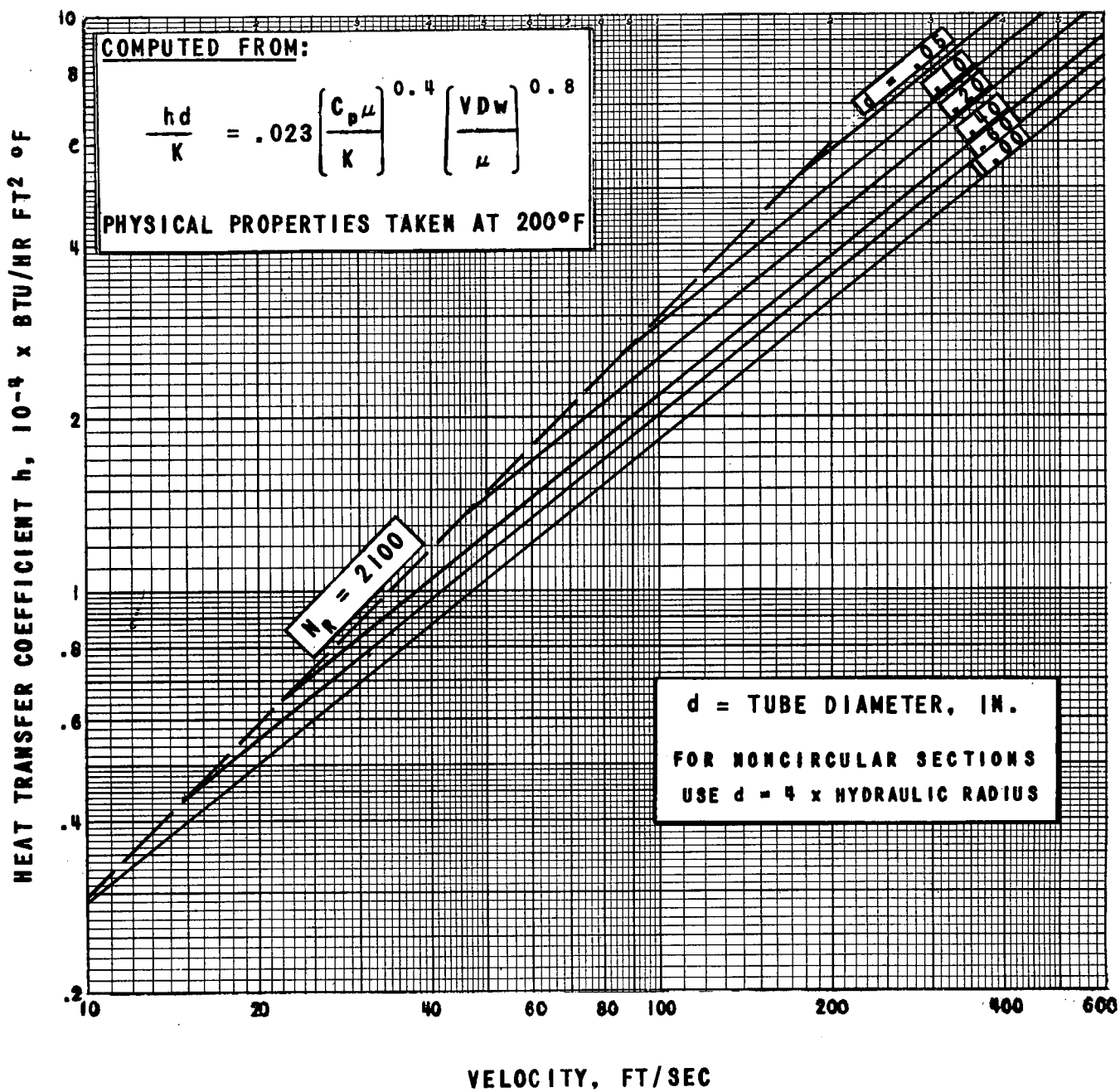


FIGURE 18. HEAT TRANSFER COEFFICIENT FOR WATER IN ROUND TUBES.
 NO BOILING.

Table 3
Physical Properties
(a) Liquid Metals

<u>Metal</u>	<u>Temperature °F</u>	$\frac{c}{K} \frac{W}{Hr/Ft^2}$	$\frac{k}{°F Ft} \frac{BTU}{Hr}$
Na	1300	.43	34.3
NaK (56% Na - 44% K)	1300	.70	17.0
NaK (22% Na - 78% K)	1300	.66	16.4
Li	1300	1.29	25.0
Pb	1300	2.74	8.7
Bi	1300	1.85	8.95

(b) Non-Metals

<u>Fluid</u>	<u>Temp. °F</u>	$\frac{c}{BTU/Lb °F}$	$\frac{W}{Lb/Ft^3}$	$\frac{\mu}{Lb/Hr Ft}$	$\frac{k}{°F Ft} \frac{BTU}{Hr}$
Flinak:					
NaF 11.5 M %)	1400	.45	121	5.81	2.60
KF 42.0 M %)					
LiF 46.5 M %)					
NaOH	800	.48	108	6.00	.60
H ₂ O	200	.99	60.2	.74	.41

PERFORMANCE OF A SERIES OF TYPICAL COUNTERFLOW HEAT EXCHANGERS

The complex interrelationships of tube spacing and diameter, tube length, fluid velocity, etc., make it difficult to visualize the effects of variations in various parameters. A series of charts, presented in Figures 19(a) to 19(k), was therefore prepared to show the performance characteristics of some typical heat exchangers and to aid in the rapid determination of effects of changes in design conditions. These charts were intended as a means for quickly surveying a spectrum of heat exchangers rather than providing finely detailed information for a finished design. Proportions were chosen to cover the ranges that seemed of most interest. Pure counterflow was assumed in all cases with the temperature drop in the hot fluid equal to the temperature rise in the cold fluid. The logarithmic and arithmetic mean temperatures were thus made equal to each other and to the local temperature difference. The power transmitted was set equal to 400,000 KW in a heat exchanger volume of 40 cubic feet.

The charts are applicable to any size of heat exchanger with the same core matrix geometry directly if power density and temperature rise correspond to those of the charts, or with a simple correction if power density or temperature rise or both differ from the chart values. Three cases in which the desired values of power density or temperature rise deviate from the chart values present themselves:

- 1) power density is the same but temperature rise is different;
- 2) power density is different but temperature rise is the same;
- 3) both power density and temperature rise are different.

In the first case it is apparent that for a constant power density the fluid velocities through the heat exchanger must change in inverse proportions to the temperature rise. Because of the moderately complex variation of over-all heat transfer coefficient with fluid velocity it is difficult to state explicitly the effect of velocity changes on temperature difference. However, because of the way in which the charts are set up, circumventing this problem becomes relatively simple. The charts are computed for a constant heat exchanger volume so that the flow passage area of the exchanger varies in inverse proportions to tube length with the result that flow velocities are directly proportional to tube length. Hence, it is possible to select a tube length from the chart such that the velocities through and around the tubes will correspond to those in the proposed heat exchanger. The over-all heat transfer coefficients for the proposed and chart heat exchangers are then equal and the over-all temperature difference may be read directly from the chart at the new tube length. This new tube length is simply the tube length for the proposed heat exchanger multiplied by the ratio of the chart temperature rise to the proposed temperature rise.

Pressure drop is directly proportional to tube length, so that values read at the new tube length must be divided by the ratio of the temperature rises to get the pressure drops corrected to the proposed tube length.

In order to clarify the procedure, a numerical example is given here:

Sample problem No. 7

Given: Flinak to NaK, 1/8" tubes, .018" spacing, 4' tube length, 10,000 KW/Ft³, 200° temperature rise.

Find: Pressure drops in both circuits and temperature difference.

Solution: Use Figure 19(b). The chart temperature rise is twice the given temperature rise, read values at a tube length = 2 x 4 = 8 ft. Then ΔP inside tubes = 210 psi; ΔP outside tubes = 67 psi; ΔT = 43°F. The pressure drops are for a tube length twice that of the proposed exchanger; the temperature difference is correct as read. The final answers then are:

$$\begin{aligned}\Delta P \text{ inside tubes} &= 1/2 \times 210 = 105 \text{ psi} \\ \Delta P \text{ outside tubes} &= 1/2 \times 67 = 33.5 \text{ psi} \\ \Delta T &= 43^\circ\text{F}\end{aligned}$$

For comparison, the figures for a 400°F temperature rise (the chart value) are:

$$\begin{aligned}\Delta P \text{ inside tubes} &= 33 \text{ psi} \\ \Delta P \text{ outside tubes} &= 10 \text{ psi} \\ \Delta T &= 56^\circ\text{F}\end{aligned}$$

Case two, in which power density is changed but temperature rise is kept at the chart value, can be analyzed in a manner similar to that of case one. For a constant temperature rise, if the power density is multiplied by any factor k the flow velocities must be multiplied by the same factor k. As in the first case, values for pressure drops and temperature difference are therefore read at a tube length k times that of the proposed exchanger. The pressure drops are then divided by k to get the corrected values. The temperature difference read from the chart is that required to transmit 10,000 KW/ft³ at the new velocities. Transmission of 10,000 k KW/ft³, then, requires k times the chart temperature difference.

The procedure is best illustrated by an example.

Sample problem No. 8

Given: Funak to NaK, 3/16" tubes, .037" spacing, 5' tube length, 400°F temperature rise, 15,000 KW/ft³.

Find: Pressure drops in both circuits and temperature difference.

Solution: Use Figure 19(i). $k = 15,000/10,000 = 1.5$. Read chart at a tube length = 1.5 x 5 = 7.5 ft. ΔP inside tubes = 72 psi; ΔP outside tubes = 64 psi; ΔT = 146°F. Corrected values are:

$$\Delta P \text{ inside tubes} = 72/1.5 = 48 \text{ psi}$$

$$\Delta P \text{ outside tubes} = 64/1.5 = 42.7 \text{ psi}$$

$$\Delta T = 146 \times 1.5 = 218^{\circ}\text{F}$$

The performance for a 10,000 KW/ft³ power density (the chart value) is:

$$\Delta P \text{ inside tubes} = 25 \text{ psi}$$

$$\Delta P \text{ outside tubes} = 21 \text{ psi}$$

$$\Delta T = 187^{\circ}\text{F}$$

Case three, in which both power density and temperature difference differ from chart values, can be readily analyzed by combining the procedures for cases one and two. Determine a chart tube length from

$$\text{Chart tube length} = (\text{Proposed tube length}) \times \frac{\text{Proposed power density}/10,000}{\text{Proposed temperature rise}/400}$$

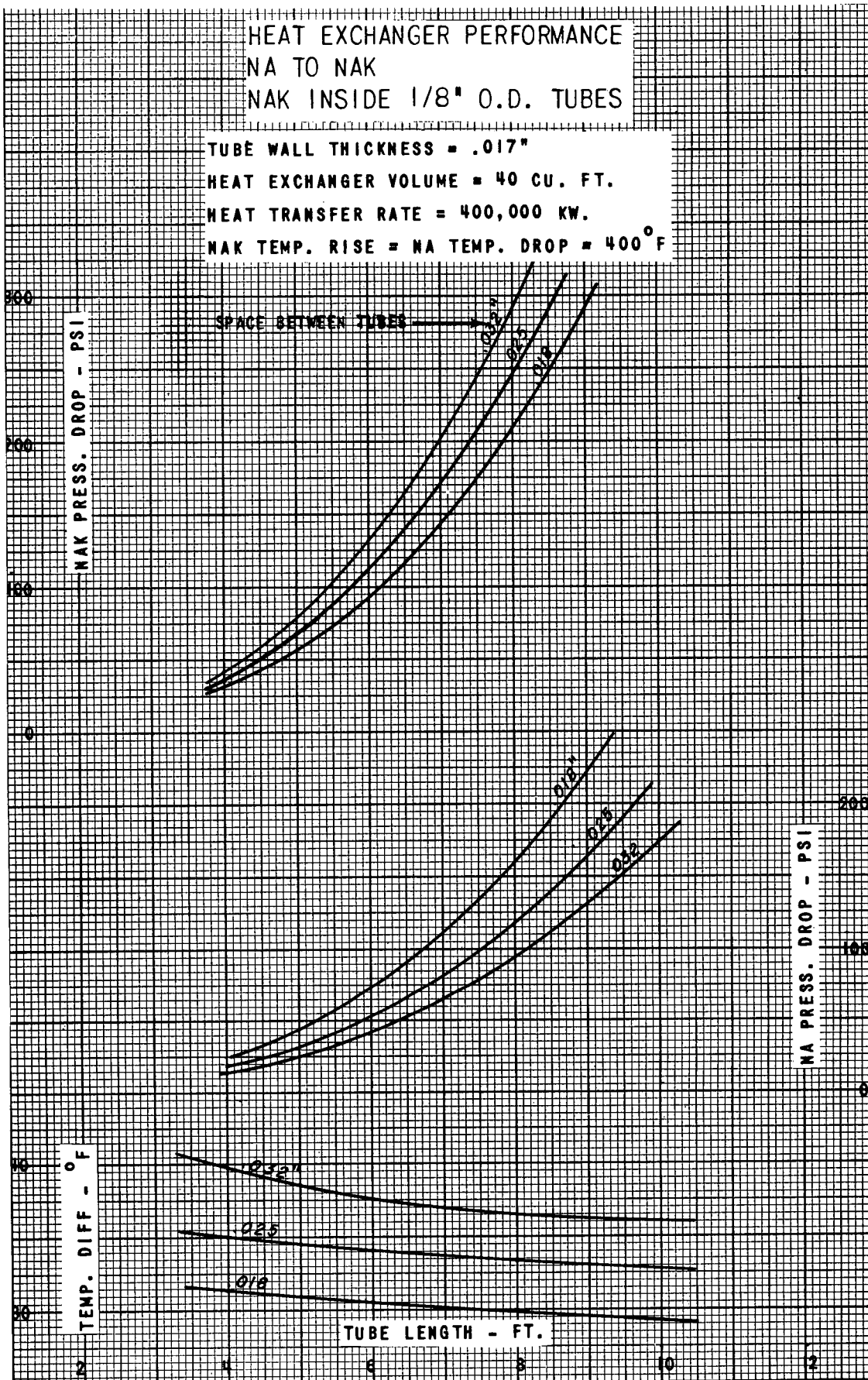
Read both pressure drops and the temperature difference at this chart tube length. Then, the pressure drops in the proposed heat exchanger are given by

$$\Delta P \text{ in proposed heat exchanger} = (\text{Chart } \Delta P) \times \frac{\text{Proposed temperature rise}/400}{\text{Proposed power density}/10,000}$$

and the temperature difference is given by

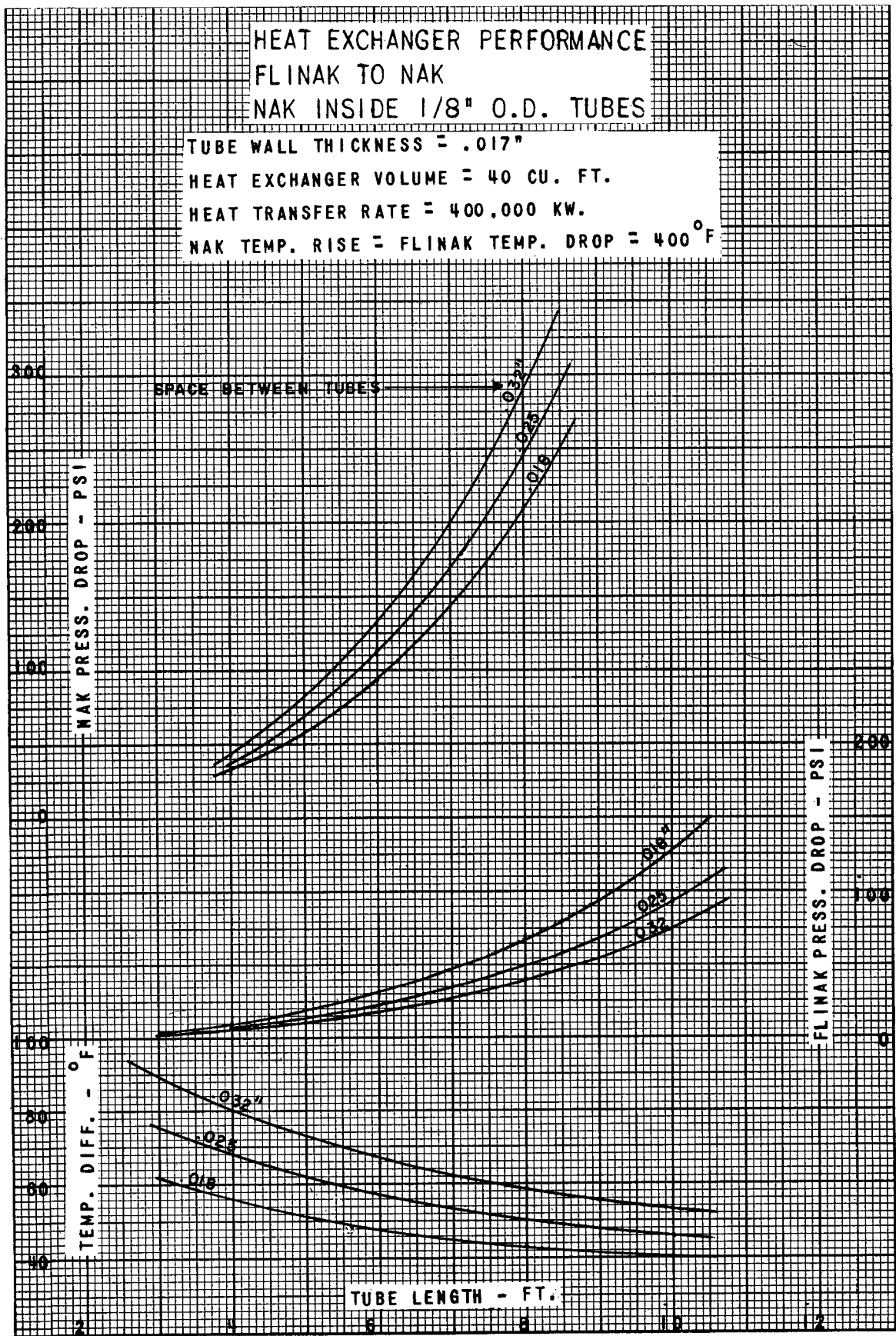
$$\Delta T \text{ in proposed heat exchanger} = (\text{Chart } \Delta T) \times \frac{\text{Proposed power density}}{10,000}$$

The effect of varying the tube wall thickness has not been taken into account either in the preparation of the charts of this section nor in the directions for their extended use. While tube wall thickness changes can have significant effects, particularly in the liquid-metal to liquid-metal heat exchangers, the tube wall thickness chosen for the charts probably will not be too much different in most cases from that likely to be selected for some new proposed heat exchanger and hence the effect generally will not be too great.



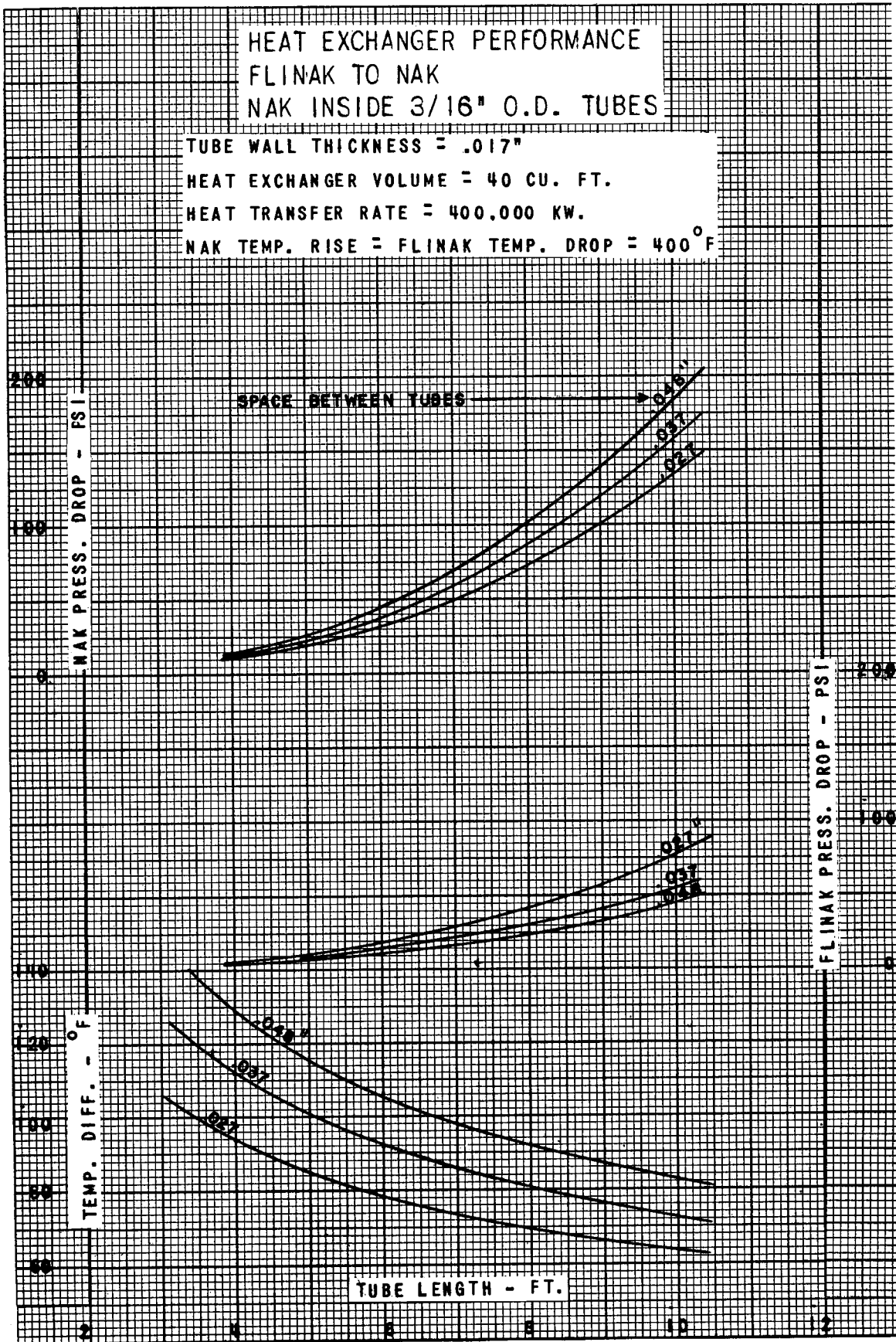
(a) NA-NAK. 1/8" TUBES.

FIGURE 19. PERFORMANCE OF 400,000 KW HEAT EXCHANGER.



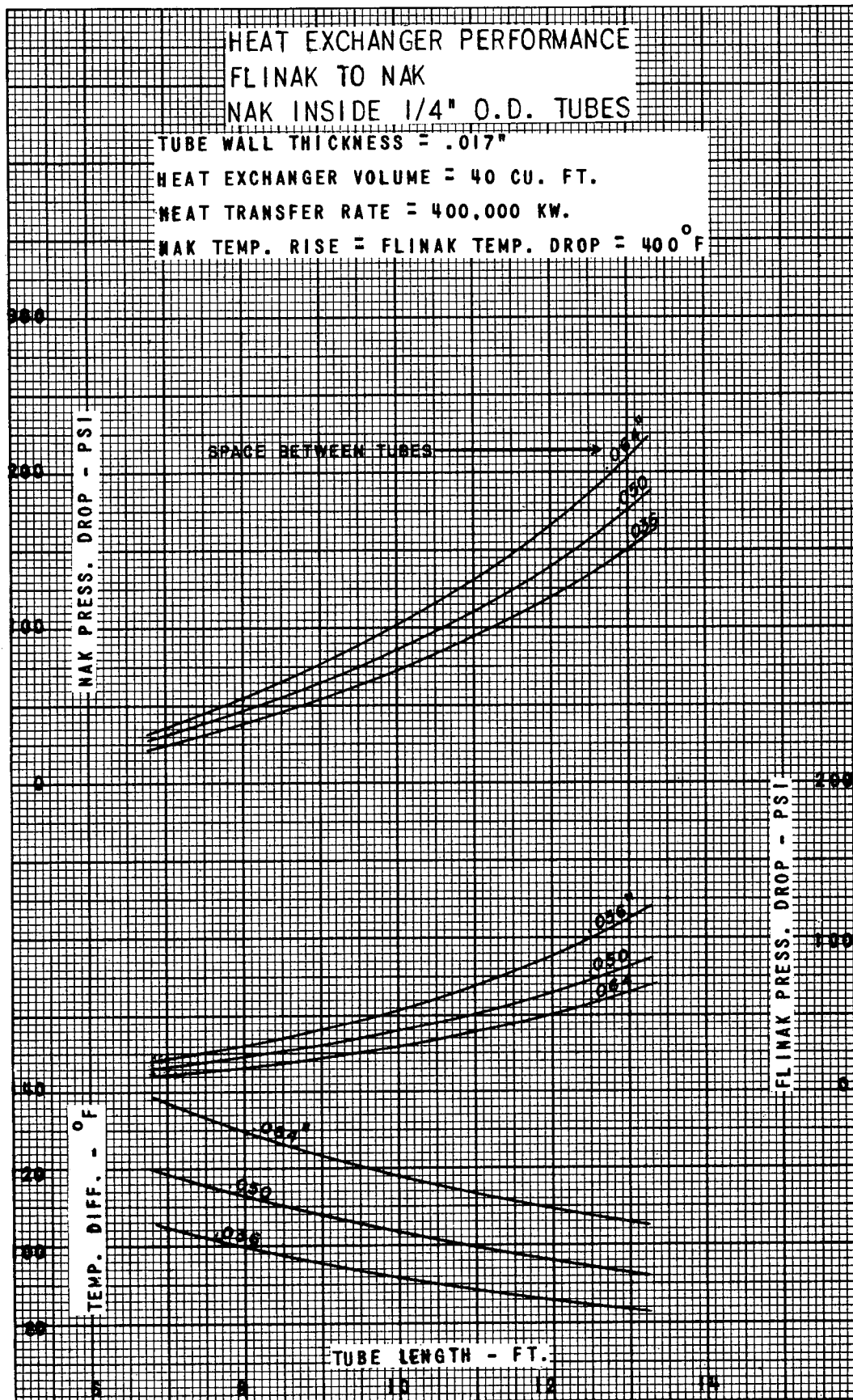
(b) FLINAK-NAK. 1/8" TUBES.

FIGURE 19. PERFORMANCE OF 400,000 KW HEAT EXCHANGER.



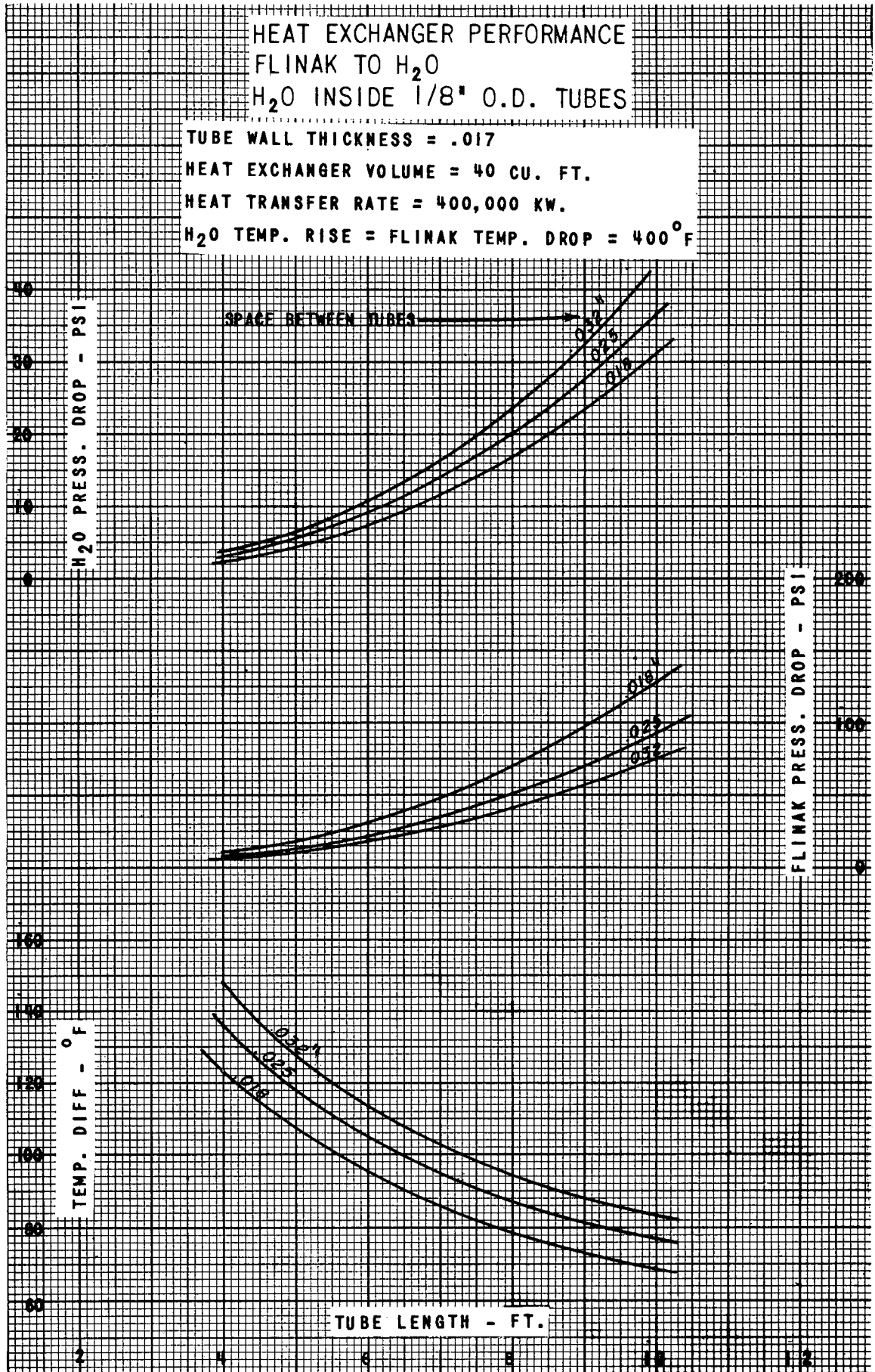
(c) FLINAK-NAK. 3/16" TUBES.

FIGURE 19. PERFORMANCE OF 400,000 KW HEAT EXCHANGER.



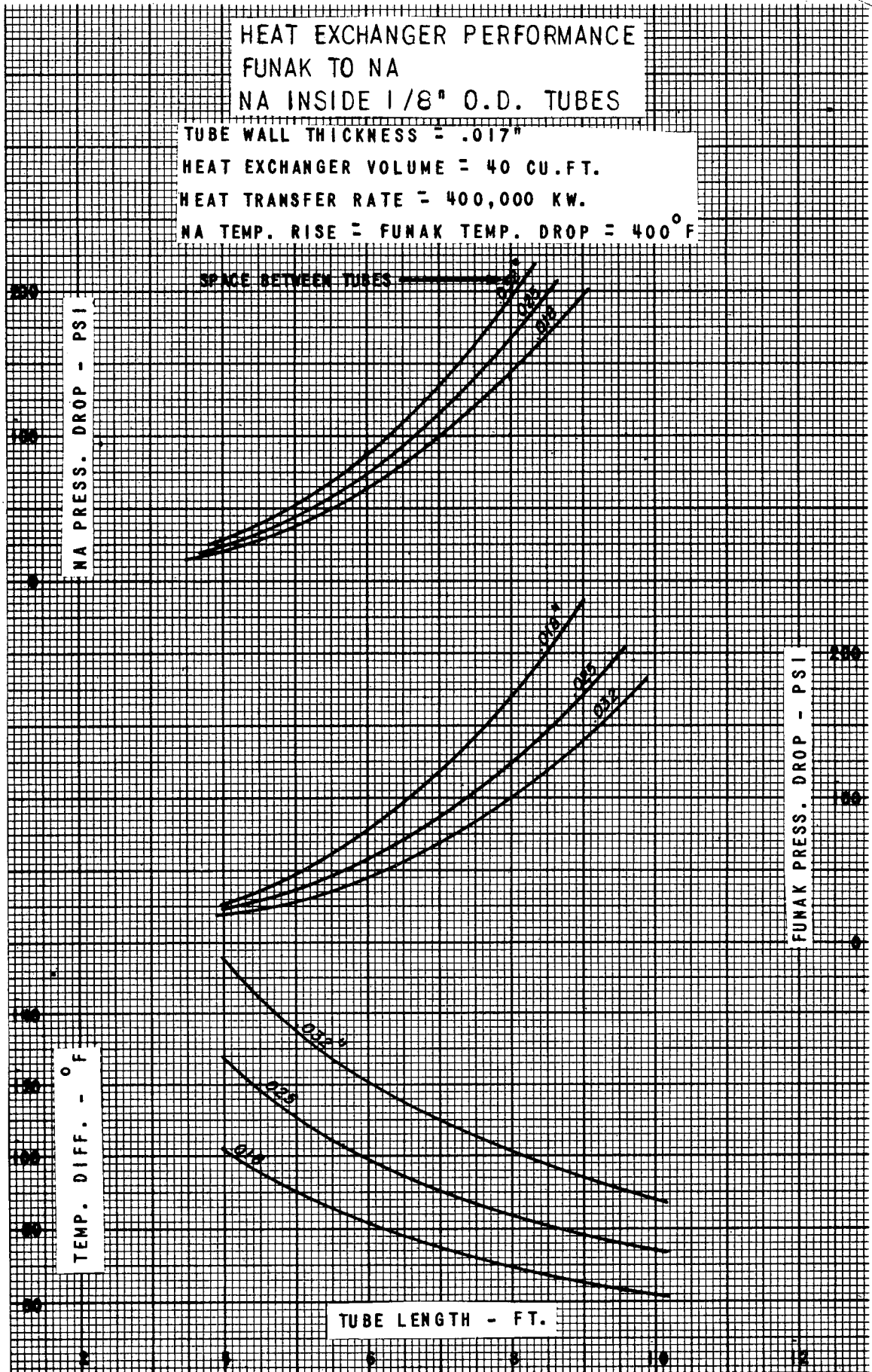
(d) FLINAK-NAK. 1/4" TUBES.

FIGURE 19. PERFORMANCE OF 400,000 KW HEAT EXCHANGER.



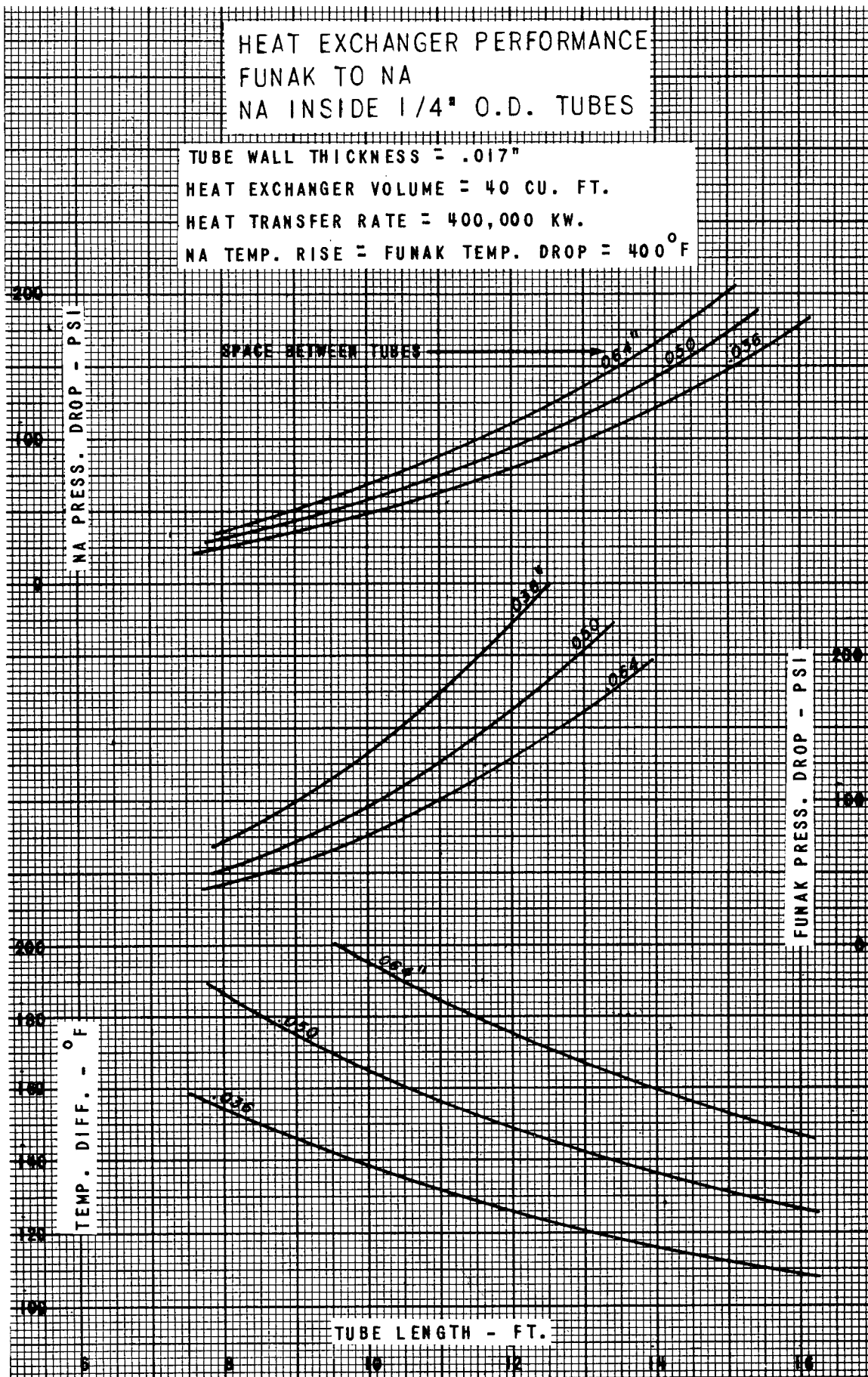
(e) FLINAK-H₂O. 1/8" TUBES.

FIGURE 19. PERFORMANCE OF 400,000 KW HEAT EXCHANGER.



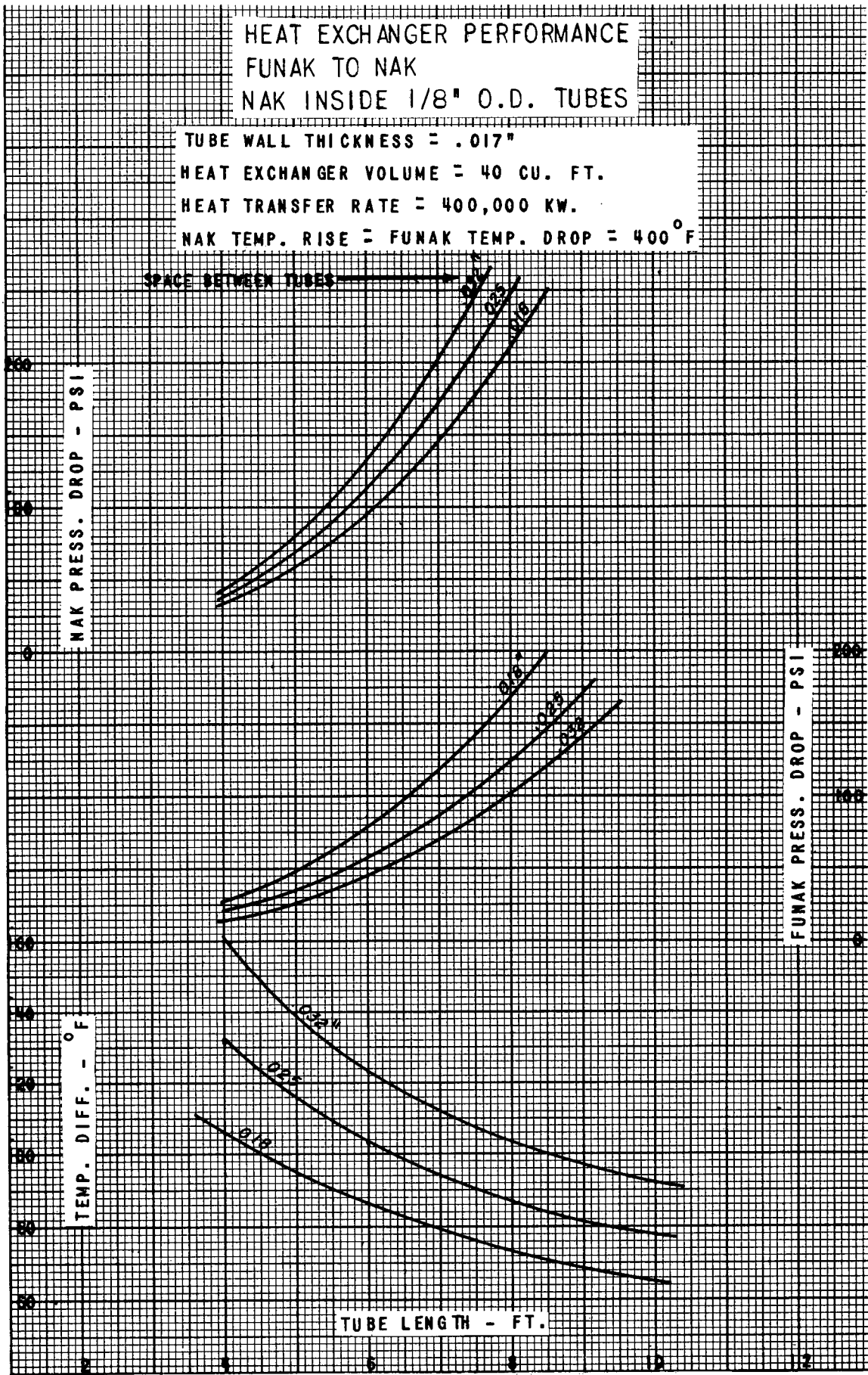
(f) FUNAK-NA. 1/8" TUBES.

FIGURE 19. PERFORMANCE OF 400,000 KW HEAT EXCHANGER.



(g) FUNAK-NA. 1/4" TUBES

FIGURE 19. PERFORMANCE OF 400,000 KW HEAT EXCHANGER.



(h) FUNAK-NAK. 1/8" TUBES.

FIGURE 19. PERFORMANCE OF 400,000 KW HEAT EXCHANGER.

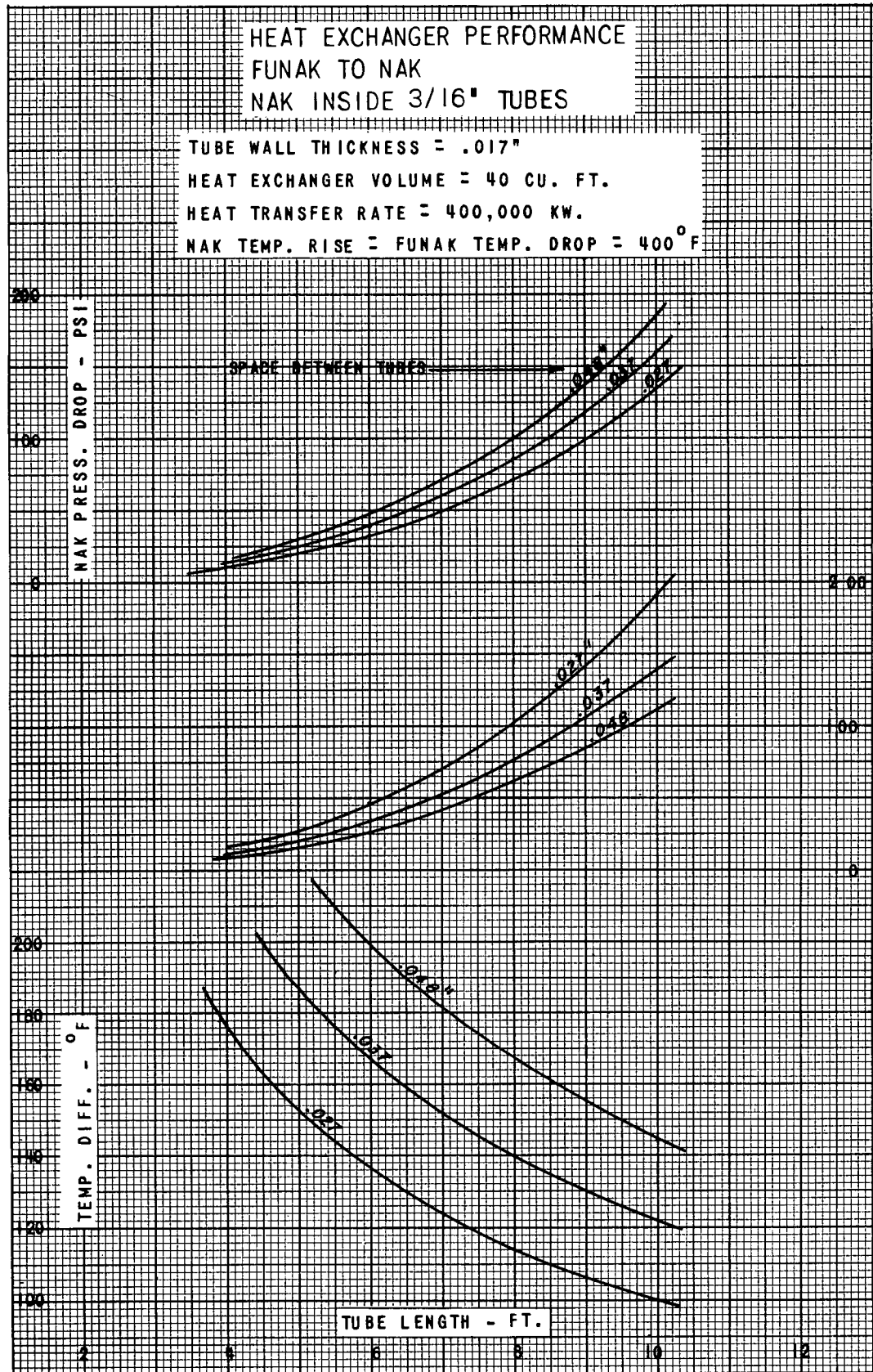
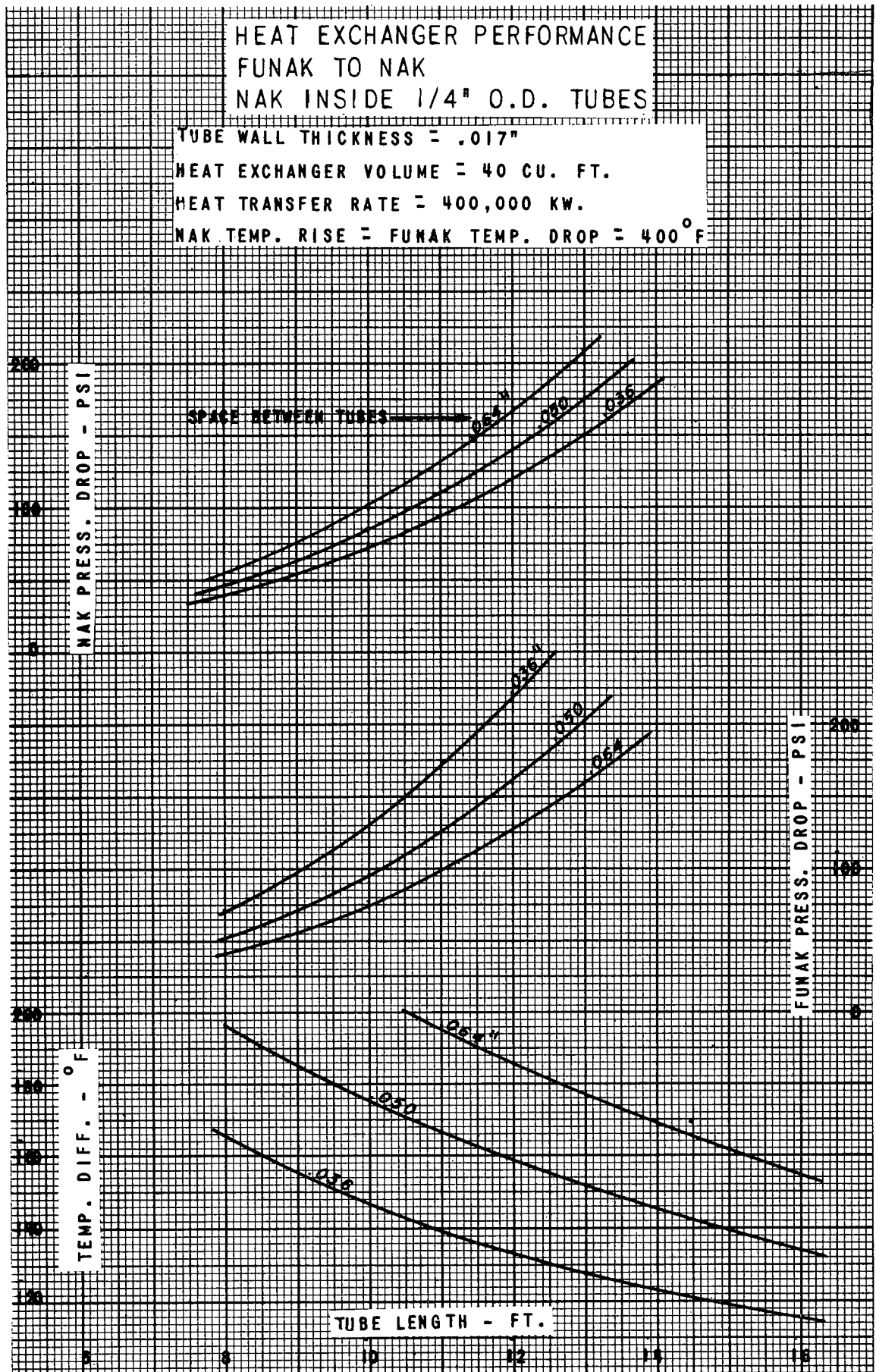
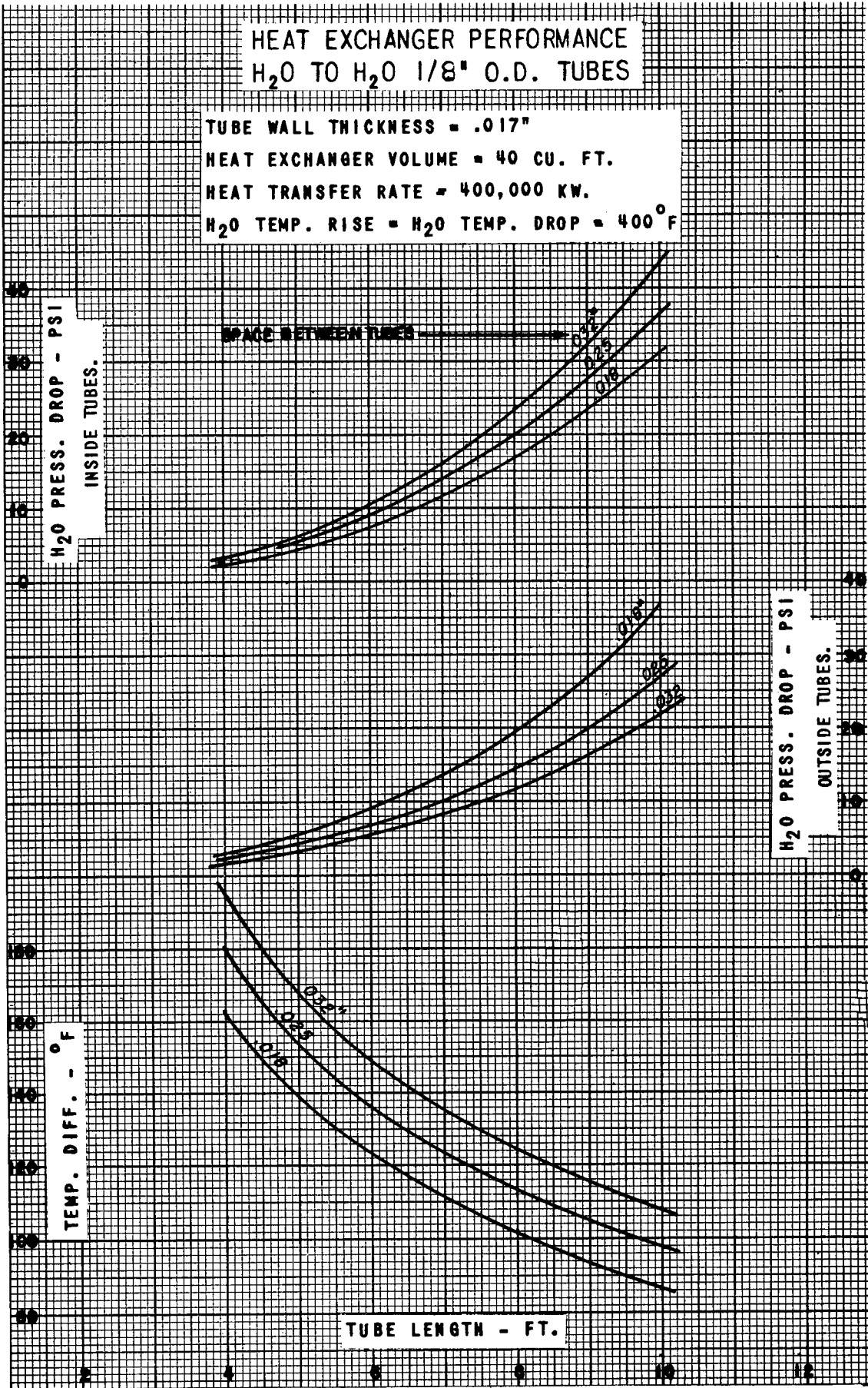


FIGURE 19. PERFORMANCE OF 400,000 KW HEAT EXCHANGER.



(j) FUNAK-NAK. 1/4" TUBES.

FIGURE 19. PERFORMANCE OF 400,000 KW HEAT EXCHANGER.



(k) H₂O-H₂O. 1/8" TUBES.

FIGURE 19. PERFORMANCE OF 400,000 KW HEAT EXCHANGER.